University of Otago

RESEARCH REPORT

Characterising TRIB1 Nanobodies using a Yeast Surface Display Platform with Flow Cytometry

Saffron Whitta

A thesis submitted in partial fulfilment of the Degree of
Bachelor of Biomedical Science with Honours.
University of Otago, Dunedin, New Zealand

October 2020

Abstract

The mammalian tribble (TRIB) pseudokinase family has three homologues, which act as an adaptor protein to regulate cell signalling pathways. TRIB proteins can bind the E3 ligase, Constitutive Photomorphogenesis Protein 1 (COP1), allowing TRIB regulatory function over essential proteins via the ubiquitin (Ub)-proteasomal pathway. For example, TRIB can cause the degradation of the transcription factor C/EBP-α which, regulates the differentiation of haematopoietic cells and adipocytes. TRIB also regulates critical signalling pathways such as the mitogen-activated protein kinase (MAPK) and serine/threonine-specific protein kinase (Akt) pathways, that controls mitosis, cell differentiation and survival. With different TRIB activities, TRIB proteins have various conformations with its substrates. Dysregulation of TRIB expression has been related to some cancer pathology such as Acute Myeloid Leukaemia (AML) and adenocarcinoma; however, the full molecular mechanism of how TRIB leads to pathogenesis is yet understood.

Single-domain antibodies called, nanobodies (Nbs), currently show promise in furthering discoveries in protein function and structure due to their ability to stabilise protein conformations with their small size of ~15 kDa, which allows; Nbs the ability to bind smaller epitopes that conventional antibodies are incapable of doing, and Nbs to be expressed intracellularly. Therefore, it is hypothesised that TRIB-specific Nbs as a research tool, may be used to discover further TRIB proteins' functional mechanisms that lead to the pathology of cancers. Understanding how TRIB-substrate conformations link with its cell signalling consequences, may reveal new therapeutic avenues.

Focusing on TRIB1 alone, TRIB1-specific Nbs previously screened from the McMahon Library, were expressed on the surface of the cell walls of *S. cerevesiae* (yeast). This allowed for the use of flow cytometry to characterise TRIB-1 Nbs affinity and specificity to its target based on the mean fluorescence intensity of the labelled Nbs and TRIB proteins: This flow cytometry method was able to be used to obtain a binding affinity (K_D = 315 nM) similar to isothermal titration calorimetry (K_D = 366 nM) for our positive TRIB1-Nb binding control, Nb2.011. Results showed that none of the eight TRIB1-Nbs tested had better affinities to TRIB1 than Nb2.011 (K_D > 366 nM). Although no promising TRIB1-Nbs was identified from the library samples, this project did elucidate limitations and important considerations in the use of the yeast surface display system, for the rapid, initial

characterisation screening of TRIB-Nbs after panning a Nb library for potential binders at nanomolar concentrations. Overall, we were able to conclude that this method of Nb characterisation, using a yeast display system with flow cytometry, may improve the discovery pipeline of TRIB-Nbs by narrowing down the panel of potential Nbs with desirable K_D estimations and specificity to its target.

Acknowledgements

First, I would like to acknowledge my two supervisors, Dr Peter Mace and Dr Liz Ledgerwood, who have been understanding and patient with me through my fumbling research endeavours this year. Their guidance has made this year a memorable Honours year experience, and I am very thankful for the opportunities they have given me which made this project possible.

Second, I would like to thank all the individuals in the Mace Lab group for being so welcoming, and giving me support over the past year; Alice, Matthias, Pavel, Hamish, Khan, Cameron, especially Sam and Abbey who took me under their wings. Also, thank you to the Day lab for the (brief) joint lab meetings and lab company during afterhours, as well as the Ledgerwood Lab for their advice. Without their contributions and friendship, this project would not have been the same.

Third, I would like to acknowledge the School of Biomedical Sciences and the administrative staff who made this COVID year as smooth as possible. To my advisor, Keith Ireton, thank you for the assurance of support throughout the year.

Last of all, to my family and friends who supported me and kept me grounded through this chaotic year, thank you for all the love and care that got me this far.

Table of Contents

List of Abbreviations

ACC	Acetyl-coenzyme A carboxylase
AID	Auxin-inducible degron
Akt	Serine/threonine-specific protein kinase
AML	Acute Myeloid Leukaemia
ATP	Adenosine triphosphate
AU	Absorbance unit
BAD	BH3-only protein BCL-2 associated agonist of cell death
BCL-2	B-cell lymphoma 2, apoptosis regulatory protein
BT474	Breast carcinoma cell line
C/EBP-α	CCAAT/enhancer-binding protein alpha
Cdc25	Cell division cycle 25
CDR	Complimentary determining region
CHAPS	3-[(3-cholamidopropyl)dimethylammonio]-1-propanesulfonate
C-lobe	Carboxy terminal lobe
COP1	Constitutive Photomorphogenesis Protein 1
C-terminal	Carboxy terminal
DFG	Aspartic acid-Phenylalanine-Glycine/Asp-Phe-Gly
DNA	Deoxyribonucleic acid
E. coli	*Escherichia coli*
ERK	Extracellular signal-regulated kinase
FITC	Fluorescein isothiocyanate
FOXO	Forkhead family of transcription factors
g	Grams
Gal	Galactose
GFP	Green fluorescent protein
GPCR	G-protein coupled receptor
HepG2	Immortalised human liver carcinoma cell line
His_6 tag	Polyhistidine tag comprising of 6 histidine residues
ITC	Isothermal titration calorimetry
K_D	Equilibrium dissociation constant
kDa	Kilo-Daltons
L	Litre
LB	Lysogeny broth

LMNG	Lauryl maltose-neopentyl glycol
M	Molar
MACs	Magnetic-activated cell sorting
MAPK	Mitogen-activated protein kinas
MFI	Mean fluorescence intensity
mRNA	Messenger ribonucleic acid
mTORC2	Rapamycin-insensitive protein complex 2
MYC	Proto-oncogene, BHLH Transcription Factor
Nb/Nbs	Nanobody/nanobodies
Ni^{2+}	Nickel
N-lobe	Amino terminal lobe
N-terminal	Amino terminal
PE	Phycoerythrin
PKB	Protein kinase B
POI	Protein of interest
RT-PCR	Reverse transcription polymerase chain reaction
S. cerevesiae	*Saccharomyces cerevisiae*
SDS-PAGE	Sodium dodecyl sulfate polyacrylamide gel
SEC	Size exclusion chromatography
SLE	Serine-leucine-glutamic acid/Ser-Leu-Glu
TB	Terrific broth
TRIB	Tribble
Ub	Ubiquitin
v/v	Volume per volume
Vhh	Antigen binding fragment of heavy chain only antibodies
w/v	Weight per volume
α	Anti

List of Figures

List of Tables

1. Introduction

1.1 Introduction to Tribble (TRIB) Pseudokinase.

The Tribble (TRIB) protein family was first discovered in *Drosophila melanogaster* and later discovered in humans. In D*rosophila* flies, only one TRIB homologue exists, and its function was first discovered to coordinate cell division and proliferation during morphogenesis necessary for mesoderm formation, by inducing proteasomal degradation of Cdc25 (M-phase inducer) activators String and Twine (Grosshans and Wieschaus, 2000; Mata *et al*., 2000; Seher and Leptin, 2000). The human TRIB pseudokinase family, unlike in *Drosophila*, comprises of three homologues (TRIB1, TRIB2, and TRIB3). Within human tribbles, sequence identity lies at 71.3% between TRIB1/2, 53.3% between TRIB1/3, and 53.7% between TRIB2/3 (Yokoyama and Nakamura, 2011).

Unlike canonical kinases that can regulate substrate activity through phosphorylation, TRIB proteins have obtained atypical residues which makes them unable to regulate efficient phosphoryl-transfer from adenosine triphosphate (ATP) to substrates (Bailey *et al*., 2015; Foulkes *et al*., 2018). Instead, TRIB proteins indirectly modulate various signalling pathways as an adaptor protein. Most studied are the mitogen-activated protein kinase (MAPK)/extracellular signal-regulated kinase (ERK) pathway, the Protein kinase B (PKB or Akt - a serine/threonine-specific protein kinase) pathway, and CCAT-enhancer-binding protein (C/EBP) pathway, which is involved in cell growth, cell survival and cell differentiation (Chen *et al*., 2018; Eyers, 2015; Eyers *et al*., 2017; Mashima *et al*., 2014; Ohoka *et al*., 2005). Non-homeostatic expression of TRIB proteins has therefore been associated with the pathogenesis of diseases such as cancer.

As TRIB proteins can associate with multiple substrates and induce various cellular outcomes, TRIB proteins are assumed to have a high degree of structural plasticity that give rise to multiple, transient complexes. However, this makes functional research on TRIB proteins difficult, as to understand the mechanisms underlying *TRIB*-related pathology, an understanding of the different TRIB protein complexes and how it relates to cell signalling events is required. Hence, new research tools are required to study further the TRIB family structure and how this relates to its various functional outcomes.

1.2 The TRIB Pseudokinase Domain.

TRIB proteins cannot phosphorylate substrates like regular kinases and have evolved to become regulatory scaffold proteins. Despite all three human TRIB homologues showing residual ability to bind ATP by retaining key lysine residues seen in kinases (*Figure 1.2.1.A* –

in red, the β3 lysine residue is shown to be conserved), they have no functional kinase activity (Lohan and Keeshan, 2013). Unlike canonical kinases, human TRIB homologues lack specific sequences needed for phosphoryl transfer, and this gives rise to their 'pseudo' kinase domain (Yokoyama and Nakamura, 2011). The DFG (Asp-Phe-Gly) motif in kinases, that acts to orient ATP into the binding site, is replaced in TRIB proteins (Eyers *et al*., 2017; Jamieson *et al*., 2018; Lohan and Keeshan, 2013). In TRIB1/2, the DFG motif is replaced by an SLE (Ser-Leu-Glu) sequence (*Figure 1.2.1.A* – highlighted DFG motif in red is not seen in human TRIB proteins), which stabilises the activation loop blocking the ATP binding pocket (Jamieson *et al*., 2018; Murphy *et al*., 2015). Furthermore, human TRIBs lack the necessary sequence for sufficient ATP binding (GXGX2GXV/'glycine-rich' motif in subdomain 1) and also lacks the HRD (His-Arg-Asp) residue that transfers the phosphate group from ATP to the substrate in the catalytic cleft (Bailey *et al*., 2015; Lohan and Keeshan, 2013). In short, human TRIBs lack the necessary sequences found in kinase proteins, summarised in *Figure 1.2.1.A*, that allows functional and optimal phosphoryl-transfer to substrates.

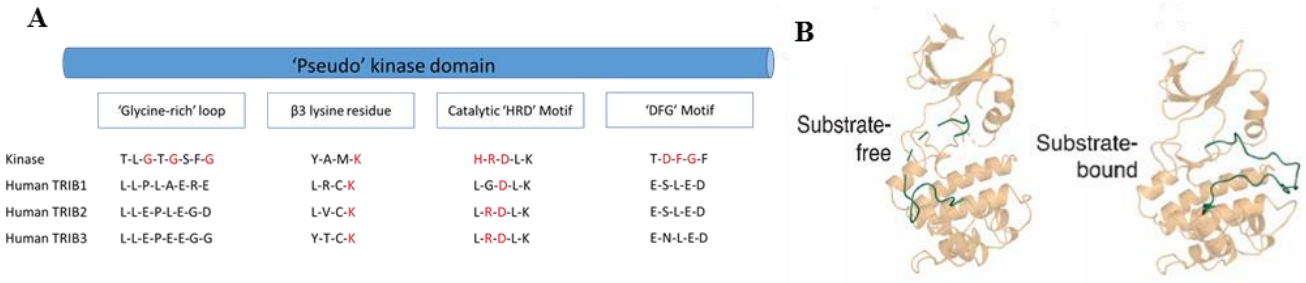

Figure 1.2.1: **The TRIB pseudokinase domain. A.** Adapted from (Eyers, 2015), functional kinase sequences, highlighted in red, are lost in TRIB pseudokinases (unable to phosphorylate substrates). In TRIB1/2, the DFG motif that act to orient ATP into the binding site, is replaced by the SLE motif that stabilises the activation loop to act as an autoinhibitory structure of COP1 binding when a substrate is not bound, shown in Figure 1.2.1.B. **B.** A protein structure of the TRIB1 pseudokinase domain (UniProt ID: Q96RU8) obtained from (Jamieson *et al*., 2018), shows how the activation loop (in green) conforms when substrate binds to expose the COP1 motif.

1.3 TRIB signalling pathways.

TRIB proteins have distinct motifs that facilitate different signalling modulation. As a family of pseudokinases, TRIB proteins acquired distinct amino acid sequences/motifs that allow scaffolding of effector proteins to their substrates. Site-directed mutagenesis has shown that an ILLHPW motif in the C-lobe of all TRIB homologues' pseudokinase domain, is what allows docking and upregulation of phosphorylating MEK proteins (dual-specificity tyrosine and serine/threonine kinases) in the MAPK pathway (Eyers *et al*., 2017; Jin *et al*., 2007; Yokoyama *et al*., 2010). Another conserved motif is the DQxVPx (generally DQLVPE) motif

in the C-terminal tail of all three TRIB homologues, which allows the recruitment of the E3 ligase, Constitutive Photomorphogenesis Protein 1 (COP1). Coupled with TRIB proteins having a degron (degradation signalling sequence) binding site in the pseudokinase domain, that may recruit the degrons of substrate proteins such as CEBPα and acetyl-coenzyme A carboxylase (ACC), TRIB proteins can regulate protein function via the ubiquitin (Ub)-proteasomal degradation pathway (Dedhia *et al*., 2010; Eyers *et al*., 2017; Keeshan *et al*., 2010).

A solved crystal structure of human TRIB1 pseudokinase domain has shown that substrate (e.g. C/EBPα) binding to the TRIB degron in the pseudokinase domain, leads to folding of the activation loop toward the αC-helix which allows for the COP1 motif to be released from the autoinhibitory conformation facilitated by the SLE motif (refer to *Figure 1.2.1.A-B*) (Jamieson *et al*., 2018). Subsequently, COP1 can bind to the C-terminal tail of TRIB proteins. As the COP1 motif is tethered to the N-lobe of the pseudokinase domain, TRIB proteins can scaffold COP1 to substrates bound at the pseudokinase domain (Dedhia *et al*., 2010); This induces poly-ubiquitylation of the substrate at a distinct lysine residue (K48) which marks it for 26S proteasomal degradation. Summarily, the distinct motifs and its position along the TRIBs' protein structure for MEKs (C-lobe of pseudokinase domain) and COP1 (tethered to the N-lobe of the pseudokinase domain) *(Figure 1.3.1)*, allows for different protein regulations. With TRIB proteins being able to associate with multiple substrates, TRIB exists in different conformations (only one conformation has been solved, *Figure 1.2.1.B*), which may be better studied using nanobodies that can stabilise them.

TRIB can act as a tumour suppressor or oncogenic factor by modulating the activity of MEK and Akt. As a tumour suppressor, TRIB2/3 interact with Akt to reduce its activation by mTORC2 (rapamycin-insensitive protein complex 2) phosphorylation (in the case of TRIB3) (Salazar *et al*., 2014). The direct mechanism of this Akt modulation is still yet established for all TRIB homologues (refer to *Figure 1.3.1*) (Eyers *et al*., 2017). This suppression of Akt activity by TRIB proteins is linked to an increase in FOXO (forkhead family of transcription factors) and BH3-only protein BCL-2 associated agonist of cell death (BAD) which promotes apoptosis (Salazar *et al*., 2014; Tsuzuki *et al*., 2019; Zareen *et al*., 2013). However, this tumour suppressing role of TRIB proteins with Akt modulation is contradictory to TRIB's oncogenic role via the MAPK pathway.

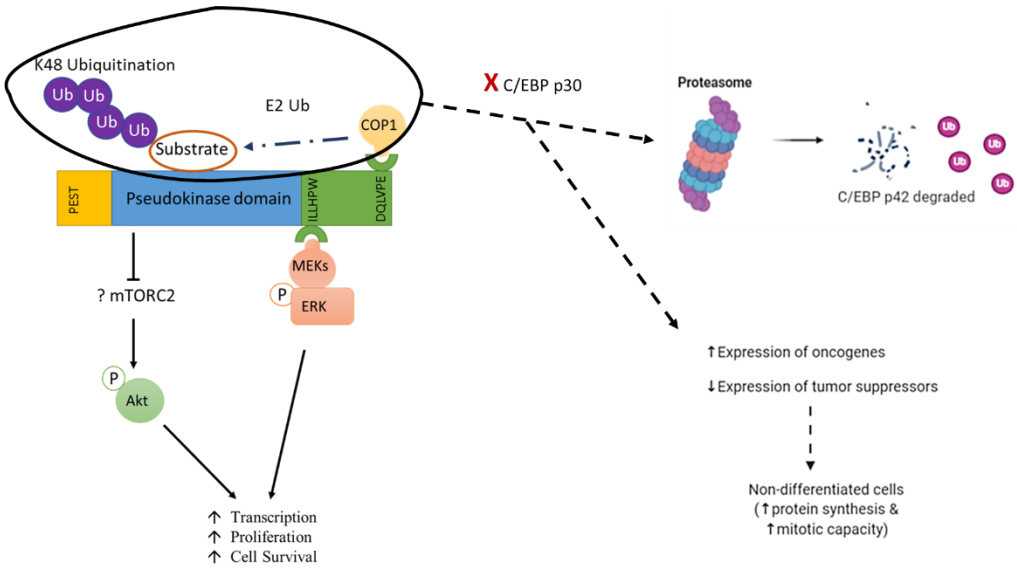

Figure 1.3.1: **A brief view of the human Tribble signalling pathway. LHS:** Schematic adapted from (Eyers et al., 2017) showing TRIB proteins' signalling interactions, the variable **PEST domain** that makes TRIB proteins unstable, and the distinct C-terminal motifs; **ILLHPW** allows TRIB direct interaction with MEKs increasing **MAPK pathway signalling; DQLVPE** allows TRIB to act as an adaptor, facilitating E3 ligase (e.g. COP1) to contact its protein target bound to the TRIB pseudokinase domain. TRIB homologues also modulate the **Akt signalling pathway** – the mechanism is yet fully known; however, TRIB3 is suggested to modulate mTORC2 phosphorylation of AKT. **RHS:** The dotted arrows show an example of **COP1-mediated degradation of a substrate;** the example substrate shown is C/EBPα p42. Degradation C/EBPα p42 leads to loss of differentiation in myeloid cells that can lead to acute myeloid leukaemia. LHS: left-hand side. RHS: right-hand side. This figure was made using BioRender.

As previously stated, MEK binds TRIB proteins to the ILLHPW motif in the C-lobe. MEK binding to TRIB has been shown to increase the phosphorylation of ERK proteins and subsequently, cell survival and growth (Jin *et al*., 2007). Preventing ERK phosphorylation by inhibiting MEK1 (using UO126), showed there was a correlation between decreased phosphorylated-ERK concentration and significantly reduced TRIB-induced C/EBP degradation (Yokoyama *et al*., 2010). ERK1/2 has been shown to phosphorylate C/EBP, which upregulate its degradation. C/EBP is a transcription factor that drives the differentiation of myeloid cells and adipocytes. Upregulated degradation of the C/EBP then compounds the oncogenic effects of TRIB-MEK interaction, that increases the likelihood of oncogenesis. Subsequently, TRIB proteins' contradictory role in maintaining cell homeostasis may suggest exclusive MEK or AKT modulation at a given time: Understanding TRIB allostery/conformations may be the key to deciphering its multifaceted role in cell homeostasis and the development of TRIB-related human cancers.

1.4 TRIB association with human cancers.

TRIB homologue expression levels occur inversely in cells. TRIB proteins are generally associated with myeloid-derived cells due to its relationship with the C/EBP family of transcription factors; however, it is also expressed in other cells types. It has been speculated that TRIB proteins regulate each other's expressions through negative and feedforward mechanisms (Rishi *et al*., 2014; Salomé *et al*., 2018). TRIB1/3 and TRIB2 mRNA (messenger ribonucleic acid) are inversely expressed in different blood cell lineages under normal conditions: Myeloid-derived cells express high levels of TRIB1/3 and low levels of TRIB2, whereas lymphoid derived cells express high levels of TRIB2 and low levels of TRIB1/3 (Salomé *et al*., 2018). This differential expression (inverse correlated TRIB1-TRIB2 and proportional TRIB1-TRIB3 expression) may conditionally pertain to other cells. In HepG2 (immortalised human liver carcinoma) cells, insulin stimulation increased TRIB1 and TRIB3 mRNA expression but reduced TRIB2 mRNA expression (Tsuzuki *et al*., 2019). A general trend has been seen that TRIB1 and TRIB3 mRNA are expressed in inverse proportion to TRIB2 mRNA.

TRIB1/2 overexpression is linked to the development of Acute Myeloid Leukaemia (AML). Non-homeostatic levels of TRIB1/TRIB2 within myeloid cells, lead to dysplasia that can pathologically result in (AML) (Jackson and Taylor, 2002). Under pathologic conditions, murine models with transfected haemopoietic stem cells (Dedhia *et al*., 2010) and mRNA analysis of human AML cells (Salomé *et al*., 2018), show that some AML subtypes may be attributed to overexpression of either TRIB1 or TRIB 2. An RT-PCR (reverse transcription polymerase chain reaction) study has shown that 8q24 amplification in AML cells, not only increased MYC (Proto-Oncogene, BHLH Transcription Factor) mRNA expression but also TRIB1 when compared to healthy donor cells (Röthlisberger *et al*., 2007). Overexpression of TRIB1/2 reduces the cellular concentration of the full (p42) C/EBPα isoform and increases levels of the truncated (p30) C/EBPα isoform (refer to *Figure 1.3.1* - RHS) (Keeshan *et al*., 2006). The literature agrees that C/EBPα p30 increase in haematopoietic stem cells may be a key driver for AML development, as it lacks the N-terminus transactivation domain (present in C/EBPα p42) that prevents cell cycle progression in its mitotic stage via E2F (E2 transcription factor) regulation (Rishi *et al*., 2014). Although transient overexpression of TRIB1/2 has been found to act as tumour suppressors by upregulating apoptosis through inhibiting JNK and the proceeding dephosphorylation of BCL-2 (apoptosis regulatory

protein) on residue Ser70 (Gilby *et al*., 2010), it may stand that constitutive TRIB1/2 overexpression does induce leukemogenesis.

In adenocarcinoma, low expression of TRIB3 is linked to evasion of apoptosis. TRIB3 research has revealed its involvement in the endoplasmic reticulum (ER) stress response downstream of ER stress sensors (Ohoka *et al*., 2005), that may directly be regulated by TRIB1 (Mashima *et al*., 2014). Although both TRIB1 and TRIB3 affect the ER stress response, TRIB3 expression, unlike TRIB1 and TRIB2, has no significant contribution to the pathogenesis of blood cancers but in adenocarcinoma (Dedhia *et al*., 2010). Unlike most TRIB1/2-related cancers, TRIB3 mRNA levels are disproportionately expressed to the degree of cancer lesions in breast carcinoma (BT474) and hepatocellular carcinoma (HepG2) (Salazar *et al*., 2014). Furthermore, unlike the overexpression seen in TRIB1/2-related cancers that confers advantageous upregulation of MAPK pathway, TRIB3 expression in adenocarcinoma is downregulated for reduced stress-induced apoptosis (Ohoka *et al*., 2005). TRIB3 overexpression studies in neurons have proven its pro-apoptotic effects by downregulating Akt phosphorylation which decreases dephosphorylation of FOXO proteins (Aimé *et al*., 2015; Zareen *et al*., 2013); in dopaminergic neurons of the substantia nigra, TRIB3 overexpression does increase cell death occurrences as it reduces pro-survival protein Parkin (Aimé *et al*., 2015). It is unknown how or why TRIB3 has a bias in Akt regulation over MAPK regulation (seen in TRIB1/2), and how TRIB3's tumour suppressing activity is reduced through underexpression in adenocarcinoma.

PEST domain may be the key to sustained overexpression or under expression of TRIB proteins in diseases such as cancer. TRIB proteins are hard to research, not only because of the difficulty present in isolating its different transient complexes as it interacts with its different substrates: Each of the homologues have an N-terminal PEST domain (a peptide sequence rich of proline, glutamic acid, serine and threonine that signals for protein degradation) with distinct motifs, that gives it varying short intracellular half-lives (Eyers *et al*., 2017). The difference in TRIB protein turnover in normal and diseased conditions may then determine the duration of effects seen, e.g. increased MEK phosphorylation with longer active TRIB compared with more transient TRIB presence, generating more extensive cell survival and mitotic events that contribute to gaining cancer hallmarks like resistance to cell death. Imaging the half-lives of TRIB protein homologues *in vitro* and being able to trap the multiple transient conformations of TRIB proteins as it acts with its substrates, may be useful

to prove whether the PEST domain is an important feature in TRIB homeostasis and TRIB-related diseases.

1.5 Prospects of using nanobodies in potentiating human TRIB research.

Nanobodies are emerging to be a useful research tool. Derived from camelid antibodies, Nbs consist of only two variable heavy chains (Vhh) and lack the light-heavy chains of conventional antibodies (refer to *Figure 3*). Therefore, the antigen-binding sites of nanobodies are not fragmented between two variable light and heavy chains, and Nbs can easily be expressed in the cytoplasm of bacteria (*E. coli*) and yeast *(S. cerevesiae*) (Desmyter *et al*., 2015; Hassanzadeh-Ghassabeh *et al*., 2013). Nanobodies are also resistant to oxidative changes, having no significant change in antigen affinity with reduced disulphide bonds, as well as reduced thermostability at 47 °C (Pleiner *et al*., 2015). These characteristics make Nbs an easy to reproduce, useful research tool. Being approximately 15 kDa (kilodaltons) in size, Nbs can bind smaller epitopes with nanomolar affinity, which conventional antibodies (~150 kDa) are incapable of doing (Desmyter *et al*., 2015). It has the ability to provide stability to G-coupled protein receptors (GPCRs) and their different allosteric states, allowing for the discovery that a heterogeneous mechanism lies with how agonists may induce variable biological responses according to which transient converting receptor states become stabilised with substrate interaction (Staus *et al*., 2016). Hence, using Nbs to trap TRIB conformations may potentiate the understanding of the human TRIBs-protein interactions and how this relates to its various functional outcomes. Despite the possible uses for Nbs in TRIB research, no TRIB-Nbs have yet to be fully developed for research use.

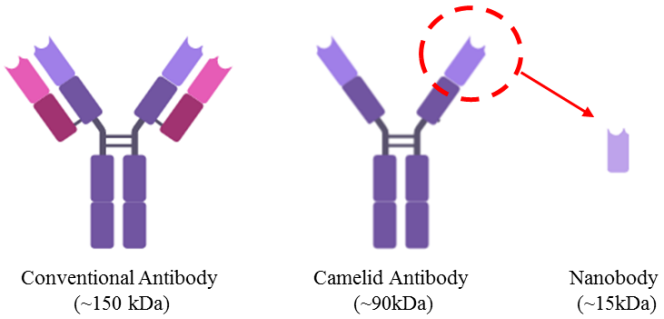

Figure 1.5.1: **Conventional antibodies vs Camelid derived nanobodies**. Nanobodies consists of only heavy chains (light purple blocks) and are small (~15 kDa), unlike conventional antibodies that are big (~150kDa) and consist of two heavy chains and two light chains (magenta blocks). This figure was made using BioRender.

Nanobodies may allow profiling of TRIB function in cells. Whilst some literature has found evidence that overexpression of TRIB proteins is present in subtypes of cancer (Dedhia *et al*., 2010; Mashima *et al*., 2014), there are some studies that have found TRIB expression

to decrease (Ohoka *et al*., 2005; Salazar *et al*., 2014). Despite there being no clarity in what determines TRIB proteins as a tumour suppressor or as an oncogenic factor, related oncogenic stimuli that increase TRIB expression may result in increased or suppressed mitotic ability in cancer cells, that is dependent on the context of cell type and status of other cancer-related genes (Röthlisberger *et al*., 2007; Yokoyama *et al*., 2010). Most TRIB study done is limited to observing TRIB mRNA expression without confirming protein presence, and looks indirectly at TRIB protein interaction through cell morphogenesis or phosphorylation of its downstream effectors like ERK and Akt (Dedhia *et al*., 2010; Salazar *et al*., 2014; Salomé *et al*., 2018). The development of specific Nbs for TRIB proteins will therefore facilitate further study of; TRIB1/2 protein expression within myeloid and lymphoid derived cells and its association to AML through C/EBP regulation, the non-redundant function between TRIB homologue expressions in different cell types, as well as more in-depth structural analysis on TRIB conformations that determine its tumour suppressor/oncogenic role (MAPK or Akt modulating bias) under homeostatic and diseased states (Ohoka *et al*., 2005; Salazar *et al*., 2014).

In recent years, a new screening method using flow cytometry have been developed where synthetic Nbs may be expressed on the surface of yeast cells via an Aga1p-Aga2p tether or Aga1p-Aga2p mimicking tether (Feldhaus *et al*., 2003; McMahon *et al*., 2018; Uchański *et al*., 2019); The use of conjugated fluorophores to Nbs and proteins of interest (POI), allows for flow cytometric visualisation of Nb affinity and specificity to POIs, generating results that are equivalent to previous antibody screening methodologies such as surface plasmon resonance (Michael *et al*., 2003). Using this method may improve the discovery pipeline for TRIB-specific Nbs.

1.6 Aims

The discovery and use of TRIB-specific Nbs may potentiate further human TRIB studies and reduce the gap in knowledge for understanding the contradictory roles of TRIB as a tumour suppressor and an oncogenic factor in diseased states. Therefore, with a focus on the initial development of human TRIB1-Nbs, this project will utilise a yeast surface display system and aim to:

1. Optimise the flow cytometric analysis of the yeast surface display system to characterise TRIB1-Nbs.
2. Characterise the affinity and specificity of TRIB1-Nbs.

2. Materials and Methods

2.1 Materials

2.1.1 Bacterial Strains and Plasmids

Table 2.1.1 1: **Bacterial Strains**

Strain	**Description**
BL21(DE3)	*Escherichia coli. fhuA2 [ion] ompT gal [dcm]ΔhsdS*
MC1061	*Escherichia coli. araD139, Δ(ara, leu)7697, ΔlacX74, galU-, galK-, hsm+, strA*

Table 2.1.1.2: **Plasmids.** His_6 fusion tag was used in this study.

Insert	**Vector backbone**	**Resistance**
Long TRIB1 - $M627_{84-372}$	LIC N-terminal His_6 tag	Kanamycin (Kan)
Long TRIB2 – $M924_{53-343}$	LIC N-terminal His_6 tag	Kan

2.1.2 Yeast Strain and Nanobody Clones

In this study, Nb2.011 which has been shown to co-elute and co-crystalise with TRIB1 is used as a positive control. Whereas Nb5.018 (a Nb known to bind PPTrap – an unrelated, membrane bound protein), is used as a negative control for Nb-binders. *Table 2.1.2.2* summarises the Nbs characterised in this study, using the yeast display system and flow cytometry.

Table 2.1.2.1: **Yeast Strain**. The common Brewer's Yeast strain BJ5465 was used in this study, for surface Nb expression.

Strain	**Description**
BJ5465	*Saccharomyces cerevisiae. MATα ura352 trp1 leu2Δ1 his3Δ200 pep4::HIS3 prb1Δ1.6 R can1 GAL*

Table 2.1.2.2: **Nanobody Clones used in this project**. The TRIB1 Nb clones (*S. cerevesiae*, refer to Table 2.1.2.1) used in this study, was previously generated, and screened against its target protein by the Mace Lab, as specified by the McMahon yeast display screening method *(*McMahon *et al.*, 2018*).*

Nanobody	**Protein Target**	**Sequence**
Nb5.018	PPTrap	QVQLQESGGGLVQAGGSLRLSCAASGYIFTKLYMG WYRQAPGKEREFVAGIGRGSTTYYADSVKGRFTISR DNAKNTVYLQMNSLKPEDTAVYYCAVYPVLRPYF GYWGQGTQVTVSS
Nb2.011	TRIB1	QVQLQESGGGLVQAGGSLRLSCAASGNISYSVVMG WYRQAPGKEREFVATIADGGSTYYADSVKGRFTISR DNAKNTVYLQMNSLKPEDTAVYYCAAWDNRDPFL TYWGQGTQVTVSS
Nb2.012	TRIB1	QVQLQESGGGLVQAGGSLRLSCAASGNIFQITSMG WYRQAPGKERELVAGINSGGTTYYADSVKGRFTIS RDNAKNTVYLQMNSLKPEDTAVYYCAAYAQRYGY LSYWGQGTQVTVSS
Nb2.029	TRIB1	QVQLQESGGGLVQAGGSLRLSCAASGTISLVRAMG WYRQAPGKERELVAGIARGSITYYADSVKGRFTISR DNAKNTVYLQMNSLKPEDTAVYYCAAYGRNWSRL AYWGQGTQVTVSS
Nb2.031	TRIB1	QVQLQESGGGLVQAGGSLRLSCAASGSISTYRRMG WYRQAPGKEREFVAGITAGGNTYYADSVKGRFTIS RDNAKNTVYLQMNSLKPEDTAVYYCAVGHRLLNI YADTPIDGLAYWGQGTQVTVSS
Nb2.038	TRIB1	QVQLQESGGGLVQAGGSLRLSCAASGNISVIRGMG WYRQAPGKEREFVAAINSGANTYYADSVKGRFTIS RDNAKNTVYLQMNSLKPEDTAVYYCAAAVYDKRY HSYWGQGTQVTVSS
Nb2.049	TRIB1	QVQLQESGGGLVQAGGSLRLSCAASGNISDLYAMG WYRQAPGKEREFVAGIATGSNTYYADSVKGRFTISR DNAKNTVYLQMNSLKPEDTAVYYCAAVSKVPLRL RYWGQGTQVTVSS
Nb2.060	TRIB1	QVQLQESGGGLVQAGGSLRLSCAASGNIFDIIAMG WYRQAPGKEREFVAGINGGSITYYADSVKGRFTISR DNAKNTVYLQMNSLKPEDTAVYYCAALGSYQRPR DGRHSYWGQGTQVTVSS

Nb2.066	TRIB1	QVQLQESGGGLVQAGGSLRLSCAASGNISIIHYMG WYRQAPGKEREFVAGIGYGATTYYADSVKGRFTIS RDNAKNTVYLQMNSLKPEDTAVYYCAAGNYRNRG YRYWGQGTQVTVSS
Nb2.074	TRIB1	QVQLQESGGGLVQAGGSLRLSCAASGTISGIRRMG WYRQAPGKEREFVASITSGANTNYADSVKGRFTISR DNAKNTVYLQMNSLKPEDTAVYYCAALYRKDQYV TSYHIYWGQGTQVTVSS

2.1.3 Media for bacterial cell culture

Bacterial cell culture media was prepared with type 1 deionised water (18.2 MΩ) from a Milli-Q Advantage A10 academic water purification system (Millipore). Media was then autoclaved at 121 °C, 0.1 MPa for 20 minutes. *Escherichia coli* strains were grown in Terrific Broth (TB) media (FORMEDIUM, for protein expression), Lysogeny Broth (LB) media (FORMEDIUM, for DNA plasmid amplification) or on LB agar (colony growth). LB media was made of 10 g peptone, 10 g NaCl and 5 g yeast extract per Litre: 7.5 g of agar was added per 500 mL, for LB agar. TB media was made of 12 g tryptone and 24 g of yeast extract per Litre. Supplementation of media with Kanamycin (50 μg/mL) was done before use.

2.1.4 Media for yeast cell culture

All yeast cell culture media was prepared with type 1 deionised water (18.2 MΩ) from a Milli-Q A10 academic water purification system (Millipore). Media was then autoclaved at 121 °C, 0.1 MPa for 20 minutes. *Saccharomyces cerevisiae* nanobody clones were grown in Yglc4.5-Trp media (pH 4.5) until stationary phase, which consisted of (per 1 Litre); 3.8 g Trp drop-out media supplement (Kaiser), 6.7 g yeast nitrogen base w/out amino acids (FORMEDIUM), 10.4 g tri-sodium citrate dihydrate (SCHARLAU), 7.4 g citric acid monohydrate (Fisher Chemical). Yglc4.5-Trp media was then supplemented with 1% Penicillin/Streptavidin (Pen/Strep) antibiotic (10,000 units/mL stock, Gibco), and 10% sterifiltered D-glucose (20% stock solution, FORMEDIUM). *Saccharomyces cerevisiae* Nb clones were induced to express Nbs in yeast-Trp media (pH 6) which consisted of (per 1 Litre); 3.8 g Trp drop-out media supplement (FORMEDIUM), 6.7 g yeast nitrogen base w/out amino acids (FORMEDIUM). Yeast-Trp media was then supplemented with 1% Pen/Strep and 10% of sterifiltered D-glucose (20% stock solution) or 10% sterifiltered D-galactose (20% stock solution, FORMEDIUM).

2.1.5 Solutions

Except where otherwise stated, buffers and solutions were made up with type 1 deionised water (18.2 MΩ) from a Milli-Q Advantage A10 academic water purification system (Millipore). Chromatography buffers were filtered with a 0.45 μm vacuum filter and degassed for ~20 minutes. Yeast selection buffers were filtered with a 0.45 μm Sterifilter (Corning), and yeast glucose/galactose supplements was syringe-sterifiltered with a 0.2 μm Sterifilter (Corning).

Table 2.1.5.1: **Solutions and its ingredients used in this study**.

Solutions	**Ingredients**
Cell freezing buffer	20 mM Tris (pH 8.0), 300 mM NaCl
Standard purification buffer	50 mM Tris (pH 8.0), 300 mM NaCl, 10% sucrose (*w/v*), 10% glycerol (*v/v*), 10 mM imidazole
Elution buffer	50 mM Tris (pH 8.0), 300 mM NaCl, 10% sucrose (*w/v*), 10% glycerol (*v/v*), 300 mM imidazole
Size exclusion chromatography buffer	20 mM HEPES (pH 7.6), 150 mM NaCl
Resolving buffer (for SDS-PAGE)	1.5 M Tris (pH 8.8)
Stacking buffer (for SDS-PAGE)	0.5 M Tris (pH 6.8)
2x SDS-sample buffer	4% (*w/v*) SDS, 125 mM Tris (pH 6.8), 0.01% (*w/v*) bromophenol blue, 100 mM DTT, 20.4% glycerol
10x SDS-PAGE running buffer	1% SDS, 192 mM glycine, 25 mM Tris (pH 8)

Coomassie stain	50% (*v/v*) ethanol, 10% (*v/v*) glacial acetic acid, 0.25% (*w/v*) Coomassie brilliant blue R250
SDS-PAGE de-stain	50% (*v/v*) ethanol, 10% (*v/v*) glacial acetic acid
Standard selection buffer	150 mM NaCl, 20 mM HEPES (pH 7.6), 0.1% (*w/v*) BSA, 5 mM maltose

2.1.6 Fluorophores

Table 2.1.6.1: **Fluorophores used in this study for flow cytometry**.

Fluorophores	**Excitation/Emission Wavelength (nm)**
Mouse monoclonal [16B12] to HA tag conjugated to PE (ab72479, abcam)	488/575
FITC, general α-protein (Pierce FITC Antibody Labelling Kit, Thermo Scientific)	494/518

2.2 Methods

2.2.1 Bacterial cell culture techniques

2.2.1.1 Bacterial transformation

Competent BL21 (DE3) cells (for protein expression), or MC1061 cells (for DNA cloning), were transformed by incubating 20 µL of cells with 0.5 µL of plasmid. First, cells were incubated on ice for 10 minutes, followed by a 45 second heat shock at 42 °C. Cells were placed back on ice for 2 minutes before the addition of 350 µL of LB media. Cells were then incubated for 45 minutes in a 37 °C shaker, before being spread on LB agar plates bearing Kan antibiotic. Plates were incubated at 37 °C overnight.

2.2.1.2 Protein and DNA expression

For protein expression, cell plates transformed in *Section 2.2.1.1*, were resuspended with 3 mL of LB for 1 L cultures. In 1 L cultures, 1 mL of antibiotics and 1 mL of resuspended cells were added. Cells were grown at 37 °C on a shaker, until the optical density at 600 nm (OD_{600}) reached 0.5-0.8. Cultures were moved to an 18 °C shaker and left to acclimatise for 45 minutes. Expression was then induced with 20 µL of isopropyl β-D-1-

thiogalactopyranoside (final concentration of 0.2 mM) per 100 mL of culture. Protein expression was left to occur overnight.

For DNA expression, one colony from the cell plates transformed in *Section 2.2.1.1,* was extracted, and grown overnight in 3 mL LB media, at 37 °C on a shaker. Cells were harvested the following day in 1.7 mL microcentrifuge tubes and pelleted using a HERAEUS Pico17 centrifuge (Thermo Scientific) at 13 rpm, for 2 minutes. A Zyppy™ plasmid miniprep kit (Zymo Research) was then used to purify DNA plasmids from bacterial cultures. The Zyppy™ plasmid miniprep protocol was altered to include the resuspension of cells in 1 mL of water following centrifugation of the 3 mL overnight culture. Fourty microlitres of DNase-free water was used to elute DNA plasmids; DNA was then stored at -20 °C.

One L cultures were harvested in 1 L centrifuge bottles using the Avanti JXN-26 centrifuge (Beckman Coulter) and the JA-17 rotor at 25,000 rpm for 30 minutes at 4 °C. Supernatant was discarded, and cell pellets were resuspended in 10 mL of freeze buffer (*Table 2.1.5.1).* Resuspended cells were then frozen at -20 °C, until required.

2.2.1.3 Bacterial cell lysis

For 1 L cultures, resuspended cells were thawed at room temperature and made up to 30 mL with standard purification buffer. DNase and lysozyme were each added to final concentrations of 3 μg/mL and 0.8 mg/mL, respectively. Cells were emulsified using an Avestin Emulsiflex C3 (ATA Scientific), following the manufacturer's instructions; samples were lysed through homogenisation with a high-pressure valve at ~15,000 psi.

2.2.1.4 Ni^{2+} affinity purification

Protein constructs expressed (1 L culture) had a His_6 tag, therefore, were purified using Ni^{2+} affinity purification. A 5 μL sample was collected from the initial cell lysate as an insoluble fraction. This sample was pelleted at 10,000 rpm for 2 mins. Post centrifugation, 5 μL of supernatant was kept as a soluble fraction. The remaining supernatant was loaded onto 2 mL His-select Ni^{2+} affinity resin (Sigma), pre-equilibrated with purification buffer. A 50 mL tube with mixed resin/supernatant was left to bind on a rotator at 4 °C, for 30 minutes. The resin was then transferred to a Poly-Prep Chromatography handheld-column (BioRad). Samples were washed with purification buffer and a 5 μL flow through sample was kept. Protein was eluted with 300 mM of imidazole in purification buffer; 4x 1 mL elutions were taken for 1 L cultures. Eluted protein concentrations were measured using the NanoDrop (*Section 2.2.2.2*).

Pooled elution fractions were incubated overnight at 18 °C with 5 µL 3C protease and 0.2% DTT, for the removal of the His_6 tag. The soluble, insoluble, flow through, post His_6 tag removal, and elution fractions from Ni^{2+} affinity chromatography were then analysed by SDS-PAGE (*Section 2.2.2.1*).

2.2.1.5 Size exclusion chromatography (SEC)

Elution fractions from Ni^{2+} affinity purification were pooled and concentrated further, to ~500 µL in an ultrafiltration concentrator (PALL) with a 10 kDa molecular weight cut-off filter. Protein was loaded onto a Superdex™ S200 size exclusion column (GE Healthcare), pre-equilibrated with SEC buffer. Size exclusion chromatography was performed using an ÄKTA pure chromatography system (GE Healthcare), where SEC buffer was run through the column at a flow rate of ~0.5 mL/min and 500 µL fractions were collected. A real-time chromatogram of 280 nm absorbance was used to predict protein concentrations and mass was compared to proteins of known size run on the same Superdex™ S200 column. To confirm purification of proteins of interest, fractions of eluted proteins were then analysed using SDS-PAGE, followed by analysis on the nanodrop. Samples were snap frozen using liquid nitrogen and stored at -80 °C.

2.2.2 General protein techniques

2.2.2.1 SDS-PAGE

Proteins expressed and extracted from *E. coli* BL21 cells were separated for analysis, using sodium dodecyl sulfate-polyacrylamide gel electrophoresis (SDS-PAGE). SDS-PAGE gradient gels were made using a gradient former (Model 385, BioRad) and a peristaltic pump (Pharmacia). Low (10%) and high (20%) percentage-acrylamide gel solution reagents, plus the stacking gel reagents are found in *Table 2.2.2.1.* Gradient gels were poured and set, before the stacking buffer was added. A 15-well comb was inserted into this stacking gel to create wells for sample loading.

Table 2.2.2.1: **SDS-PAGE gradient gel reagents.**

High % gel	
40% acrylamide	15 mL
Resolving buffer	7.5 mL

MQ water	1.82 mL
10% SDS	300 µL
Bromophenol blue	210 µL
TEMED	15 µL
10% APS	150 µL
Low % gel	
40% acrylamide	7.5 mL
Resolving buffer	7.5 mL
MQ water	14.54 mL
10% SDS	300 mL
TEMED	15 µL
10% APS	150 µL
Stacking gel	
40% acrylamide	3.75 mL
Resolving buffer	7.77 mL
MQ water	18 mL
Bromophenol blue	10 µL
TEMED	25 µL
10% APS	150 µL

Protein samples were diluted in 2x SDS-PAGE sample buffer (*Table 2.1.5.1*). Soluble and insoluble fractions obtained from bacterial cell culture lysates, were boiled at 95 °C for 5 minutes and briefly spun down. Three microlitres of Precision Plus Protein Marker (BioRad) was loaded into the first lane and 5-10 μL of diluted samples were loaded into separate wells of the gel. Gels were run with an Electrophoresis Power Supply (EPS-600, Pharmacia) at 220 V for 45 minutes with water cooling. Gels were stained for ~15 minutes in Coomassie Blue and destained overnight. The processed gels were imaged with an Image Scanner III (GE Healthcare).

2.2.2.2 Protein quantification using NanoDrop

Protein concentrations (bacterial cell culture) were quantified using a NanoDrop 1000 Spectrophotometer (Thermo Scientific). The absorbance of protein solutions at 280 nm was measured using a 1 μL sample. Extinction coefficients for each protein construct was previously calculated by inputting amino acid sequences into ExPASy ProtParam; this was used to calculate protein concentration using Beer-Lambert law.

2.2.3 Yeast cell culture techniques

Yeast cell culture techniques were performed under sterile conditions in the presence of an open flame. During recovery, growth, and induction of yeast cells, the 24 well blocks used for culture were covered with sterile BS25 Aera Seal (Excel Scientific Incorporated).

2.2.3.1 Recovery of yeast Nb clones

Previously, the Mace Lab had built a TRIB1-Nb library using the McMahon method, whereby yeast was enriched for high affinity Nb-binders through 4 rounds of magnetic-activated cell sorting (MACS) selection with successively lower concentration of labelled TRIB1 (McMahon *et al*., 2018). Enriched yeasts were plated as single colonies in a 96-well plate and stored at -80 °C. Tribble-1 nanobodies characterised in this study was recovered from that library.

A sample of frozen yeast Nb library aliquots of selected TRIB1-Nb to be characterised in this study was taken and revived in 5 mL of Yglc4.5-Trp media in a 24 deep-well block overnight in an incubator at 30 °C and 230 rpm. Clonal expansion was checked by centrifugation at 5000g and 4 °C, for 4 minutes using a 5810R centrifuge (Eppendorf). Following successful revival, yeast culture was centrifuged for Yglc4.5-Trp media replacement, to allow yeast

growth to stationary phase (~48 hours). An OD_{600} measurement was then taken to calculate yeast population density (OD_{600} of $1 \approx 1.5 \times 10^7$ yeast cells).

Initially, TRIB1-Nb clones revived (for this study) from the Mace Lab's *TRIB*1-Nb library, were kept as frozen aliquots to passage for characterisation experiments. Yeast culture was centrifuged after reaching stationary phase, followed by removal of supernatant and resuspension of cells in 1 mL of Yglc4.5-Trp media supplemented with 10% DMSO; 450 uL aliquots (final density is ~ 10^{10} cells/mL) were stored at -80°C, using an isopropanol cell freezing chamber (Thermo Fisher Scientific cat# 5100-0001) to maintain cell integrity.

2.2.3.2 Nanobody expression

Once yeast cells were revived from the frozen TRIB1-Nb stock and incubated to reach stationary phase as mentioned in *Section 2.2.3.1*, the yeast cultures were centrifuged for the replacement of Yglc4.5-Trp media to pH 6 yeast media supplemented with glucose. This was followed by an overnight incubation at 30 °C and 230 rpm, to acclimate yeast cells to the more basic yeast media. For the expression of Nbs on the surface of yeast cells, the yeast cultures were centrifuged, and media replaced with pH6 yeast media supplemented with galactose. Yeast culture was then incubated for 24-48 hours, at 25 °C and 230 rpm.

A reverse time course induction experiment was performed using Nb2.011, to determine Nb-expression levels in yeast over time. Induction of yeast over a 48-hour period was performed with 3 induction replicates at 0 hours, 12 hours, and 24 hours. After 48 hours, cells were prepped for flow cytometry analysis by PE labelling as described in *Section 2.2.4*.

Optimisation of the standard selection buffer (*Table 2.1.5.1*) was carried out to minimise non-specific binding of TRIB proteins to yeast and Nbs. In this experiment, the standard selection buffer was supplemented with either:

- 0.002% LMNG
- 1%, 2% or 3% TWEEN® 20 (Sigma Life Science)
- 2%, 4% or 6% Glycerol
- 0.5% CHAPS (GLYCON Biochemicals GmbH)

These supplemented selection buffers were used to prepare uninduced and induced Nb-yeast clones for flow cytometry with 480 nM TRIB1-FITC as described in *Section 2.2.4*; An additional wash step with only standard selection buffer was done after removal of excess TRIB1-FITC.

2.2.4 Characterisation of nanobody affinity and specificity

For the characterisation of TRIB1-Nbs, yeast cell culture post Nb-induction, was prepped for flow cytometry analysis on the Guava ExpressPlus (Guava® easyCyte™-5HT, Merck Millipore). For each Nb-yeast clone, an OD_{600} measurement of a 1 in 10 dilution sample was taken to calculate 1.5x cells needed for the experiments (1×10^6 cells for each sample, a total of 3 induction replicates) and for PE bulk labelling. An unlabelled control and a TRIB-FITC only control sample was also prepared for each yeast clone tested, with a PE only control gained from PE bulk labelling. Cells were centrifuged in 2 mL eppendorf tubes, at 5000g for 3 min at 4 °C using 5424R centrifuge (Eppendorf). The yeast media was removed and replaced with 500 µL selection buffer, followed by another centrifuging step and removal of the supernatant. Cells were then added to 200 µL αHA-PE (1 in 10 dilution, 0.1 mg/ml), and incubated in foil, on a rotator for 1 hour at 4 °C. Following PE labelling of Nbs, yeast cells underwent 2x 500 µL selection buffer washes, before resuspension in 1.5 mL selection buffer. Resuspended yeast cells were dispensed as 90 µL samples in a 2 mL 96 well block. Cells were then incubated on a shaker at 500 rpm at room temperature for 60 minutes, with serial TRIB1-FITC/TRIB2-FITC concentrations (0-480 nM). Samples were then washed 2x with 500 µL selection buffer and resuspended with 1 mL of selection buffe. In a 96-well plate (flat-bottomed), 300 µL of samples were dispensed, ready for flow cytometry.

2.2.4.1 Characterisation of TRIB1-Nb affinity

For the affinity characterisation of TRIB1-Nb affinity against TRIB1, TRIB1 purified from *E. coli* was labelled with FITC (Pierce FITC Antibody Labelling Kit, Thermo Scientific) as stated by the manufacturer's protocol, then snap frozen using liquid nitrogen and stored at -80 °C. A serial dilution of TRIB1-FITC with selection buffer was performed to gain concentrations of; 480 nM, 240 nM, 120 nM, 60 nM, 30 nM, 15 nM, 7.5 nM, 0 nM. These concentrations were used for TRIB1-Nb incubation with TRIB1-FITC as described in *Section 2.2.4*.

2.2.4.2 Characterisation of TRIB1-Nb specificity

For the specificity characterisation of TRIB1-Nb affinity over TRIB2, TRIB2 purified from *E. coli* was labelled with FITC (Pierce FITC Antibody Labelling Kit, Thermo Scientific) as stated by the manufacturer's protocol, then snap frozen using liquid nitrogen and stored at -80 °C.

To characterise whether TRIB1-Nb had the ability to bind TRIB2, and consequently the potential to have less specificity against TRIB1, Nb-expressing yeast was incubated with TRIB2-FITC at 200 nM concentration as described in *Section 2.2.4*. Following, separate Nb-expressing yeast samples was incubated with varying molar ratio concentrations of TRIB1-FITC (200 nM) with unlabelled TRIB2 (200 nM) to gain concentrations of; 200 nM TRIB1-FITC against 0 nM TRIB2 (1:0 molar ratio), 200 nM TRIB1-FITC against 200 nM TRIB2 (1:1 molar ratio), 200 nM TRIB1-FITC against 1 µM TRIB2 (1:5 molar ratio), 200 nM TRIB1-FITC against 2 µM TRIB2 (1:10 molar ratio). These concentrations were used for TRIB1-Nb incubation with TRIB1-FITC as described in *Section 2.2.4*.

2.2.5 Statistical analysis

Analysis of flow cytometry data gained from Guava, was done using FlowJo 10.7.1. Yeast population was isolated from dead cells and debris, using the polygon gating tool. Control samples was then used to compensate FITC signal spillover into the PE channel. Following, a quadrant gating tool was applied to the unlabelled yeast clone controls, to separate the yeast population into Nb-expressors and non-Nb-expressors, and TRIB1/2 Nb-binders and non-binders.

For the analysis of the reverse time course induction performed on Nb2.011 yeast clones (*n=3, Section 2.2.3.2)*, the bisector gating tool was set on the unlabelled control (PE histogram) in order to set an expression threshold for Nb-expressing yeast (Nb Pos). A mean fluorescence intensity (MFI) of the PE channel, as well as the population percentage of Nb-Pos was then taken and exported for analysis on GraphPad Prism 8.4.3. A one-way ANOVA with Dunnett's post hoc test was performed on the PE MFI data and Nb-Pos population data (%), to see how 48- and 36- hours of induction compared to 24 hours of induction (statistical significance of $p < 0.05$).

For the analysis of the optimisation of standard selection buffer (*n=3, Section 2.2.3.2)* the bisector gating tool was set on the unlabelled control (FITC histogram) in order to set

threshold for non-specific binding of TRIB1-FITC to yeast. A FITC MFI of non-specific binding population was then taken and exported for analysis on GraphPad Prism 8.4.3. A one-way ANOVA with Dunnett's post hoc test was performed on the FITC MFI data, to see whether the level of non-specific binding changed with modifications made to the selection buffer, when compared to the use of standard selection buffer for flow cytometry preparation (statistical significance of $p < 0.05$).

For the characterisation analysis of TRIB1-Nb affinity (*Section 2.2.4.1)* and specificity (*Section 2.2.4.2)*, a bisector gating tool was set on the unlabelled control (PE histogram) to identify the Nb-expressing yeast populations. From the Nb-Pos population, the mean fluorescence intensity of the compensated FITC channel was then taken and exported for analysis on GraphPad Prism 8.4.3. To characterise TRIB1-Nb affinity, a non-linear regression analysis was performed, where a one-site specific binding test was done to determine the dissociation constant (K_D) of TRIB1-Nbs. To characterise the specificity of TRIB1-Nbs over TRIB2, a one-way ANOVA with Dunnett's post hoc test was performed, where the TRIB1-FITC MFI at TRIB1 to TRIB2 molar ratio concentration of 1:0 was compared with every other TRIB1 to TRIB2 molar ratio concentrations (statistical significance of $p < 0.05$).

3. Results

The development of antibodies against proteins of interest for the use as a research tool takes time which may be streamlined by easy methods that can rapidly characterise multiple nanobodies in each experiment. In the passing years, as it is easy to express Nbs in bacteria and yeast due to its small size, Nbs surface display systems have been developed as a platform to accelerate the discovery of conformationally-selective Nbs against proteins of interest.

To streamline the development of TRIB1 selective Nbs and further TRIB1 research, the McMahon yeast surface display platform was utilised alongside flow cytometry to characterise an approximate Nb affinity and specificity quickly; This was hypothesised to limit the putative TRIB1-Nbs to be taken into the next steps of the discovery pipeline from an existing Nb-library. Flow cytometry is a method that utilises the excitation of fluorophore-labelled proteins by a laser, and detection of the resulting fluorescence of fluorophores to determine presence or interaction between proteins of interests. By labelling our protein of interest, TRIB1, with FITC in conjunction to using PE to label expressed Nbs by yeast clones, this would allow us to observe four different yeast populations from our flow cytometry analysis (*Figure 3*); Q1 – non-specific binding of TRIB1-FITC to yeast, Q2/Q3 – Nb-expressing yeast, Q2 – TRIB1-Nb binders, Q4 – unlabelled yeast.

To characterise TRIB1-Nbs using the yeast surface display system and flow cytometry, we had to first make unlabelled and fluorophore-labelled TRIB1/2 proteins for TRIB1-Nb affinity and specificity characterisation. Next, a check of the induction time for optimal Nb-expression in our yeast clones. Non-specific binding of our target protein (TRIB1 to yeast) also had to be accounted for as this would affect the MFI readings from flow cytometry that we used to calculate the Nb-affinities. Finally, TRIB1-Nbs were able to be characterised for its affinity, which narrowed the Nbs selected for the specificity characterisation.

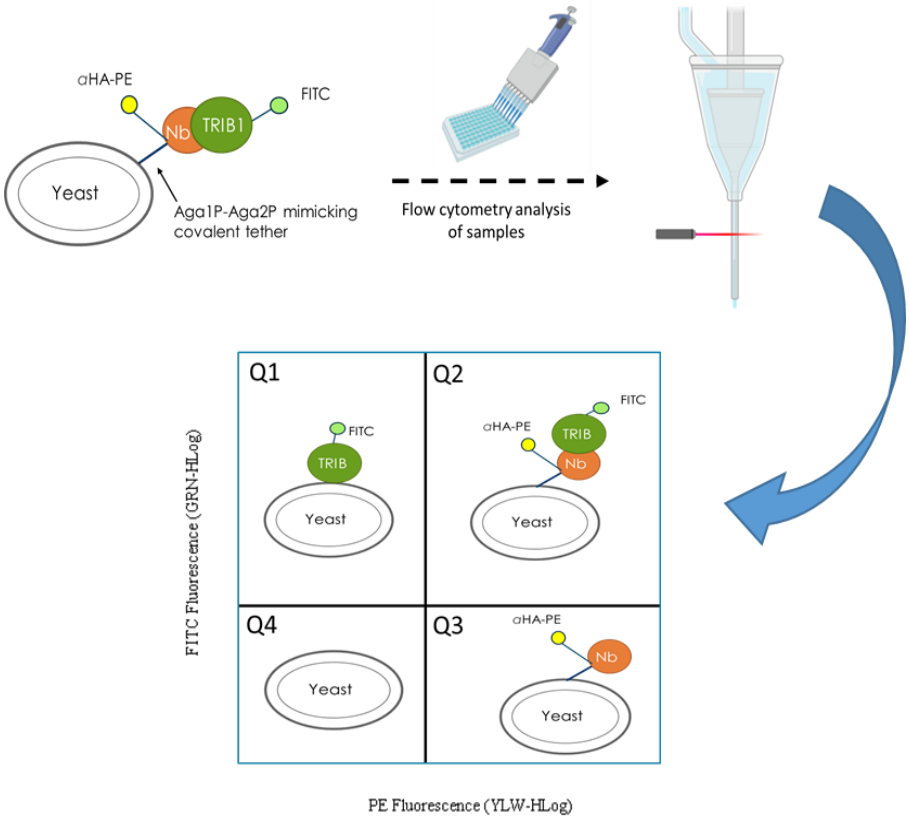

Figure 3: **Schematic of the yeast surface display system used to characterise TRIB1-Nbs using flow cytometry.** Nbs are expressed on the surface of the yeast cell wall via an Aga1p-Aga2p mimicking covalent tether. The Nbs have an HA epitope that is labelled with PE. TRIB1 is labelled with FITC. Flow cytometry analysis of labelled yeast cells will generate a yeast population dot plot that can be separated into four different groups; Q1 – non-specific binding of TRIB1-FITC to yeast, Q2/Q3 – Nb-expressing yeast, Q2 – TRIB1-Nb binders, Q4 – unlabelled yeast. This figure was made using BioRender.

3.1 TRIB1 and TRIB2 expression and purification.

To investigate the affinities and specificities of putative TRIB-1 Nbs to its target using flow cytometry, TRIB1 and TRIB2 had to be expressed and purified for labelling with fluorophores. Previously, the Mace Lab cloned full-length TRIB1 (M627), and full-length TRIB2 (M924) constructs into expression vectors through Ligation Independent Cloning (LIC). *Escherichia coli* were transformed with either TRIB1 or TRIB2 constructs for the expression of proteins *(Section 2.2.1, Figure 3.1.A).* Proteins were expressed with a His_6-tag which allowed for purification of proteins using His-select Ni^{2+}-affinity resin (*Section 2.2.1.4, Figure 3.1.A – outlined by a purple box).* SDS-PAGE was used to analyse samples; soluble, insoluble, flow-through, post-His_6-tag-removal, and elution fractions from Ni^{2+}-affinity purification (*Section 2.2.2.1).* A clear single band at ~33 kDa corresponding to the size of TRIB1 and TRIB2 proteins; This indicated success in the overexpression and purification of each TRIB construct from *E. coli.* The protein band of samples incubated with 3C protease, being slightly below the Ni^{2+}-affinity purification elution bands *(Figure 3.1.B),*

indicated the successful removal of the His_6-tag from TRIB1; a similar observation was made for TRIB2 *(Figure 3.1.D)*. A secondary purification of the eluted protein was performed post-cleavage of the His_6-tag, by using SEC. TRIB1 (~33.1 kDa) and TRIB2 (~33.3 kDa) proteins were eluted into B panel fractions which is at the expected size according to the S200 column (refer to *Figure 3.1C and 3.1E*, respectively). Purified TRIB1 and TRIB2 samples were then left unlabelled or labelled with FITC through primary amines (lysine side chains). FITC-labelled TRIB1 and TRIB2 proteins were run through a desalting column, then analysed using a NanoDrop to check for successful FITC labelling. The yield of purified proteins (80 uM TRIB1-FITC, 30 uM TRIB1, 100 uM TRIB2-FITC) in *Section 3.1* allowed for the characterisation of TRIB1-Nbs in *Sections 3.3 and 3.4.*

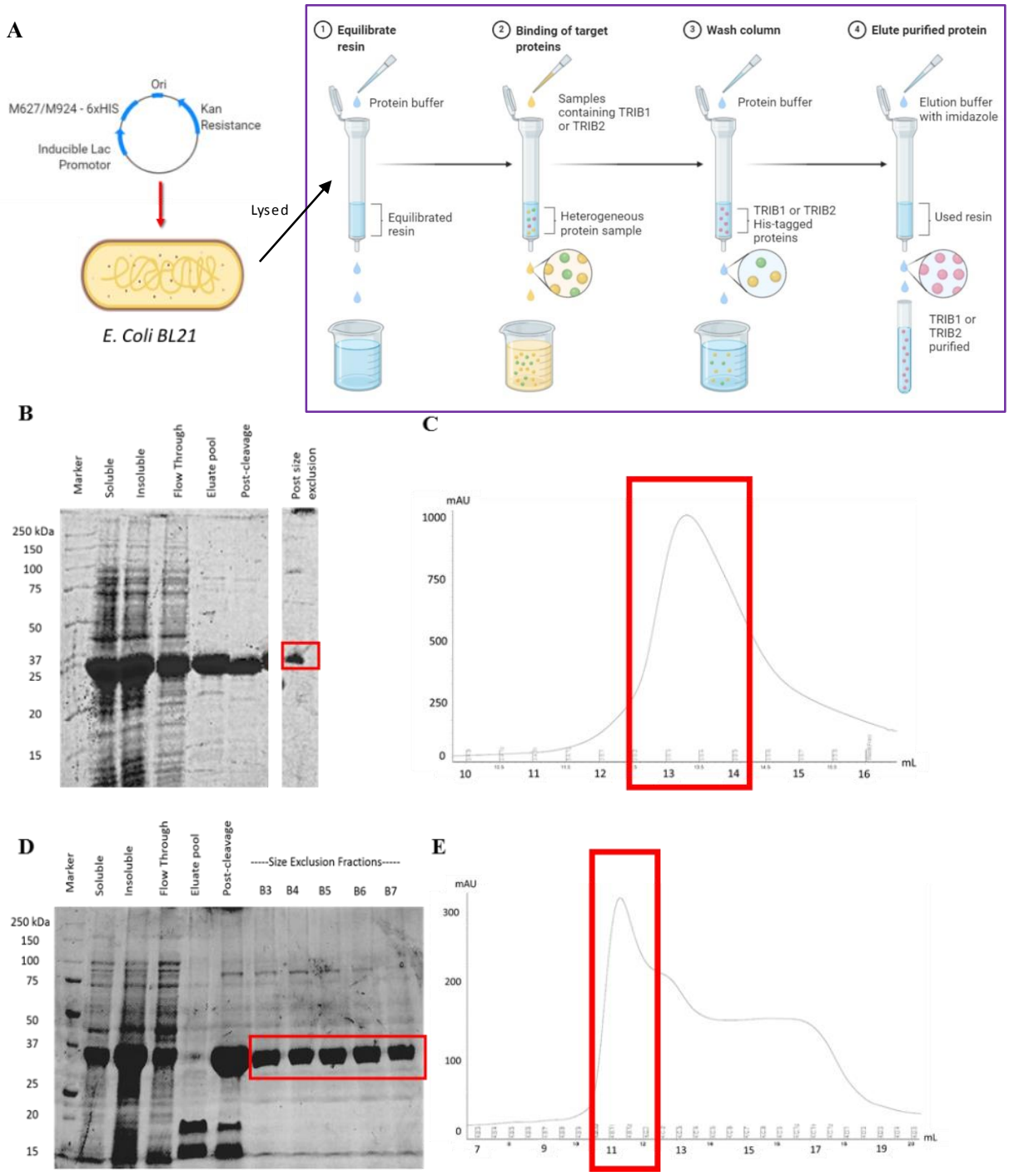

Figure 3.1: **Expression and purification of TRIB1 and TRIB2 from *E. coli* BL21**. **A.** Schematic made in BioRender of TRIB1/2 expressed in *E. coli*, which was followed by cell lysis and protein purification using Ni^{2+}-affinity chromatography, outlined by the purple box. **B**. SDS-PAGE gel showing TRIB1 (31.1 kDa) expression (soluble and insoluble fractions, eluate pool, post-cleavage of His_6-tag, post size exclusion pool fraction). **C.** Shows UV chromatography elution profile from a Superdex 200 (S200) SEC TRIB1 run, using post-cleavage TRIB1 proteins purified in A. **D.** SDS-PAGE gel showing TRIB2 (33.3 kDa) expression (soluble and insoluble fractions, eluate pool, post-cleavage of His_6-tag, post size exclusion fractions). **E.** Shows UV chromatography elution profile from an S200 SEC TRIB2 run, using post-cleavage TRIB2 proteins purified in C. Red boxes indicate purified TRIB proteins. SEC: size exclusion chromatography. mAU: milli absorbance unit.

3.2 Optimisation of yeast display system and flow cytometry methods.

3.2.1 The optimal Nb-induction of yeast clones under galactose is 24 hours.

To utilise the yeast display system in conjunction to flow cytometry as a tool for initial characterisation screening of TRIB1-Nbs, the period for optimal Nb-expression in Nb-yeast clones was investigated through a reverse time course induction experiment (t=24 hours, t=36 hours, t=48 hours; *Section 2.2.3.2)*. For this investigation, only the Nb2.011 clone was used. A timeline of the experiment is shown in *Figure 3.2.1.A, S. cerevesiae* was induced to express Nbs under galactose. This was followed by labelling the HA epitope tag on Nbs expressed by yeast, using an αHA-PE antibody as described in *Section 2.2.4.* The flow cytometry data were analysed using FlowJo 10.7.1, with PE histograms generated out of the yeast population, then gated for positive Nb-expressers (Nb-Pos) using a bisector tool (*Figure 3.2.1.B* and *Appendix A.1*) to gain a PE MFI and a percentage of Nb-Pos yeast population as described in *Section 2.2.5.* The raw data for PE MFI can be seen in *Appendix A.2*, whilst the data for the percentage population of Nb-Pos yeast can be seen in *Appendix A.3*. To see any significant changes within Nb expression in yeast, the percentage population of Nb-Pos yeast was normalised against unlabelled yeast controls – this minimised any background PE signal that was present. A one-way ANOVA with Dunnett's post hoc test performed for sets of induction data: Induction times (t=36 and t=48) were compared against 24 hours. PE MFI was used as a measure of the level of Nb expressed in yeast clones. Overall, no statistical significance ($p < 0.05$) was found in the PE MFI across the time points (refer to *Figure 3.2.1.C* and *Appendix 1.4*). However, there was a statistically significant drop found in the percentage population of Nb-Pos yeast between 24 hours and 48 hours of induction (p-value = 0.001, refer to *Figure 3.2.1.D* and *Appendix 1.5*). The level of Nb-PE fluorescence was relatively stable throughout the different induction times; however, the proportion of yeast population expression expressing Nbs drops as induction time increased.

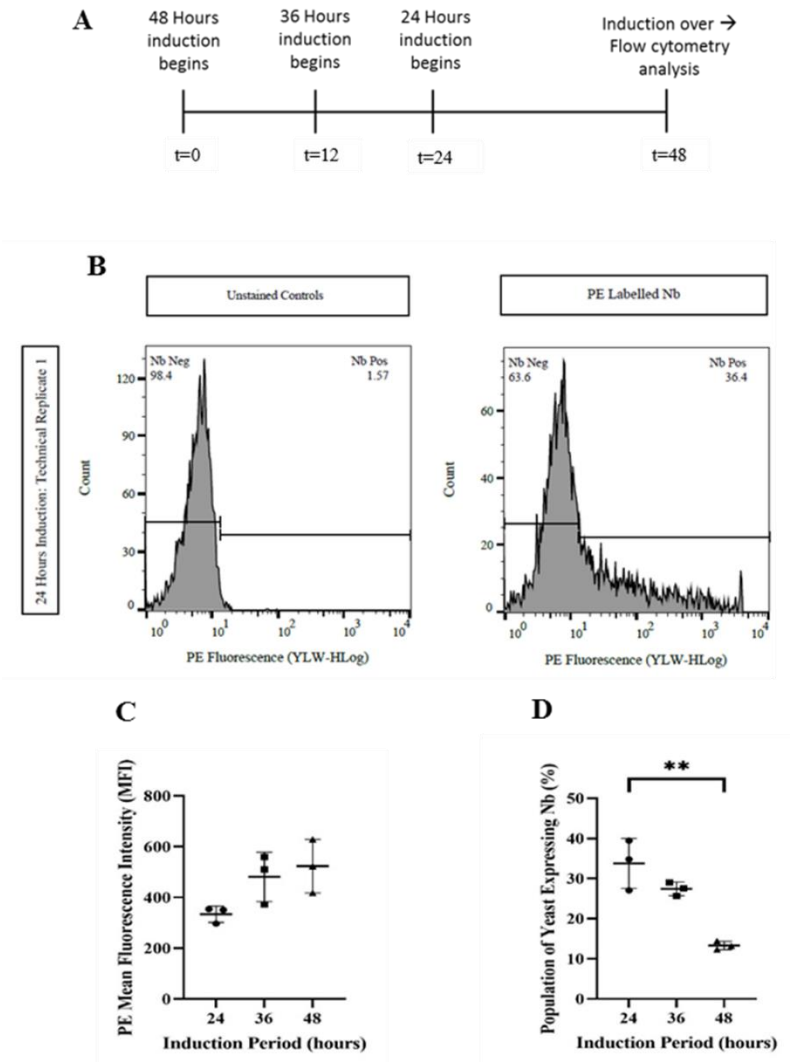

Figure 3.2.1: **Reverse time course induction of *S. cerevesiae* (yeast) Nb clones, under galactose-supplement pH 6 yeast media *(n=3).*** Nbs were labelled with αHA-PE before flow cytometry runs using Guava ExpressPlus. Column graphs with mean and standard deviation (SD) were generated using GraphPad Prism 8.4.3, with a one-way ANOVA with Dunnett post-hoc test performed to find significant difference *($p < 0.05$), ** ($p < 0.005$). **A.** A schematic of the reverse time course induction experiment performed for t=24 hours, t=36 hours and t=48 hours of induction. **B.** An example of bisector gating in FlowJo 10.7.1, for Nb-Pos population using an unlabelled yeast control, which was then applied to other samples for analysis. **C.** No significant difference is seen in overall Nb expression (PE MFI) on the surface of yeast between 24-48 hours of galactose induction. **D.** Population of Nb-expressing yeast decreased significantly between 24 and 48 hours of galactose induction. Nb: Nanobody. Nbs: Nanobodies. MFI: Mean fluorescence intensity.

3.2.2 Standard selection buffer is optimal for flow cytometry analysis.

To try and minimise potential affinity and specificity overestimation of TRIB1-Nbs investigated in this study, non-specific binding of labelled TRIB proteins to yeast had to be minimised. One of the limitations to using flow cytometry to characterise Nb affinity and specificity using a yeast surface display system is that it is highly dependent on the signal intensity of the fluorophores used to label the Nbs of interest and the protein of interest it targets. We must ensure that the fluorophores used, as an indicator of Nb binding to our target

protein, fluoresce at a level that generates a meaningful observation. As we use the FITC MFI to calculate the affinity of the Nbs, any changes to the MFI observed that is not due to true binding of our TRIB1-Nbs to TRIB1-FITC will skew our affinity calculations.

When yeast populations of induced and uninduced Nb-yeast clones (Nb5.018 – negative control, Nb2.012 – positive control, Nb2.038, Nb2.049, Nb2.066) was observed using flow cytometry, it was shown that TRIB1-FITC non-specifically bound to the surface of yeast (Q1 population, *Appendix B.1*). Consequently, uninduced yeast clones (Nb5.018 – negative control, Nb2.012 – positive control), were prepared for flow cytometry using the standard selection buffer and standard selection buffer supplemented by varying concentrations of detergents (TWEEN-20, CHAPS, and LMNG) and glycerol as described in *Section 2.2.3.2*, to see whether non-specific binding could be lowered. Flow cytometry data on Guava ExpressPlus (*Appendix B.2-3*) was processed using FlowJo, where a quadrant gate was applied to show the different yeast populations. A bisector gate was applied to the FITC histogram was used to determine the unlabelled yeast population (showing specific binding) against the yeast population non-specifically binding to TRIB1-FITC. A one-way ANOVA with Dunnett's post hoc test was performed on the TRIB1-FITC MFI of non-specific TRIB1 binding to yeast *(Appendix B.4)*, and on the percentage of yeast population non-specifically binding to yeast (*Appendix B.5*). Column graphs were generated using GraphPad Prism 8.4.3, with mean and SD shown (Nb 5.018 graphs see *Figure 3.2.2.A-B*, Nb 2.011 graphs see *Figure 3.2.2.C-D*). Results showed, that when using modified standard selection buffer compared to standard selection buffer, no significant reduction in the level (*Appendix B.6*) or percentage of yeast population (*Appendix B.7*) of non-specific binding of TRIB1-FITC to yeast was seen ($p < 0.05$). Similarly, any significant reduction in non-specific binding, for a supplemented selection buffer, that was not present across both Nb clones tested (Nb5.018 and Nb2.011) was reconsidered as being not significant overall. Consequently, it was determined that the standard selection buffer was already optimal for flow cytometry analysis of TRIB1 binding to TRIB1-Nbs.

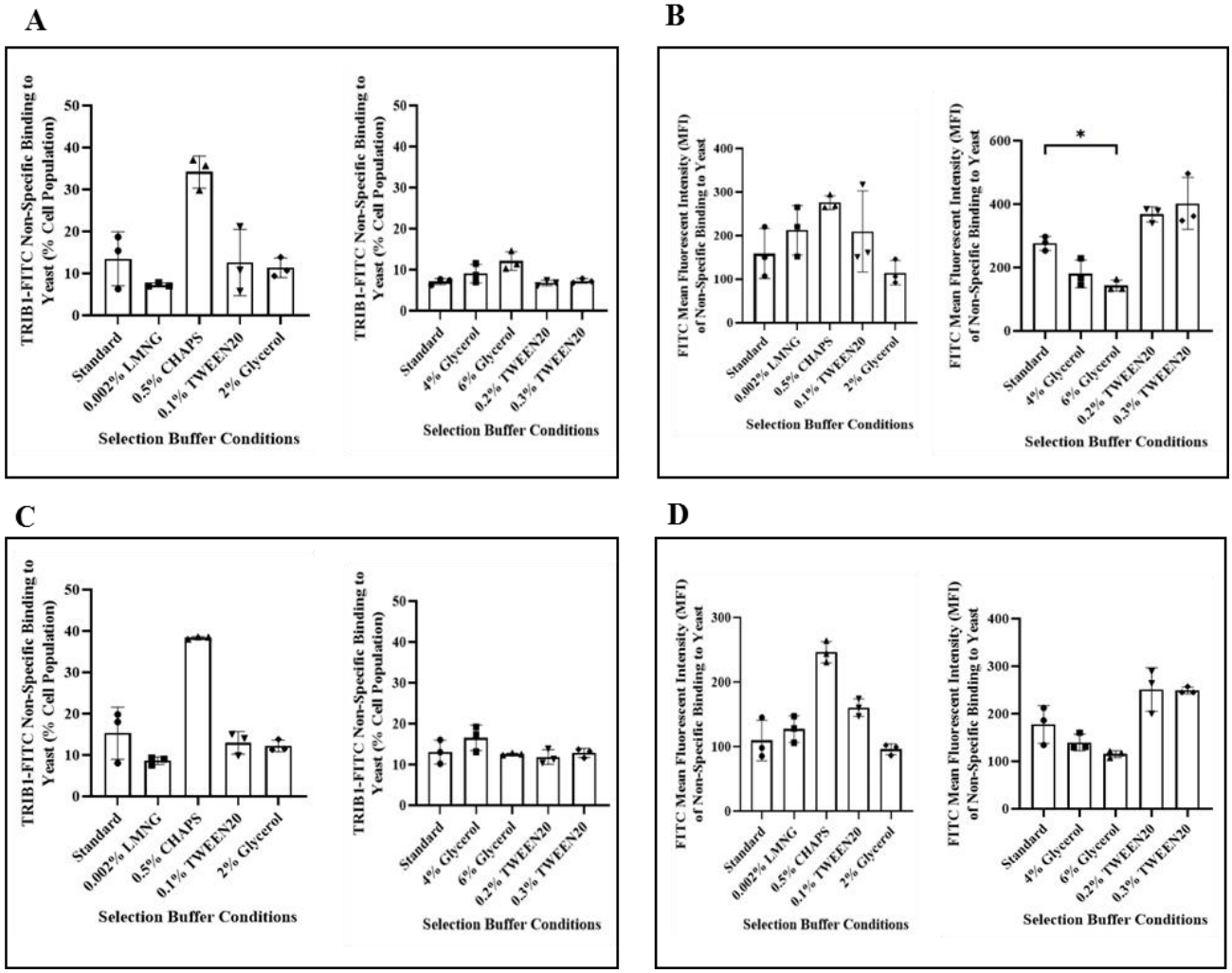

Figure 3.2.2: **Optimisation of selection buffer for flow cytometry analysis – standard selection buffer is optimal.** Uninduced Nb yeast clones (Nb5.018 and Nb2.011) was incubated with 480 nM of TRIB1-FITC, then analysed using Guava Express Plus. Flow cytometry data was gathered and processed using FlowJo 10.4.1. Column graphs were generated using GraphPad Prism 8.4.3, with mean and SD (*n=3*) showed with statistical significance shown * ($p < 0.05$). **A.** No significant difference was observed in Nb5.018 yeast population of yeast non-specifically binding TRIB1-FITC when standard selection buffer was modified by the addition of reagents. **B.** A significant difference in the level (MFI) of non-specific binding of yeast to TRIB1-FITC was seen in Nb5.018 yeast when standard selection buffer was supplemented 6% glycerol. However, this result was not translated over to Nb2.012 in D. **C.** No significant difference was observed in Nb2.011 yeast population of yeast non-specifically binding TRIB1-FITC when standard selection buffer was modified by the addition of reagents. **D.** No significant difference in the level (MFI) of non-specific binding of yeast to TRIB1-FITC was seen in Nb2.011 yeast when standard selection buffer was supplemented with reagents. Nb5.018: Nanobody yeast clone against an unrelated protein (negative control). Nb2.011: Nanobody yeast clone that is known to bind TRIB1 (positive control). MFI: Mean fluorescence intensity.

3.2.3 Compensation of FITC-PE spillover and gating of yeast populations.

It is known that FITC (green) fluorescence bleeds over into the PE (yellow) channel due to an overlap in their emission spectrum. Therefore, before any analysis could be done using PE and FITC fluorescence on flow cytometry data, FITC signalling must be compensated. Compensation of FITC to PE spillover was done using the compensation matrix in FlowJo. A

bisector gate was used to determine the threshold for FITC and PE signalling (*Figure 3.2.3.1.A*); the bisector gate was chosen as this would remove the likelihood of accounting any yeast cells into both negative and positive groups. This was followed by adjustment of the fluorescent readouts so that the FITC signal no longer resulted in a false-positive PE signal (*Figure 3.2.3.1.B*). Compensation of the FITC-PE spillover was recognised when the FITC only control of samples, no longer showed cells in Q2 and Q3 (*Figure 3.2.3.1.C*). Refer to *Appendix C* for example of compensation applied to all characterisation experiments in this study.

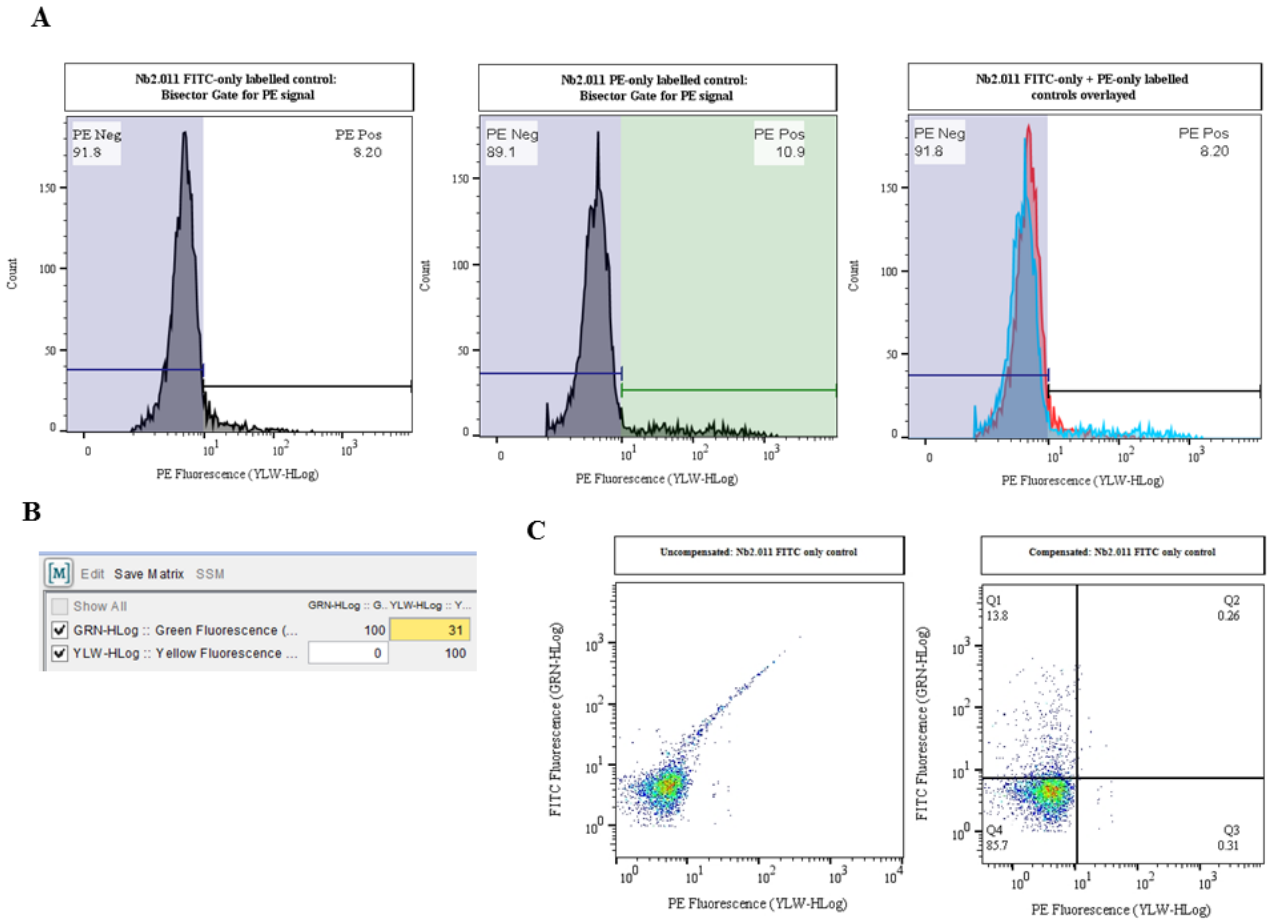

Figure 3.2.3.1: **Compensation of FITC-PE fluorescence spillover using FlowJo and Nb2.011 as an example. A**. An unlabelled control was used to determine the gate for FITC-negative and FITC-positive outcomes in the green fluorescence channel (GRN-HLog) using the bisector tool. FITC-positive population from the FITC-only control sample for Nb2.011 was then viewed for PE fluorescence in the yellow channel as a histogram to set a PE-negative gate using the bisector tool which was then transferred to Nb2.011 PE-only control. **B.** The compensation tool in FlowJo was then utilised to correct for FITC signalling bleeding into the PE channel, with the matrix edited manually to ensure more accurate compensation was applied to sample populations. **C.** With compensation applied, FITC-only control samples are expected to no longer show positive signalling in the PE channel as shown in the before and after dot plot of Nb2.011 FITC-only controls.

Once compensation of FITC-PE is done, flow cytometry data gained from characterisation experiments may be analysed using FlowJo (*Figure 3.2.3.2*). First, a polygon gating tool was used to select for the yeast population, removing readouts from debris and potential dead cells. The dot plot of side scatter (cell granularity) vs forward scatter (cell size) is then converted into a dot plot of PE (Nb) fluorescence vs FITC (TRIB1) fluorescence; a quadrant gate is used on negative control samples to be able to differentiate different yeast populations as shown in *Figure 3*. The dot plot is then converted into a PE histogram, where an unlabelled control is separated into non-Nb expressers (Nb Neg) and Nb Pos populations. The FITC MFI used to calculate TRIB1-Nb affinities is gained from the Nb Pos population.

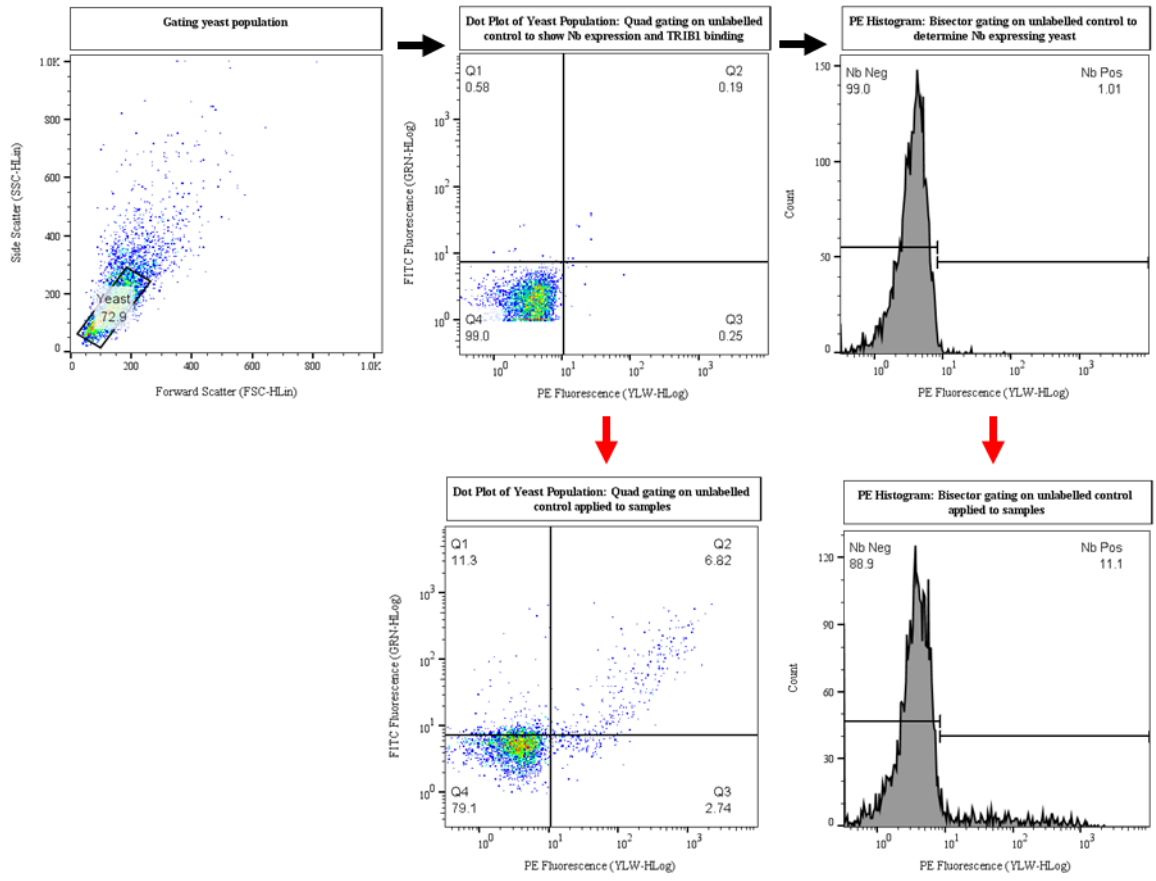

Figure 3.2.3.2: **Example of gating the yeast population to characterise TRIB1-Nbs.** Nb2.011 samples were used in this example. FlowJo 10.7.1 was used to first gate the yeast population from dead cells and debris. The yeast population was then graphed onto a dot plot of PE vs FITC fluorescence, where a quadrant gate was applied to show the different yeast populations. This was then converted into a PE histogram to gain FITC MFI of Nb Pos population: An unlabelled control was used to set a PE threshold using the bisector gating tool - this classified yeast cells as either Nb expressers (Nb Pos) or non-Nb expressers (Nb Neg). Red arrows indicate what application of the gates set with an unlabelled control looks like on labelled samples.

3.3 Affinity characterisation of TRIB1-Nbs.

Eight TRIB1-Nbs, previously screened as putative TRIB1 binders were studied based on sequence enrichment form the naïve library (*Table 2.1.2.2*). Yeast cells were cultured, induced, and prepared for flow cytometry as described in *Section 2.2.3.* The affinity of TRIB1-Nbs was measured by the FITC MFI of the Nb-Pos yeast population (Q1 and Q2, *Figure 3, Appendix D-H*). The raw data of MFI gathered using FlowJo 10.7.1 (Appendix I) was analysed using non-linear regression, one-site specific binding test, where a binding curve was generated for each profiled Nb (*Figure 3.3*). This calculated an equilibrium dissociation constant (K_D), where the value of the K_D is inversely proportional to the strength of the binding affinity that a ligand has to its target.

The initial affinity characterisation of TRIB1-Nbs was performed using eight titrations of TRIB1-FITC concentrations (0-480 nM). The maximum TRIB1-FITC concentration of 480 nM was chosen, as the non-specific binding of TRIB1-FITC to yeast increased by a large amount past this concentration, and the desired TRIB1-Nbs to use in future studies are those with low nM K_D. Results showed that most of the Nbs did not have a very high affinity to TRIB1 at the nanomolar range (*Table 3.3.1*). Three TRIB1-Nbs showed good binding against TRIB1 (Nb2.038, Nb2.049, and Nb2.066 – highlighted in *Table 3.3.1*) and was further tested for its affinity using 12 TRIB1-FITC concentrations (0-480 nM – 1 nM, 2 nM, 4 nM and 10 nM concentrations replaced the 7.5 nM titration) (*Appendix I.15*). By starting with lower concentrations of TRIB1-FITC, the non-linear regression curve able to be generated will be a more accurate representation of the binding kinetics between TRIB1-Nb with its target TRIB1. These Nbs were also tested again, within the same experiment, so that a more accurate K_D could be calculated using normalised data; where the FITC MFI of Nb5.018 is subtracted from the FITC MFI generated by TRIB1-Nb binding TRIB1-FITC to account for non-specific binding. However, the second trial of affinity characterisation using more TRIB1 dilutions showed that Nb2.038 *(Figure 3.3.2.A)*, Nb2.049 *(Figure 3.3.2.B)* and Nb2.066 *(Figure 3.3.2.C)* did not have a higher affinity to TRIB1 when compared to the positive control, Nb2.011.

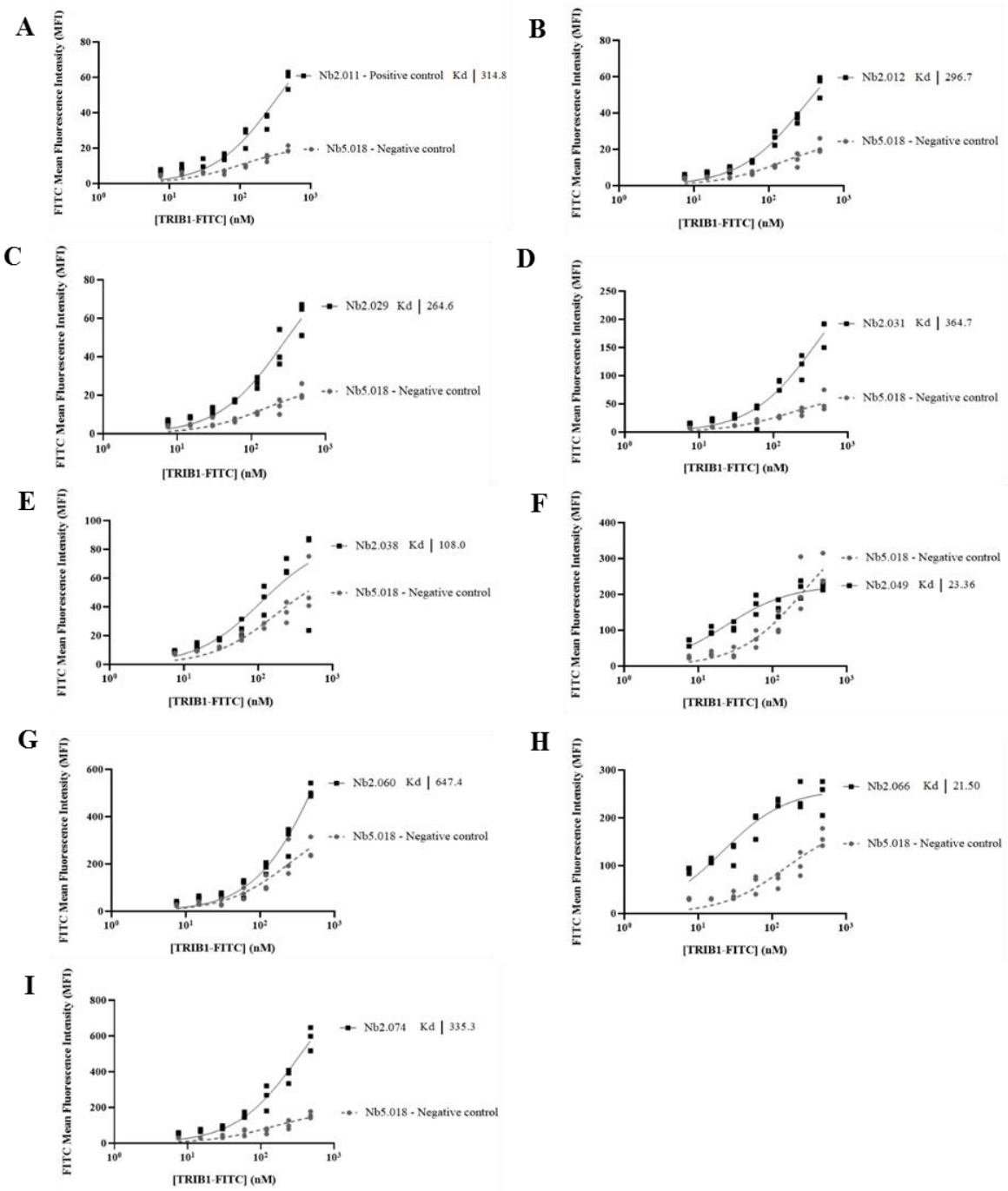

Figure 3.3.1: **Binding curves of TRIB1-Nbs against 8 TRIB1-FITC titrations (0-480 nM).** An affinity characterisation study using the yeast display system in conjunction with flow cytometry was performed on TRIB1-Nbs with 8 titrations of TRIB1-FITC. Each TRIB1-Nb binding study was carried out with the negative control, Nb5.018. Non-linear regression, one-site specific binding test (*n=3*) was done using GraphPad Prism 8.4.3. Each graph shows the non-linear regression curve, with each replicate shown apart from data at 0 nM of TRIB1-FITC due to the nature of a log scale. **A.** Nb.2.011 (positive control), **B.** Nb2.012, **C.** Nb2.029, **D.** Nb2.031, **E.** Nb2.038, **F.** Nb2.049, **G.** Nb2.060, **H.** Nb2.066, and **I.** Nb2.074. TRIB1 binding curve in Nb2.038 (E), Nb2.049 (F), and Nb2.066 (G) nice sigmoidal trend expected of a good binder; A second affinity characterisation trial was performed with 12 titrations of TRIB1-FITC.

Table 3.3.1: **Summary table of TRIB1-Nb affinity to TRIB1.**

	Kd (nM)	
Nanobody	**Best-Fit**	**95% CI (profile likelihood)**
2.011	315	183 to 604
2.012	297	205 to 451
2.029	265	164 to 455
2.031	365	213 to 714
2.038	108	50 to 242
2.049	23	15 to 36
2.060	647	380 to 1363
2.066	22	13 to 22
2.074	353	216 to 560

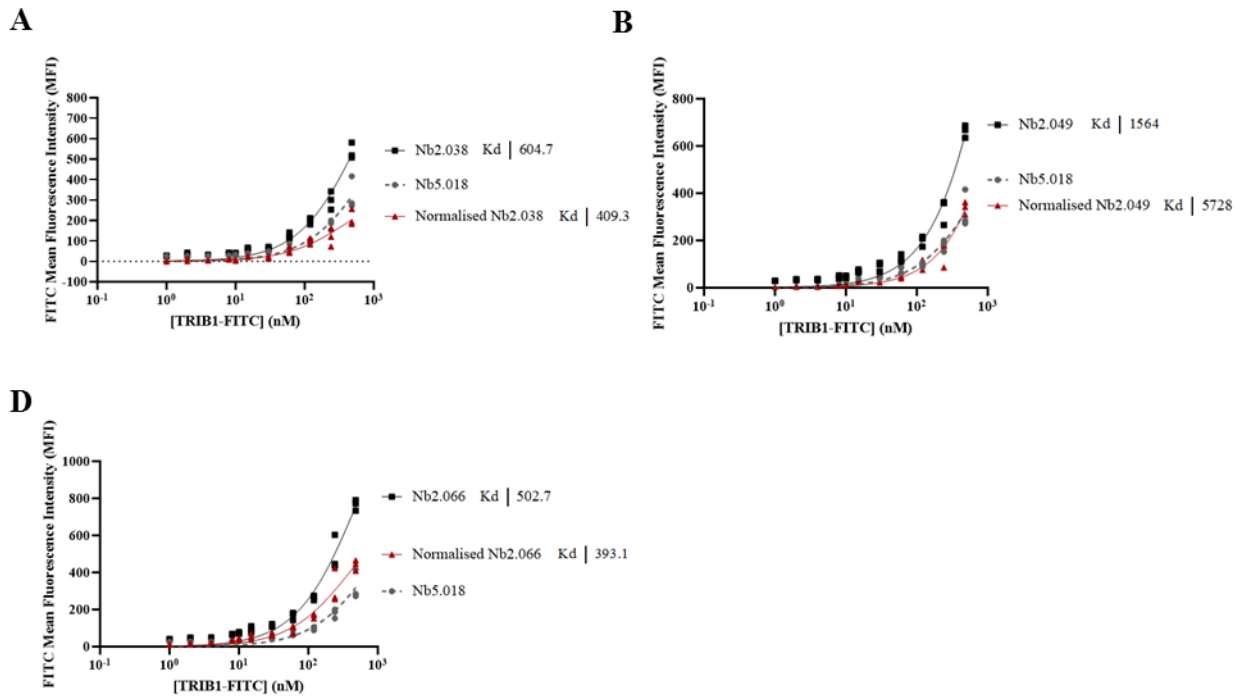

Figure 3.3.2: **Binding curves of TRIB1-Nbs against 12 TRIB1-FITC titrations (0-480 nM).** An affinity characterisation study using the yeast display system in conjunction with flow cytometry was performed on TRIB1-Nbs. Each TRIB1-Nb binding study was carried out with the negative control, Nb5.018. Non-linear regression, one-site specific binding test (*n=3*) was done on raw and normalised data using GraphPad Prism 8.4.3. FITC MFI of Nb5.018 binding TRIB1-FITC was subtracted from FITC MFI of TRIB1-Nbs tested, to account for non-specific binding. Each graph shows the non-linear regression curve, with each replicate shown apart from data at 0 nM of TRIB1-FITC due to the nature of a log scale. **A.** Nb2.038, **B.** Nb2.049, **C.** Nb2.066.

3.4 Specificity characterisation of TRIB1-Nbs over TRIB2.

Nanobodies are known to be highly conformationally selective, with minimal sequences. The ability of Nbs to have such high specificity against its target ligand makes it a promising tool to study specific TRIB homologue signalling pathways *in vitro,* as TRIB homologues show a high degree of homology. To investigate whether the TRIB1-Nbs studied were specific for TRIB1 over another TRIB homologue, TRIB2 (which shares ~70% sequence identity), a competition assay was done as described in *Section 2.2.4.2*. Due to time constraints, this specificity characterisation was limited to Nb2.038 and Nb2.066, alongside the negative and positive Nb controls (*n=3*). This assay allowed us to observe whether an unlabelled TRIB2 would be able to outcompete TRIB1-FITC binding to the TRIB1-Nbs: A decrease in FITC MFI then indicates a reduction in TRIB1-Nb binding to labelled TRIB1 and subsequently reduced specificity of TRIB1-Nb for TRIB1. Flow cytometry data was analysed using FlowJo 10.7.1 (*Appendix K.1*), where the raw data (FITC MFI, *Appendix K.3*) was analysed using a one-way ANOVA test with Dunnett's post hoc, to show whether there were any significant TRIB1-FITC MFI changes of samples with 200 nM TRIB1-FITC and 0 nM TRIB2 when compared to samples with fixed TRIB1-FITC concentration (200 nM) and increasing molar ratio concentrations of TRIB2. A column graph was generated to show the results of the competition assay, where each replicate was shown with the mean and standard deviation (SD) (*Figure 3.4.1.A*). Results showed that there were no significant changes ($p < 0.05$) seen in the intensity of FITC signalling (*Appendix K.4*).

To see whether the TRIB1-Nbs tested and the positive control Nb could have bound to TRIB2 due to the sequence homology, a shallow binding affinity test was executed where induced yeast clones were incubated with 200 nM of TRIB2-FITC. The FITC MFI of TRIB2 binding to TRIB1-Nbs when compared to the negative control, Nb5.018 *(Figure 3.4.1.B),* showed that Nb2.011, Nb2.038 and Nb2.066 did bind TRIB2 (but this needs to be further investigated as it could have been caused by non-specific binding seen with TRIB1). Overall, the specificity assays carried out for the three TRIB1 Nbs suggests that the two TRIB1-Nbs tested plus the positive control, Nb2.011, were specific for TRIB1 over TRIB2 despite the high sequence homology that exists between the two proteins.

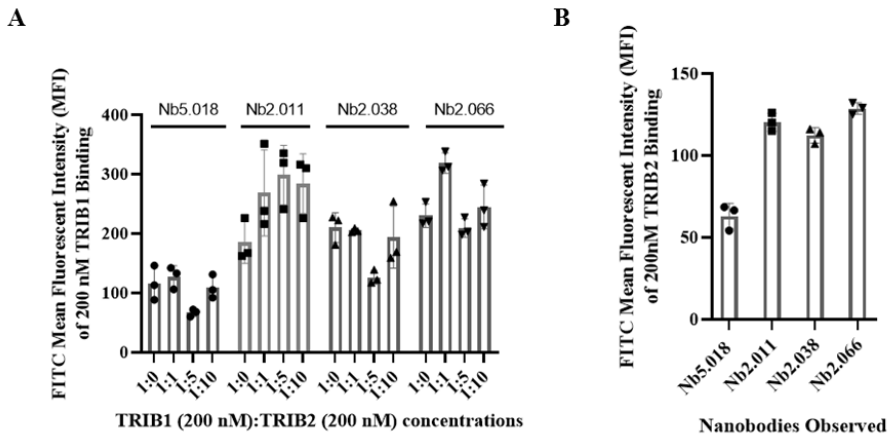

Figure 3.4.1: **Competition assay to determine the specificity of 3 TRIB1-Nbs over TRIB2, which shares ~70% sequence identity.** The competition assay (*n*=3) was done using a yeast display system, where Nbs expressed on the surface of the yeast cell wall was incubated with a set concentration of TRIB1-FITC with a fold increased molar concentration of unlabelled TRIB2: e.g. 1:5 of TRIB1: TRIB2 means 200 nM of TRIB1 with 2 µM of TRIB2. **A.** Shows column graph with mean, standard deviation (SD) and each replicate data shown. No statistical significance was seen between 1:0 molar concentrations of TRIB1 to TRIB2 and TRIB1 with 1x/5x/1x TRIB2 concentration. Nb2.011, Nb2.038 and Nb2.066 are specific for TRIB1 over TRIB2. **B.** Shows graph of FITC MFI of 200 nM TRIB2-FITC binding to TRIB1-Nb. Compared to negative control binder, Nb5.018, Nb2.011, Nb2.038 and Nb2.066 shows some binding to TRIB1.

4. Discussion

TRIB studies have made observations where it has contradictory roles in cancer pathogenesis. With its role as an adaptor protein, TRIB proteins associate with many substrates to regulate signalling pathways such as the C/EBPα, MEK and Akt pathways related to cell differentiation, growth, and survival. TRIB proteins, therefore, exist in a heterogeneous fashion, where its multiple transient complexes allow it to modulate varying signalling pathways in either inhibitory or stimulatory manner. Studying one aspect of TRIB signalling and how it consequently results in disease when dysregulated, is hard without an efficient research tool that can stabilise its selective conformations. TRIB-specific Nbs may potentiate further human TRIB studies and reduce the gap in knowledge for understanding the contradictory roles of TRIB as a tumour suppressor and an oncogenic factor in diseased states. This study used a yeast display system with flow cytometry and aimed to characterise the affinity and specificity of TRIB1-Nbs. The results of the TRIB1-Nb characterisation study will be discussed, as well as whether the use of the yeast display system with flow cytometry is efficient for the initial characterisation screen of selected TRIB-Nbs from a Nb-library, for the initial discovery pipeline.

4.1 Optimisation of yeast display system and flow cytometry methods.

4.1.1 The optimal Nb-induction of yeast clones under galactose is 24 hours.

In order to investigate the affinity and specificity of TRIB1-Nbs using the yeast display system created by the McMahon Group, Nbs had to be adequately expressed on the surface of the yeast clones to gain reasonable data for analysis. Previously, in the development of the McMahon Nb-yeast display system, an N-terminal engineered mating factor α preprotein was added to enhance the yeast expression of synthetic Nbs (McMahon *et al.,* 2018): They observed that Nb expression levels were optimal between 48-72 hours of induction under galactose. However, a similar yeast display system created by the Uchański group saw that an overnight induction under galactose was sufficient to generate ~60% of the total yeast population to display their Nbs (Uchański *et al*., 2019). Subsequently, we first wanted to observe whether our TRIB1-Nb yeast clones were able to generate the same level of expression and at what induction time was the most optimal to execute for this study through the execution of reverse time course induction.

Our findings (*Section 3.2.1*) showed that 24 hours was the optimal induction time for our yeast clones, with roughly 30% of the total yeast population expressing Nbs (*Figure 3.2.1.D*).

The expression of Nbs within the total population of Nb2.011 clones, being roughly half of what we expected based on previous literature (Uchański *et al*., 2019), may be explained by any residual glucose present strongly repressing the expression of GAL1-induced genes until a later time at which glucose levels in cells are low enough to release repression (Weinhandl *et al*., 2014). It may also be explained by our PE labelling showing depletion, as indicated by a spike in amplitude at high PE fluorescence (*Figure 3.2.1.B*): This suggests an underestimation of the level of Nb expressed by our yeast population. To overcome this, a more concentrated αHA-PE labelling of our antibody could have been done than just a 1 in 10 dilution (*Section 2.2.4*). However, this was not executed as the concentration of αHA-PE was already double than initially planned and depletion of our PE label was still observed.

Unlike the McMahon group who observed better Nb-expression at 48 hours of induction, we observed that with increasing induction time, the total population of yeast expressing Nbs decreased from ~35% at 24 hours of induction, to ~10% at 48 hours of induction, but the level of PE MFI (an indicator of overall Nb expression) did not significantly increase/decrease over time (*Figure 3.2.1.C*). Growth of yeast culture under galactose, leading to an increase of total yeast population that decreased the ratio of Nb-Pos yeast, cannot explain this observation. Yeast growth occurs at a minimum in the condition of galactose with pH 6 yeast media that was used for induction. Galactose metabolism in yeast requires a high level of energy diverted into producing GAL enzymes (Stockwell *et al*., 2015) and, *S. cerevesiae* is an acidophilic organism that better grows in lower pH media (Peña *et al*., 2015) that does not require the diversion of energy into maintaining optimal pH environment for enzymes and transport proteins associated with growth (Narendranath and Power, 2005). Since our Nb expression was controlled under the GAL1 promoter, reducing levels of galactose in our culture over 48 hours could have been the reason why we observed a very significant decrease in the number of Nb2.011 yeast cells expressing Nbs ($p = 0.001$) without seeing a change to the level of Nb expression in individual yeast cells, when compared to 24 hours of induction. Expression of GAL1 genes requires sufficient displacement of Gal80 proteins that represses the DNA-binding target protein of the GAL1 promoter, Gal4 (Johnston, 1987; Weinhandl *et al*., 2014). Without adequate removal of Gal80 repression of Gal4 by the inducer (Gal3p activated by galactose) (Stockwell *et al*., 2015), there would not have been continued, high induction of Nb expression in the total yeast population. This may be in conjunction to a build-up of waste metabolites and starvation over a 48-hour period, which may have resulted in yeast cells reverting to a

survival mode which restricted our recombinant protein expression (Petti *et al.*, 2011): Starvation leads to a metabolic change in yeast where genes related to translation is repressed and degradation of non-essential proteins increases.

4.1.2 Optimisation of selection buffer.

The characterisation of Nbs with the use of a yeast display system in conjunction with flow cytometry is very much dependent on the level of fluorescence seen in the fluorophores used and how it affects the resulting MFI which is used for analysis. Any non-specific binding of our TRIB1-Nbs to uninduced Nb-yeast clones could have potentially led to an overestimation of affinity/specificity of our tested *TRIB*1-Nbs with induced yeast clones and Nb labelling. We had observed consistent non-specific binding of TRIB1-FITC to uninduced and induced Nb-yeast clones (*Appendix B.1*). Hence, we attempted to optimise our standard selection buffer by addition of reagents (LMNG, CHAPS, TWEEN-20, and glycerol) that are typically used to minimise non-specific binding of proteins. The detergents used to supplement our selection buffer were chosen for the following reason; the zwitterionic CHAPS, non-ionic TWEEN-20 (Johnson, 2013), and integral membrane protein stabiliser, LMNG (used to enrich Nb5.018) (Chae *et al*., 2010), are reported to not compromise the integrity of proteins of interest and their protein-protein interactions studied using flow cytometry. Due to the presence of a phenyl ring in TWEEN-20, it can absorb UV light at ~280 nm (Johnson, 2013), and although this would not have any effects on our flow cytometry reading due to the excitation/emission wavelengths of the fluorophores used in this study (*Table 2.1.6.1*), additional wash steps with standard selection buffer executed (*Section 2.2.3.2*) to remove the detergent as a precaution. The addition of glycerol to standard selection buffer was also tested, to see whether increased suspension of yeast cells and TRIB1/2 proteins used in this study, would minimise the contact between TRIB1/2 proteins and the unrelated yeast surface: Previously, the Mace lab had observed that recombinant TRIB proteins behaved better in selection buffer containing glycerol.

Our results (*Section 3.2.2*) showed that in both our positive (Nb2.011) and negative (Nb5.018) control Nb-yeast clones, our modification of selection buffer had no significant effects in reducing the observed non-specific binding. Although the addition of 0.5% CHAPS was seen to significantly change non-specific binding ($p < 0.0001$), it was not the desired reduction but an increase that was observed. This may have resulted from the high concentration used, causing its aggregation and affecting the binding of TRIB1-FITC non-

specifically to yeast, and/or it also binding to hydrophobic regions of yeast surface proteins and being detected during flow cytometry analysis. Similarly, to CHAPS, any significant changes observed using modified selection buffer, which increased non-specific binding was ignored (*Appendix B.6-7*). Although glycerol at 6% did result in a significant decrease of TRIB1-FITC non-specifically binding to yeast Nb5.018 ($p = 0.0143$, *Appendix B.7*), a similar observation was not seen in yeast Nb2.011. Consequently, the use of selection buffer with 6% glycerol was not implemented, as this data implied that the level of non-specific binding varies across yeast clones and experiments: This indicated that modification to the standard selection buffer would have little to no significant effects in minimising non-specific binding. Instead, non-specific binding could be accounted for, post-flow cytometry analysis, by subtracting the mean MFI of Nb5.018 (negative binding control) from the MFI data of tested TRIB1-Nbs (Uchański *et al.*, 2019): This, however, was dependent on there being similar induction seen between the negative control yeast clone and tested yeast clones, as well as consistent non-specific binding across the yeast clones.

4.2 Characterisation of TRIB1-Nbs.

4.2.1 TRIB1-Nb affinity found suggested further library screening.

As previously mentioned, the yeast display system has been characterised as a tool for the rapid discovery of Nbs to POIs. TRIB1-Nbs were initially pooled from an existing Nb library by rounds of MACs selection against decreasing concentration of TRIB1 proteins into the nanomolar range. Positive TRIB1 binding population were enriched, followed by next generation sequencing of individual clones of recombinant yeast. The top 8 TRIB1-Nbs that were enriched, were chosen to be tested in this research project. By using the initial K_D estimates calculated from flow cytometry, it is possible to further identify the best binding candidates from the TRIB1-Nb library, to be taken into later stages of development. We implemented the yeast display system in conjunction with flow cytometry, to observe whether this method worked to streamline the affinity characterisation of TRIB1-Nbs in this study - potentially reducing the time needed for the initial Nb discovery in the development pipeline.

First, the affinity characterisation result for Nb2.011 was compared to the isothermal titration calorimetry (ITC) assay result of free Nb2.011 co-eluted with TRIB1 (another method for determining protein-protein interactions). Our results showed that Nb2.011 had ~315 nM (*Table 3.3.1*) affinity to TRIB1, which was comparable to the ITC result, which was 366 nM

(Mace Lab, unpublished data). This showed proof that affinity characterisation using the yeast display system and flow cytometry (a more rapid approach than ITC), could garner an affinity approximation that is close to the actual affinity value. The yeast display system was validated as a tool to characterise the 8 chosen TRIB1-Nbs. Although we did not see saturation in the binding between TRIB1-Nbs and TRIB1 proteins (*Figure 3.3.2*), as an initial affinity screening for high affinity binders, it was deemed unnecessary to increase the range of TRIB1 concentrations; a non-saturated binding curve with a highest TRIB1 concentration of 480 nM, would suggest that the TRIB1-Nb K_D is higher than the calculated value (low affinity), which is undesirable.

Second, initial affinity screening of TRIB1-Nbs using 8 titrations of TRIB1-FITC concentrations (nM; 0, 7.5, 15, 30, 60, 120, 240, 480), showed three potential high-affinity candidates (Nb2.038, Nb2.049, and Nb2.066) with affinities that were calculated to be higher than the positive control Nb2.011 (*Table 3.3.1*). These Nbs were then characterised using ITC, but results showed that, although they did show binding to TRIB1 proteins, it was at a lower affinity than the flow cytometry data suggested (Mace Lab, unpublished data). This led to a second affinity screening of the 3 candidates (Nb2.038, Nb2.049, and Nb2.066) using 12 titrations of TRIB1-FITC concentrations (nM: 0, 1, 2, 4, 8, 10, 15, 30, 60, 120, 240, 480). The results of the second affinity screening showed that the three (initially) promising Nbs were not actually better TRIB1 binders when compared to Nb2.011 (*Figure 3.3.2)*. This may be due to the use of lower TRIB1-FITC titrations which would make the fit of the overall binding curve and calculated K_D closer to the actual value. Also, with the second affinity screening, we were able to subtract the mean FITC MFI from the Nb5.018 data, to account for the non-specific binding of TRIB1 to yeast cells. In the first affinity screening, the mean FITC MFI values for Nb5.018 (negative controls) were too high to subtract with, when compared to the FITC MFI of TRIB1-Nbs tested; generating negative values that could not be used to calculate a K_D. Hence, the second affinity screening may have successfully accounted for the non-specific binding that may have resulted in the overestimation of TRIB1-affinity seen in the first affinity screening.

Our TRIB1-Nb affinity characterisation study showed that none of the 8 Nbs tested from the TRIB1-Nb library were better TRIB1 binders than Nb2.011. The TRIB1-Nb library used in this study was from one of the initial implementations of the McMahon method by the Mace lab. This would have limited the ability to reduce the initial Nb library down to potential

high-affinity TRIB1-Nbs. In future, starting at a lower concentration than 480 nM of TRIB1, (where we observed a higher degree of non-selective binding) may be beneficial as it would select for TRIB1-Nbs without confounding from non-selective binding. Also, stringent selection using much lower concentrations of TRIB1 would have selected for better TRIB1-binders to test. In literature, selection of Nbs from a naïve library using picomolar concentrations of their proteins of interests, yielded better affinity screening results using the yeast display system and flow cytometry (McMahon *et al*., 2018; Uchański *et al*., 2019). Since the initial use of the McMahon method, the execution should be better known, and another screening of TRIB1-Nbs from the McMahon Nb library is suggested in future for the discovery of better TRIB1-Nbs.

4.2.2 TRIB1-Nb specificity over TRIB2 attributed to inherent Nb conformation.

Although none of the tested *TRIB*1-Nbs in this study showed higher affinities to TRIB1 when compared to Nb2.011, the TRIB1-Nbs tested for TRIB1 specificity did show preferential binding to TRIB1 over the TRIB2 homologue (*Section 3.4*). The TRIB1-Nbs used in this study, despite only comprising of ~100 amino acid sequence and showing differences within only small sequence portions of their complementary determining region (CDR) loops (*Figure 4.2.2.1*), managed to show variable TRIB1 affinity but showed similar specificity profiles to TRIB1 over TRIB2 (*Figure 3.4.1.A*). The targeted sites of the TRIB1-Nbs studied in this project were, however, unknown. The specificity profile seen, may be explained by the inherent Nb characteristics, which allows it to have a high degree of specificity despite its relatively short sequence, and hence a short paratope. In future it may be of interest, to study whether small sequence variance in TRIB1-Nbs' CDR loops, result in it targeting different sites along the TRIB1 protein and if they were to target similar sites, whether their affinities/specificities are similar or different.

Point mutations in camelid Vhh's occur more frequently within or in proximation of the paratope regions that have significance in determining Nb structural loops/conformation (Kunik *et al*., 2012; Nguyen *et al*., 2000; Sela-Culang *et al*., 2013). Consequently, unlike the high sequence variance in framework regions or CDR loops seen in conventional antibodies, it is theorised that Nb specificity to bind antigens is dependent on the increased structural diversity in their CDR loops (in particular, the lengthened CDR3) in the Vhh (Mitchell and Colwell, 2018; Nguyen *et al*., 2000). The absence of the light chain may have resulted in the

evolved nature of VHH in nanobodies to be specific for novel paratopes (Nguyen *et al.*, 2000). Little changes to the Nb sequence, can result in a different conformational state that is able to exploit different epitopes compared to conventional antibodies which require higher variability to gain the same result (Mitchell and Colwell, 2018).

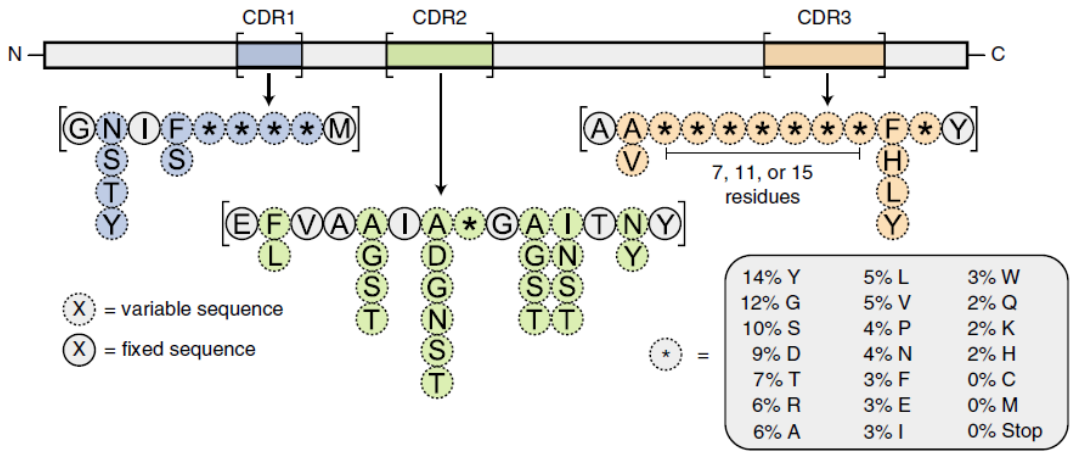

Figure 4.2.2.1: **The construction of synthetic Nbs using the McMahon method.** This schematic was obtained from (McMahon *et al.*, 2018). The complementary determining (CDR) loops that have been studied to determine the affinity and specificity of Nbs to its target, were modified to result in a range of Nbs with different characteristics. Dotted lines show the CDR amino acid residues that may differ across the Nbs used in this study. The Nb framework regions in grey, were kept the same across all Nbs used in this study. Nbs: Nanobodies.

4.3 Future Directions

Overall, this study had shown that the yeast display system previously developed by the McMahon group to rapidly discover GPCR Nbs, could be implemented for the rapid discovery of TRIB1-Nbs (also suggested for TRIB2 and TRIB3). Compensation is necessary for flow cytometry when fluorophores have overlapping emission spectrums. We had successfully overcome compensation of our FITC and PE channels (*Section 3.2.3*); however, it is noted that our FITC signal at our highest concentration of TRIB1-FITC (480 nm) was not as high as we had expected it to be and therefore, compensation may not have been executed evenly between experiments. To overcome this compensation issue, future studies for the characterisation of TRIB-specific Nbs may be improved through the use of fluorescent beads for more accurate flow cytometry compensation of FITC spill-over into the PE channel, or through the use of a different labelling methodology that utilises fluorophores without overlapping spectrums. Also, another labelling system should be used for the Nbs expressed on the surface of yeast cells, so that no depletion of our PE labelling is observed like within this study, (as mentioned in *Section 4.1.1*). One such labelling that could be implemented for visualising Nb expression would be CoA-547 which was shown to be effective by the

Uchański group (Uchański *et al*., 2019). Furthermore, future specificity trials using the yeast display system could be expanded by using a positive TRIB2-Nb control (tested against TRIB1) for comparison of TRIB1-Nbs, as well as using positive control of unlabelled TRIB1 against labelled TRIB2 proteins: If TRIB1-Nbs were specific against TRIB1 proteins, you would expect near 100% blocking of TRIB2 binding to TRIB1-Nbs.

By implementing the changes mentioned above, it may be possible to develop TRIB-specific Nbs with high affinities, for the use of future *in vitro* study. Although Nbs are highly soluble in aqueous solutions, it cannot spontaneously pass through the plasma membrane to reach its target *in vitro* (Desmyter *et al*., 2015; Hassanzadeh-Ghassabeh *et al*., 2013). However, modifications like the addition of cyclic arginine-rich peptides can facilitate cellular internalisation of Nbs for *in vitro* research (Herce *et al*., 2017). In the far future, when high-affinity TRIB-Nbs has been developed and verified, Nb modification could mean facilitation of complex TRIB-signalling studies for diseases and the development of new and specific therapeutics associated with it.

Being able to study the inhibition/destabilisation/degradation of TRIB proteins can give a platform for the development of therapeutics that target the same sites as TRIB specific Nbs to induce the same beneficial response. Nanobodies can be utilised to control protein expression through degradative means for studies and discovery of new therapeutics**.** Genetic protein inactivation occurs over a period that is ineffective for therapeutic purposes. Therefore, the use of small protein inhibitors is more common in developing new therapeutics where minimising protein expression is necessary to mitigate the development of a disease. However, small protein inhibitors have low accuracy to protein targets which lead to off-target effects. The deGradFP technology consists of an F box protein called Slmb (derived from *Drosophila melanogaster*) fused to a Nb fragment (VhhGFP4), which can elicit significant target protein degradation through cullin E3 ligase recruitment, see *Figure 4.3.1*, (Caussinus *et al*., 2012; Yamaguchi *et al*., 2019): Protein degradation through this method is observed through the decrease in green fluorescence.

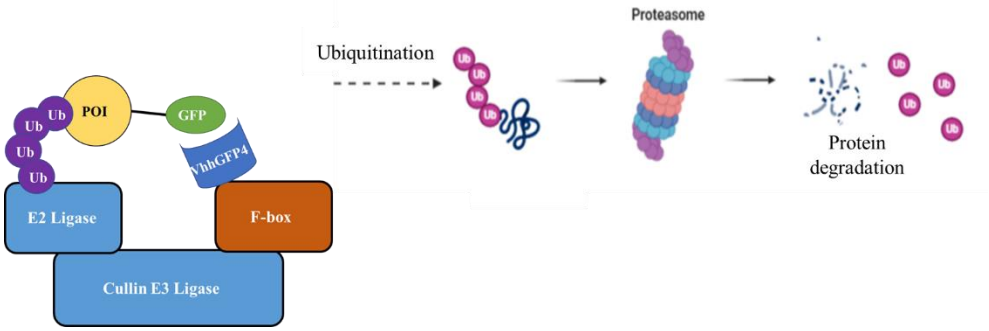

Figure 4.3.1: **Nb-protein degradation system.** deGradFP schematic adapted from (Yamaguchi et al., 2019) showing VhhGFP4 Nb fragment (dark blue) bound to F-box protein (burnt orange) which can recruit the cullin-RING ubiquitin (Ub) ligase (simply represented by E3 and E2 ligases in light blue), that facilitates K48 ubiquitination of GFP-POI (protein of interest) in drosophila flies. Figure made using BioRender.

Transgenic *drosophila* flies, expressing the Nb-Slmb fusion, illustrated the specificity of this degrading system, as it caused no deleterious, off-target effects to the development of fly embryos into adulthood (Caussinus *et al*., 2012). The deGradFP method can be further refined, by fusing auxin-inducible degron (AID) to the Nb fragment instead of an F-box protein, thereby requiring auxin binding for the recruitment of Cullin E3 ligase (Daniel *et al*., 2018): This exploits Nb selectivity toward target proteins to facilitate conditional protein degradation, allowing for temporal functional studies of proteins in cell development, growth, and repair (Daniel *et al*., 2018). For proteins that are linked with regulation of cell growth and differentiation (e.g. TRIB proteins), AID-Nb and deGradFP technology may be the way to learning/validating its functional role in specific cells at specific stages of growth, and how increased TRIB1/2/3 degradation may affect the pathogenesis of certain diseases to give an insight of possible therapeutic approaches.

4.4 Conclusion

In conclusion, this study was successful in determining whether the yeast display system, in conjunction with flow cytometry, is capable of being used as a tool for the rapid characterisation of TRIB1-Nbs. Although no new TRIB1-Nbs were discovered to be a better binder than the known TRIB1-binder (Nb2.011), this study did reveal important aspects of this method that could be accounted for/improved upon for TRIB-Nb characterisation in the future. It is important to consider the present non-specific binding between TRIB proteins to yeast, as this characterisation method was dependent on fluorophores intensity (for detecting Nb expression and TRIB1 binders) to generate MFI for analysis. This study was able to show

that the approximated TRIB1-Nb characteristics (affinity and specificity), observed using the yeast display method, was comparable to ITC. Hence, as an initial step in the discovery pipeline of TRIB-specific Nbs, this method was sufficient in screening the affinity and specificity characteristics of the tested TRIB1-Nbs in this study. Furthermore, this method may prove to be invaluable in speeding up the Nb discovery process of all human TRIB homologues from a naïve Nb-library, by allowing rapid, initial characterisation screens. This can narrow down the number of potential Nbs into a smaller Nb panel with desirable K_D estimates and specificity, to be taken into the next steps of the discovery pipeline.

References

Aimé, P., Sun, X., Zareen, N., Rao, A., Berman, Z., Volpicelli-Daley, L., Bernd, P., Crary, J.F., Levy, O.A., and Greene, L.A. (2015). Trib3 is elevated in Parkinson's Disease and mediates death in Parkinson's Disease models. Journal of Neuroscience *35*, 10731-10749.

Bailey, F.P., Byrne, D.P., Oruganty, K., Eyers, C.E., Novotny, C.J., Shokat, K.M., Kannan, N., and Eyers, P.A. (2015). The Tribbles 2 (TRB2) pseudokinase binds to ATP and autophosphorylates in a metal-independent manner. Biochemistry Journal *467*, 47-62.

Caussinus, E., Kanca, O., and Affolter, M. (2012). Fluorescent fusion protein knockout mediated by anti-GFP nanobody. Nature Structural & Molecular Biology *19*, 117-121.

Chae, P.S., Rasmussen, S.G., Rana, R.R., Gotfryd, K., Chandra, R., Goren, M.A., Kruse, A.C., Nurva, S., Loland, C.J., Pierre, Y.,*et al.* (2010). Maltose-neopentyl glycol (MNG) amphiphiles for solubilization, stabilization and crystallization of membrane proteins. Nature Methods *7*, 1003-1008.

Chen, Y., Wu, Y.-r., Yang, H.-y., Li, X.-z., Jie, M.-m., Hu, C.-j., Wu, Y.-y., Yang, S.-m., and Yang, Y.-b. (2018). Prolyl isomerase Pin1: a promoter of cancer and a target for therapy. Cell Death & Disease *9*, 883.

Daniel, K., Icha, J., Horenburg, C., Müller, D., Norden, C., and Mansfeld, J. (2018). Conditional control of fluorescent protein degradation by an auxin-dependent nanobody. Nature Communications *9*, 3297.

Dedhia, P.H., Keeshan, K., Uljon, S., Xu, L., Vega, M.E., Shestova, O., Zaks-Zilberman, M., Romany, C., Blacklow, S.C., and Pear, W.S. (2010). Differential ability of Tribbles family members to promote degradation of C/EBPalpha and induce acute myelogenous leukemia. Blood *116*, 1321-1328.

Desmyter, A., Spinelli, S., Roussel, A., and Cambillau, C. (2015). Camelid nanobodies: killing two birds with one stone. Curr Opin Struct Biol *32*, 1-8.

Eyers, Patrick A. (2015). TRIBBLES: A Twist in the Pseudokinase Tail. Structure *23*, 1974-1976.

Eyers, P.A., Keeshan, K., and Kannan, N. (2017). Tribbles in the 21st Century: The evolving roles of Tribbles Pseudokinases in biology and disease. Trends in Cell Biology *27*, 284-298.

Feldhaus, M.J., Siegel, R.W., Opresko, L.K., Coleman, J.R., Feldhaus, J.M.W., Yeung, Y.A., Cochran, J.R., Heinzelman, P., Colby, D., Swers, J.,*et al.* (2003). Flow-cytometric isolation of human antibodies from a nonimmune *Saccharomyces cerevisiae* surface display library. Nature Biotechnology *21*, 163-170.

Foulkes, D.M., Byrne, D.P., Yeung, W., Shrestha, S., Bailey, F.P., Ferries, S., Eyers, C.E., Keeshan, K., Wells, C., Drewry, D.H.,*et al.* (2018). Covalent inhibitors of EGFR family protein kinases induce degradation of human Tribbles 2 (TRIB2) pseudokinase in cancer cells. Science Signaling *11*, eaat7951.

Gilby, D.C., Sung, H.Y., Winship, P.R., Goodeve, A.C., Reilly, J.T., and Kiss-Toth, E. (2010). Tribbles-1 and -2 are tumour suppressors, down-regulated in human acute myeloid leukaemia. Immunology Letters *130*, 115-124.

Grosshans, J., and Wieschaus, E. (2000). A genetic link between morphogenesis and cell division during formation of the ventral furrow in Drosophila. Cell *101*, 523-531.

Hassanzadeh-Ghassabeh, G., Devoogdt, N., De Pauw, P., Vincke, C., and Muyldermans, S. (2013). Nanobodies and their potential applications. Nanomedicine *8*, 1013-1026.

Herce, H.D., Schumacher, D., Schneider, A.F.L., Ludwig, A.K., Mann, F.A., Fillies, M., Kasper, M.-A., Reinke, S., Krause, E., Leonhardt, H.,*et al.* (2017). Cell-permeable nanobodies for targeted immunolabelling and antigen manipulation in living cells. Nature Chemistry *9*, 762-771.

Jackson, G.H., and Taylor, P.R.A. (2002). Acute Myeloid Leukaemia: Optimising Treatment in Elderly Patients. Drugs & Aging *19*, 571-581.

Jamieson, S.A., Ruan, Z., Burgess, A.E., Curry, J.R., McMillan, H.D., Brewster, J.L., Dunbier, A.K., Axtman, A.D., Kannan, N., and Mace, P.D. (2018). Substrate binding allosterically relieves autoinhibition of the pseudokinase TRIB1. Science Signaling *11*, eaau0597.

Jin, G., Yamazaki, Y., Takuwa, M., Takahara, T., Kaneko, K., Kuwata, T., Miyata, S., and Nakamura, T. (2007). Trib1 and Evi1 cooperate with Hoxa and Meis1 in myeloid leukemogenesis. Blood *109*, 3998-4005.

Johnson, M. (2013). Detergents: Triton X-100, Tween-20, and More. Materials and Methods *3*.

Johnston, M. (1987). A model fungal gene regulatory mechanism: the GAL genes of Saccharomyces cerevisiae. Microbiological Reviews *51*, 458-476.

Keeshan, K., Bailis, W., Dedhia, P.H., Vega, M.E., Shestova, O., Xu, L., Toscano, K., Uljon, S.N., Blacklow, S.C., and Pear, W.S. (2010). Transformation by Tribbles homolog 2 (Trib2) requires both the Trib2 kinase domain and COP1 binding. Blood *116*, 4948-4957.

Keeshan, K., He, Y., Wouters, B.J., Shestova, O., Xu, L., Sai, H., Rodriguez, C.G., Maillard, I., Tobias, J.W., Valk, P.,*et al.* (2006). Tribbles homolog 2 inactivates C/EBPα and causes acute myelogenous leukemia. Cancer Cell *10*, 401-411.

Kunik, V., Peters, B., and Ofran, Y. (2012). Structural consensus among antibodies defines the antigen binding site. PLoS Computer Biology *8*, e1002388-e1002388.

Lohan, F., and Keeshan, K. (2013). The functionally diverse roles of tribbles. Biochemical Society Transactions *41*, 1096-1100.

Mashima, T., Soma-Nagae, T., Migita, T., Kinoshita, R., Iwamoto, A., Yuasa, T., Yonese, J., Ishikawa, Y., and Seimiya, H. (2014). TRIB1 supports prostate tumorigenesis and tumor-propagating cell survival by regulation of endoplasmic reticulum chaperone expression. Cancer Research *74*, 4888.

Mata, J., Curado, S., Ephrussi, A., and Rørth, P. (2000). Tribbles coordinates mitosis and morphogenesis in Drosophila by regulating string/CDC25 proteolysis. Cell *101*, 511-522.

McMahon, C., Baier, A.S., Pascolutti, R., Wegrecki, M., Zheng, S., Ong, J.X., Erlandson, S.C., Hilger, D., Rasmussen, S.G.F., Ring, A.M.,*et al.* (2018). Yeast surface display platform for rapid discovery of conformationally selective nanobodies. Nature Structural & Molecular Biology *25*, 289-296.

Michael, J.F., Robert, W.S., Lee, K.O., James, R.C., Jane, M.W.F., Yik, A.Y., Jennifer, R.C., Peter, H., David, C., Jeffrey, S.,*et al.* (2003). Flow-cytometric isolation of human antibodies from a nonimmune *Saccharomyces cerevisiae* surface display library. Nature Biotechnology *21*, 163.

Mitchell, L.S., and Colwell, L.J. (2018). Comparative analysis of nanobody sequence and structure data. Proteins *86*, 697-706.

Murphy, James M., Nakatani, Y., Jamieson, Sam A., Dai, W., Lucet, Isabelle S., and Mace, Peter D. (2015). Molecular mechanism of CCAAT-Enhancer binding protein recruitment by the TRIB1 Pseudokinase. Structure *23*, 2111-2121.

Narendranath, N.V., and Power, R. (2005). Relationship between pH and medium dissolved solids in terms of growth and metabolism of lactobacilli and Saccharomyces cerevisiae during ethanol production. Appl Environmental Microbiology *71*, 2239-2243.

Nguyen, V.K., Hamers, R., Wyns, L., and Muyldermans, S. (2000). Camel heavy-chain antibodies: diverse germline V(H)H and specific mechanisms enlarge the antigen-binding repertoire. EMBO Journal *19*, 921-930.

Ohoka, N., Yoshii, S., Hattori, T., Onozaki, K., and Hayashi, H. (2005). TRB3, a novel ER stress-inducible gene, is induced via ATF4–CHOP pathway and is involved in cell death. EMBO J *24*, 1243-1255.

Peña, A., Sánchez, N.S., Álvarez, H., Calahorra, M., and Ramírez, J. (2015). Effects of high medium pH on growth, metabolism and transport in Saccharomyces cerevisiae. FEMS Yeast Research *15*.

Petti, A.A., Crutchfield, C.A., Rabinowitz, J.D., and Botstein, D. (2011). Survival of starving yeast is correlated with oxidative stress response and nonrespiratory mitochondrial function. Proceedings of the National Academy of Sciences *108*, E1089.

Pleiner, T., Bates, M., Trakhanov, S., Lee, C.-T., Schliep, J.E., Chug, H., Böhning, M., Stark, H., Urlaub, H., and Görlich, D. (2015). Nanobodies: site-specific labeling for super-resolution imaging, rapid epitope-mapping and native protein complex isolation. eLife *4*, e11349-e11349.

Rishi, L., Hannon, M., Salomè, M., Hasemann, M., Frank, A.-K., Campos, J., Timoney, J., O'Connor, C., Cahill, M.R., Porse, B.,*et al.* (2014). Regulation of Trib2 by an E2F1-C/EBPα feedback loop in AML cell proliferation. Blood *123*, 2389-2400.

Röthlisberger, B., Heizmann, M., Bargetzi, M.J., and Huber, A.R. (2007). TRIB1 overexpression in acute myeloid leukemia. Cancer Genetics and Cytogenetics *176*, 58-60.

Salazar, M., Lorente, M., García-Taboada, E., Gómez, E.P., Dávila, D., Zúñiga-García, P., Flores, J.M., Rodríguez, A., Hegedus, Z., Mosén-Ansorena, D.,*et al.* (2014). Loss of Tribbles pseudokinase-3 promotes Akt-driven tumorigenesis via FOXO inactivation. Cell Death and Differentiation *22*.

Salomé, M., Hopcroft, L., and Keeshan, K. (2018). Inverse and correlative relationships between TRIBBLES genes indicate non-redundant functions during normal and malignant hemopoiesis. Experimental hematology *66*, 63-78.e13.

Seher, T.C., and Leptin, M. (2000). Tribbles, a cell-cycle brake that coordinates proliferation and morphogenesis during Drosophila gastrulation. Current Biology *10*, 623-629.

Sela-Culang, I., Kunik, V., and Ofran, Y. (2013). The structural basis of antibody-antigen recognition. Front Immunology *4*, 302-302.

Staus, D.P., Strachan, R.T., Manglik, A., Pani, B., Kahsai, A.W., Kim, T.H., Wingler, L.M., Ahn, S., Chatterjee, A., Masoudi, A., *et al.* (2016). Allosteric nanobodies reveal the dynamic range and diverse mechanisms of G-protein-coupled receptor activation. Nature *535*, 448-452.

Stockwell, S.R., Landry, C.R., and Rifkin, S.A. (2015). The yeast galactose network as a quantitative model for cellular memory. Molecular Biosystem *11*, 28-37.

Tsuzuki, K., Itoh, Y., Inoue, Y., and Hayashi, H. (2019). TRB1 negatively regulates gluconeogenesis by suppressing the transcriptional activity of FOXO1. FEBS Letters *593*, 369-380.

Uchański, T., Zögg, T., Yin, J., Yuan, D., Wohlkönig, A., Fischer, B., Rosenbaum, D.M., Kobilka, B.K., Pardon, E., and Steyaert, J. (2019). An improved yeast surface display platform for the screening of nanobody immune libraries. Scientific Reports *9*, 382.

Weinhandl, K., Winkler, M., Glieder, A., and Camattari, A. (2014). Carbon source dependent promoters in yeasts. Microb Cell Fact *13*, 5-5.

Yamaguchi, N., Colak-Champollion, T., and Knaut, H. (2019). zGrad is a nanobody-based degron system that inactivates proteins in zebrafish. eLife *8*, e43125.

Yokoyama, T., Kanno, Y., Yamazaki, Y., Takahara, T., Miyata, S., and Nakamura, T. (2010). Trib1 links the MEK1/ERK pathway in myeloid leukemogenesis. Blood *116*, 2768-2775.

Yokoyama, T., and Nakamura, T. (2011). Tribbles in disease: Signaling pathways important for cellular function and neoplastic transformation. Cancer Science *102*, 1115-1122.

Zareen, N., Biswas, S.C., and Greene, L.A. (2013). A feed-forward loop involving Trib3, Akt and FoxO mediates death of NGF-deprived neurons. Cell Death & Differentiation *20*, 1719-1730.

Appendices

Appendix A: **Reverse time course Nb induction of *S. cerevesiae* (yeast clone Nb2.011) between 24-48 hours , under galactose supplemented pH6 yeast media**. Nbs were labelled with αHA-PE, and MFI was measured using Guava ExpressPlus and analysed using FlowJo software. GraphPad Prism 8.4.3 was used to generate statistical analysis (*n=3*) using a one-way ANOVA, with Dunnett's post-hoc test ($p < 0.05$). **1.** Shows 1/3 induction replicate example of PE histograms made in FlowJo from the 24-, 36-, 48- hours induction flow cytometry data measured from Guava ExpressPlus. **2.** A table showing the raw data of PE MFI gathered from FlowJo analysis which represents the level of Nb-expression in Nb-expressing yeast population. **3.** A table showing the data of Nb-expressing yeast population gathered from FlowJo analysis, that was normalised for background PE signalling using the unlabelled control. **4.** A table showing the results of the one-way ANOVA test performed on the PE MFI data from *Appendix A.1 & A.2*. **5.** A table showing the results of the one-way ANOVA test, performed on the Nb-expressing yeast population data from *Appendix A1 & A.3*.

1

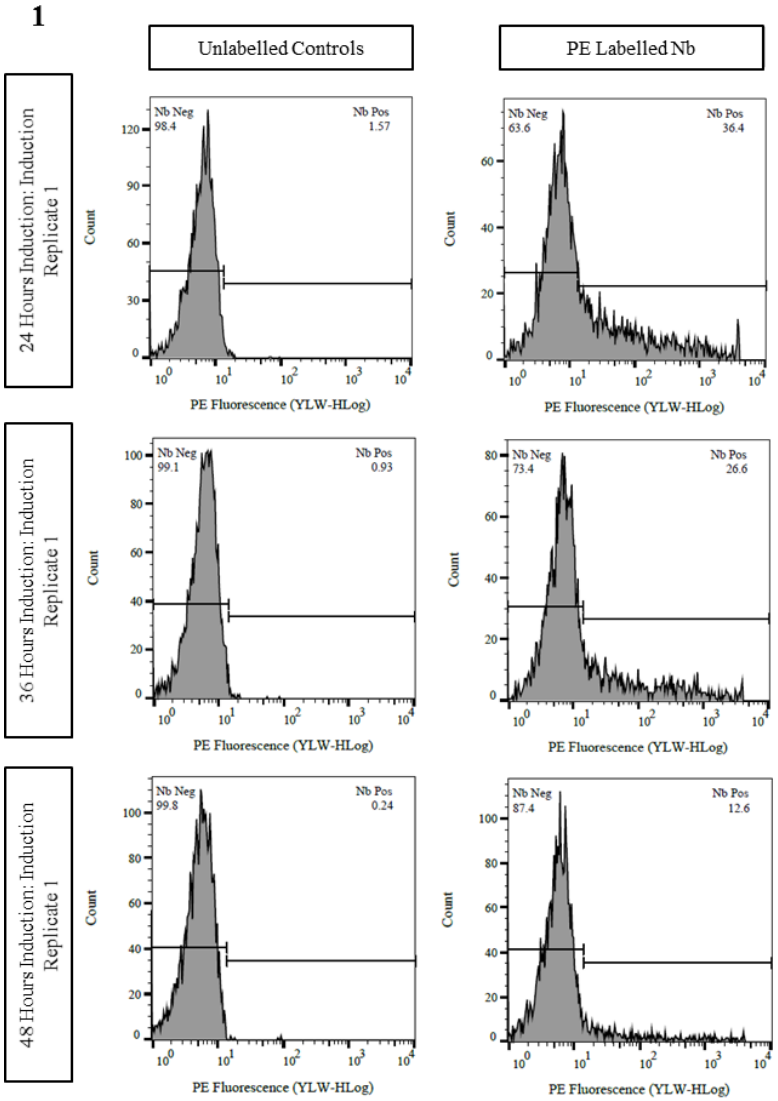

2

Induction Period (hours)	PE Mean Fluorescence Intensity (MFI)		
Induction Relplicates	1	2	3
24	351	297	354
36	373	560	511
48	418	523	629

3

Induction Period hours)	Population of Nb-expressing yeast (%)		
Induction Replicates	1	2	3
24	34.83	27.05	39.42
36	25.67	27.58	29.02
48	12.36	14.44	13.17

4

Dunnett's multiple comparisons test	Mean 1	Mean 2	Mean Difference	95% CI of difference	Significant?	Adjusted P Value
24 hours vs. 36 hours	334	481.3	-147.3	-346 to 50.9	No	0.131
24 hours vs. 48 hours	334	523.3	-189.3	-388 to 8.85	No	0.059

5

Dunnett's multiple comparisons test	Mean 1	Mean 2	Mean Difference	95% CI of difference	Significant?	Adjusted P Value
24 hours vs. 36 hours	33.8	27.4	6.34	-2.51 to 15.2	No	0.145
24 hours vs. 48 hours	33.8	13.3	20.4	11.6 to 29.3	Yes	0.001

Appendix B: **Optimisation of selection buffer for the flow cytometric characterisation of TRIB1-Nbs.** Standard selection buffer was supplemented with various concentrations of reagents to minimise non-specific binding of yeast to FITC labelled TRIB1 proteins. **1.** Dot plots of different yeast clone populations (both un-induced and induced to express Nbs) shows consistent non-specific binding of yeast to TRIB1-FITC, highlighted by red boxes (Q1). **2-3.** Shows dot plots of un-induced yeast clones incubated with TRIB1-FITC, using standard and supplemented selection buffers, with non-specific binding highlighted by red boxes: Nb5.018 (negative control) shown in the first row, and Nb2.011 (positive control) shown in the second row. **4.** Tables showing the raw data gathered from flow cytometric data exemplified by *Appendix B.2* (*n=3*). **5.** Tables showing the raw data gathered from flow cytometric data exemplified by *Appendix B.3 (n=3).* **6.** Tables showing the results of the one-way ANOVA test performed on the data from *Appendix B.4 (n=3).* **7.** Tables showing the results of the one-way ANOVA test performed on the data from *Appendix B.5 (n=3).*

1

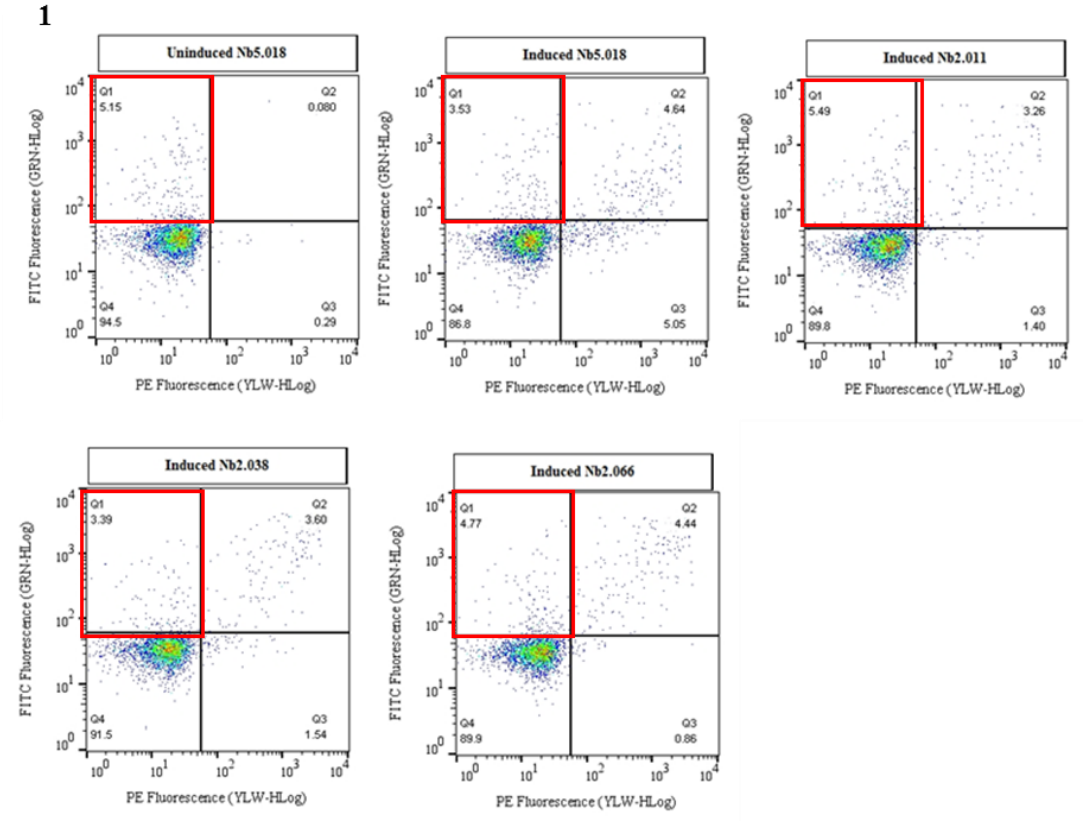

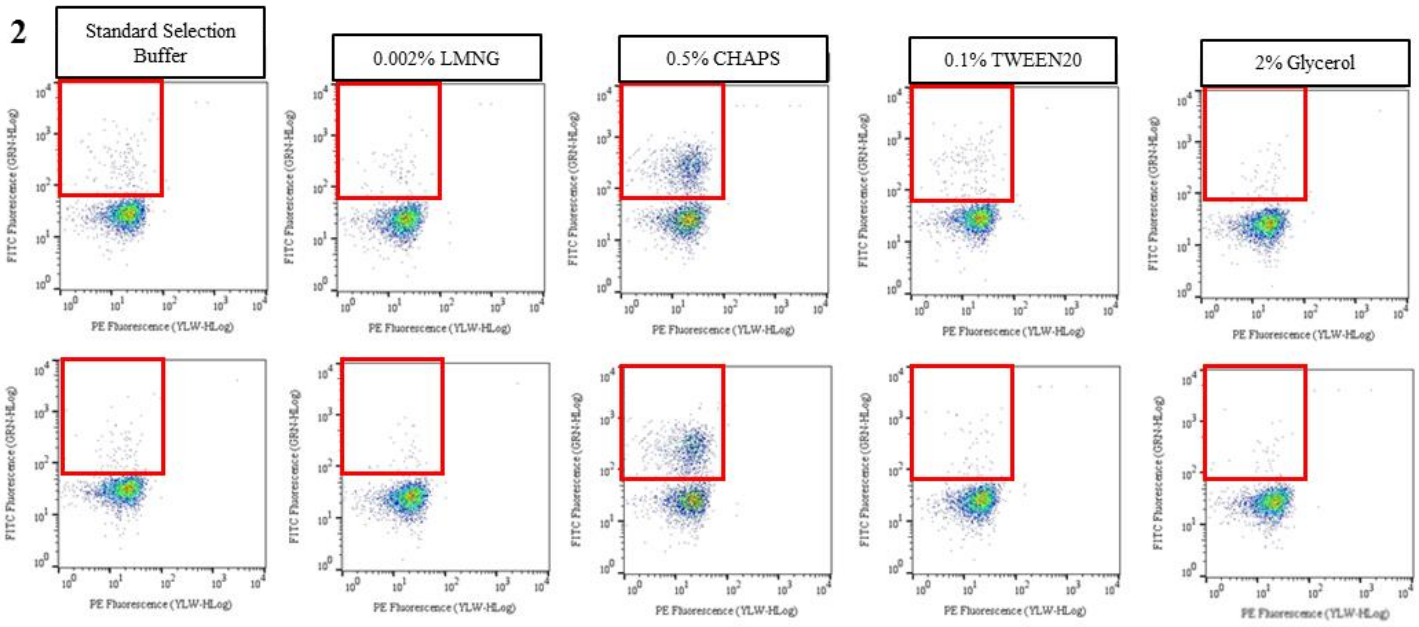
2
Standard Selection Buffer
0.002% LMNG
0.5% CHAPS
0.1% TWEEN20
2% Glycerol
FITC Fluorescence (GRN-HLog)
PE Fluorescence (YLW-HLog)

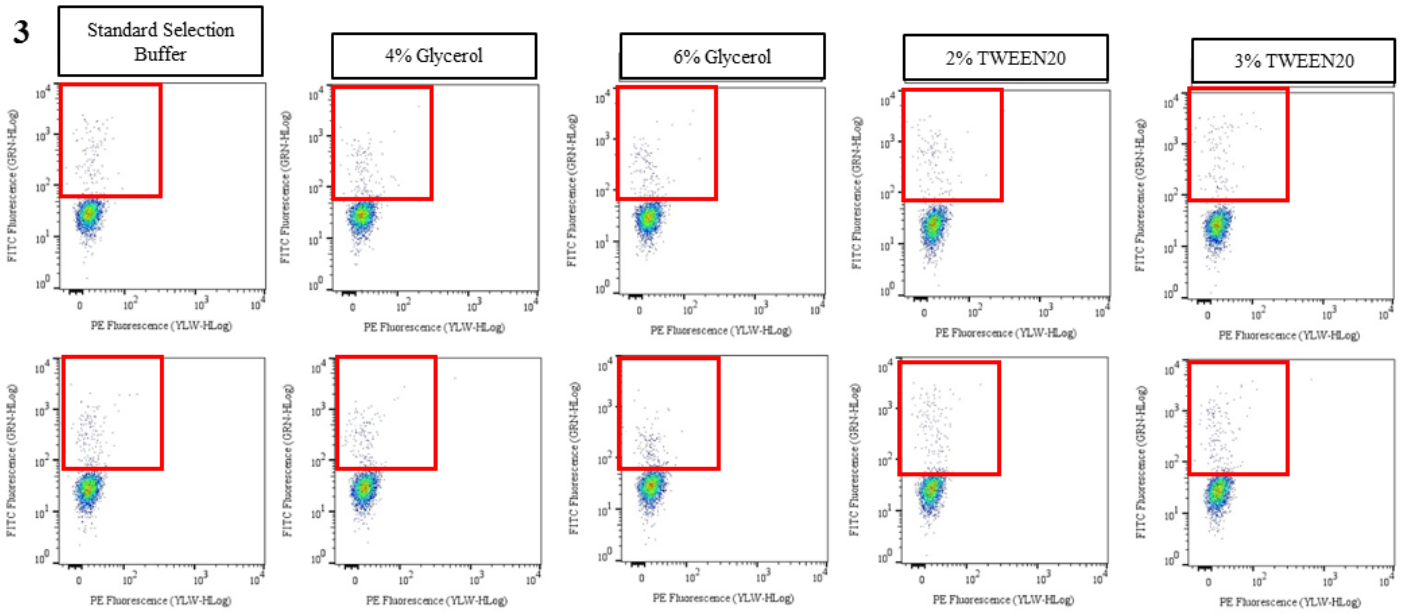
3
Standard Selection Buffer
4% Glycerol
6% Glycerol
2% TWEEN20
3% TWEEN20
FITC Fluorescence (GRN-HLog)
PE Fluorescence (YLW-HLog)

4

TRIB1-FITC Nonspecific Binding to Yeast (% of cells)					
Yeast Clone	Normal	0.002% LMNG	0.5% CHAPS	0.1% TWEEN20	2% Glycerol
Nb5.018	18.7	7.82	37	21.2	10.7
	6.32	6.97	29.8	5.75	9.41
	15.4	7.03	35.7	10.8	13.9
Nb2.011	19.8	7.56	38.6	9.85	11.5
	18	9.3	38	14	13.8
	8.08	9.02	38.5	15	11.3

FITC Mean Fluorescence Intensity (MFI) of Non-specific TRIB1 Binding Yeast					
Yeast Clone	Normal	0.002% LMNG	0.5%CHAPS	0.1% TWEEN20	2% Glycerol
Nb5.018	150	152	268	151	92.6
	220	220	294	317	146
	107	140	265	161	106
Nb2.011	85.3	106	264	174	102
	98.2	128	244	160	86.4
	145	147	231	147	99.4

5

TRIB1-FITC Nonspecific Binding to Yeast (% of cells)					
Yeast Clone	Normal	4% Glycerol	6% Glycerol	0.2% TWEEN20	0.3% TWEEN20
Nb5.018	7.66	8.64	10.3	6.09	6.81
	6.25	11.5	14.6	6.81	7.14
	7.34	7.02	11.4	7.36	7.85
Nb2.011	13	13.1	12.3	10.4	11.6
	10.2	19.2	12.5	11.3	13.7
	16	17.3	12.8	13.8	13.2

FITC Mean Fluorescence Intensity (MFI) of Non-specific TRIB1 Binding Yeast					
Yeast Clone	Normal	4% Glycerol	6% Glycerol	0.2% TWEEN20	0.3% TWEEN20
Nb5.018	279	166	163	384	496
	253	145	133	379	362
	297	229	133	340	348
Nb2.011	186	160	107	289	257
	212	130	121	264	245
	134	129	117	200	245

6 **Analysis of FITC Mean Fluorescence Intensity (MFI) of Non-specific TRIB1 Binding Yeast:**

Yeast Clone	Dunnett's multiple comparisons test	Mean 1	Mean 2	Mean Difference	95% CI of difference	Significant?	Adjusted P Value
Nb 5.018	Standard vs. 0.002% LMNG	159	212	-53.3	-188 to 80.9	No	0.624
	Standard vs. 0.5% CHAPS	159	276	-117	-251 to 17.6	No	0.093
	Standard vs. 0.1% TWEEN20	159	210	-50.7	-185 to 83.6	No	0.661
	Standard vs. 2% Glycerol	159	115	44.1	-90.1 to 178	No	0.750
Nb 2.011	Standard vs. 0.002% LMNG	110	127	-17.5	-63.9 to 28.9	No	0.662
	Standard vs. 0.5% CHAPS	110	246	-136.8	-183 to -90.4	Yes	<0.0001
	Standard vs. 0.1% TWEEN20	110	160	-50.83	-97.3 to -4.39	Yes	0.032
	Standard vs. 2% Glycerol	110	95.9	13.57	-32.9 to 60.0	No	0.813

Analysis of TRIB1-FITC Nonspecific Binding to Yeast (% of cells):

Yeast Clone	Dunnett's multiple comparisons test	Mean 1	Mean 2	Mean Difference	95% CI of difference	Significant?	Adjusted P Value
Nb 5.018	Standard vs. 0.002% LMNG	13.5	7.27	6.20	-5.53 to 17.9	No	0.400
	Standard vs. 0.5% CHAPS	13.5	34.2	-20.7	-32.4 to -8.97	Yes	0.002
	Standard vs. 0.1% TWEEN20	13.5	12.6	0.89	-10.8 to 12.6	No	0.998
	Standard vs. 2% Glycerol	13.5	11.3	2.14	-9.59 to 13.9	No	0.954
Nb 2.011	Standard vs. 0.002% LMNG	15.3	8.63	6.67	-0.811 to 14.1	No	0.083
	Standard vs. 0.5% CHAPS	15.3	38.4	-23.1	-30.6 to -15.6	Yes	<0.0001
	Standard vs. 0.1% TWEEN20	15.3	13.0	2.34	-5.14 to 9.82	No	0.777
	Standard vs. 2% Glycerol	15.3	12.2	3.09	-4.39 to 10.6	No	0.594

7 **Analysis of FITC Mean Fluorescence Intensity (MFI) of Non-specific TRIB1 Binding Yeast:**

Yeast Clone	Dunnett's multiple comparisons test	Mean 1	Mean 2	Mean Difference	95% CI of difference	Significant?	Adjusted P Value
Nb 5.018	Standard vs. 4% Glycerol	276	180	96.3	-8.99 to 202	No	0.0747
	Standard vs. 6% Glycerol	276	143	133	28.0 to 239	Yes	0.0143
	Standard vs. 0.2% TWEEN20	276	368	-91.3	-197 to 14.0	No	0.0932
	Standard vs. 0.3% TWEEN20	276	402	-126	-231 to -20.4	Yes	0.0201
Nb 2.011	Standard vs. 4% Glycerol	110	127	-17.5	-63.9 to 28.9	No	0.662
	Standard vs. 6% Glycerol	110	246	-137	-183 to -90.4	Yes	<0.0001
	Standard vs. 0.2% TWEEN20	110	160	-50.8	-97.3 to -4.39	Yes	0.032
	Standard vs. 0.3% TWEEN20	110	95.9	13.6	-32.9 to 60.0	No	0.813

Analysis of TRIB1-FITC Nonspecific Binding to Yeast (% of cells):

Yeast Clone	Dunnett's multiple comparisons test	Mean 1	Mean 2	Mean Difference	95% CI of difference	Significant?	Adjusted P Value
Nb 5.018	Standard vs. 4% Glycerol	7.08	9.05	-1.97	-5.53 to 1.59	No	0.3638
	Standard vs. 6% Glycerol	7.08	12.1	-5.02	-8.58 to -1.46	Yes	0.0074
	Standard vs. 0.2% TWEEN20	7.08	6.75	0.330	-3.23 to 3.89	No	0.996
	Standard vs. 0.3% TWEEN20	7.08	7.27	-0.183	-3.74 to 3.38	No	0.9997
Nb 2.011	Standard vs. 4% Glycerol	13.1	16.5	-3.47	-8.48 to 1.54	No	0.2055
	Standard vs. 6% Glycerol	13.1	12.5	0.533	-4.48 to 5.54	No	0.9933
	Standard vs. 0.2% TWEEN20	13.1	11.8	1.23	-3.78 to 6.24	No	0.8831
	Standard vs. 0.3% TWEEN20	13.1	12.8	1.233	-4.78 to 5.24	No	0.9998

Appendix C: **Flow cytometric compensation of FITC spillover into the PE channel.** To characterise the affinity and specificity of TRIB1-Nbs, a compensation matrix to correct the FITC fluorescence spillover to the PE fluorescent channel was made and applied in FlowJo. This minimised potential false positive TRIB1-binding results. The compensation matrix was made using an unlabelled control, a FITC only control (480 nM TRIB1-FITC, no Nb-PE labelling) and a PE only control (Nb labelled with PE, no TRIB1-FITC). **1-2.** Shows examples of dot plots before and after application of compensation matrix to FITC only controls of TRIB1-Nb yeast clones characterised in this project: After compensation, the initially skewed yeast population becomes perpendicular to the FITC channel axis (Q1).

1

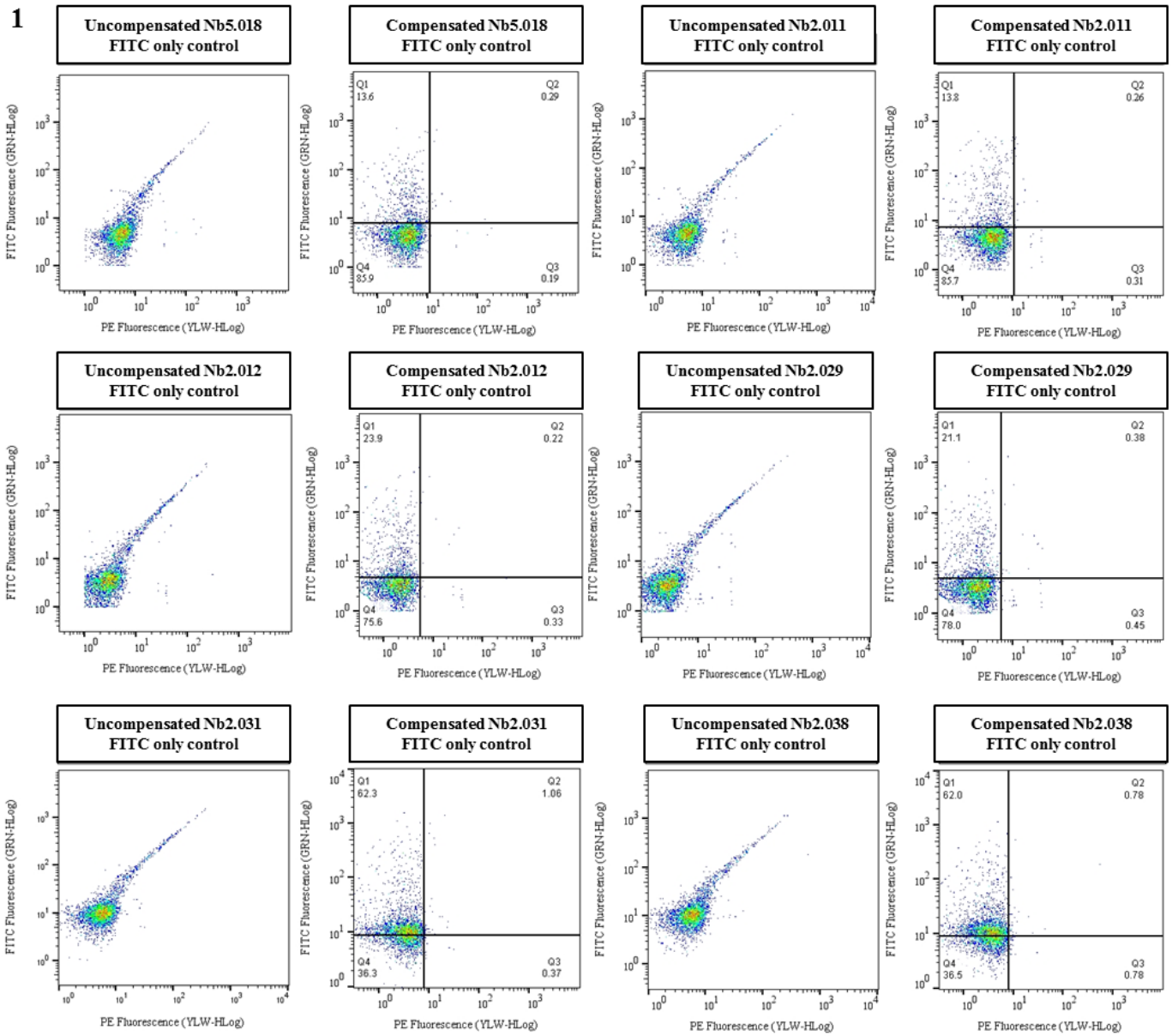

2

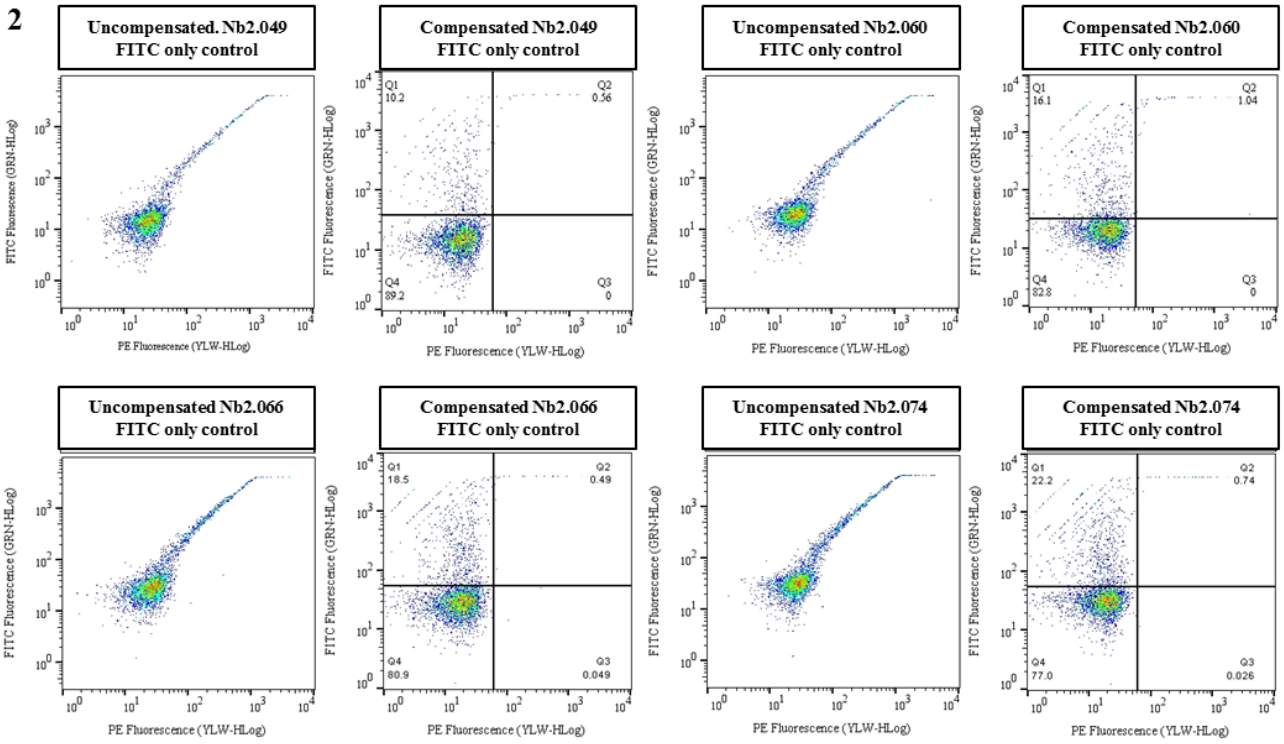
Uncompensated. Nb2.049
FITC only control
Compensated Nb2.049
FITC only control
Uncompensated Nb2.060
FITC only control
Compensated Nb2.060
FITC only control
Uncompensated Nb2.066
FITC only control
Compensated Nb2.066
FITC only control
Uncompensated Nb2.074
FITC only control
Compensated Nb2.074
FITC only control
FITC Fluorescence (GRN-HLog)
PE Fluorescence (YLW-HLog)
Q1 10.2
Q2 0.56
Q4 89.2
Q3 0
Q1 16.1
Q2 1.04
Q4 82.8
Q3 0
Q1 18.5
Q2 0.49
Q4 80.9
Q3 0.049
Q1 22.2
Q2 0.74
Q4 77.0
Q3 0.026

Appendix D: **Affinity characterisation of TRIB1-Nb yeast clone controls via yeast surface display system and flow cytometry.** Dot plots representing an induction replicate of Nb binding results to TRIB1-FITC (titrations of 0-480 nM) were generated in FlowJo – **1.** Nb5.018 (negative control) and **2.** Nb2.011 (positive control). A quadrant gate was set using an unlabelled control, to show the different yeast populations.

1

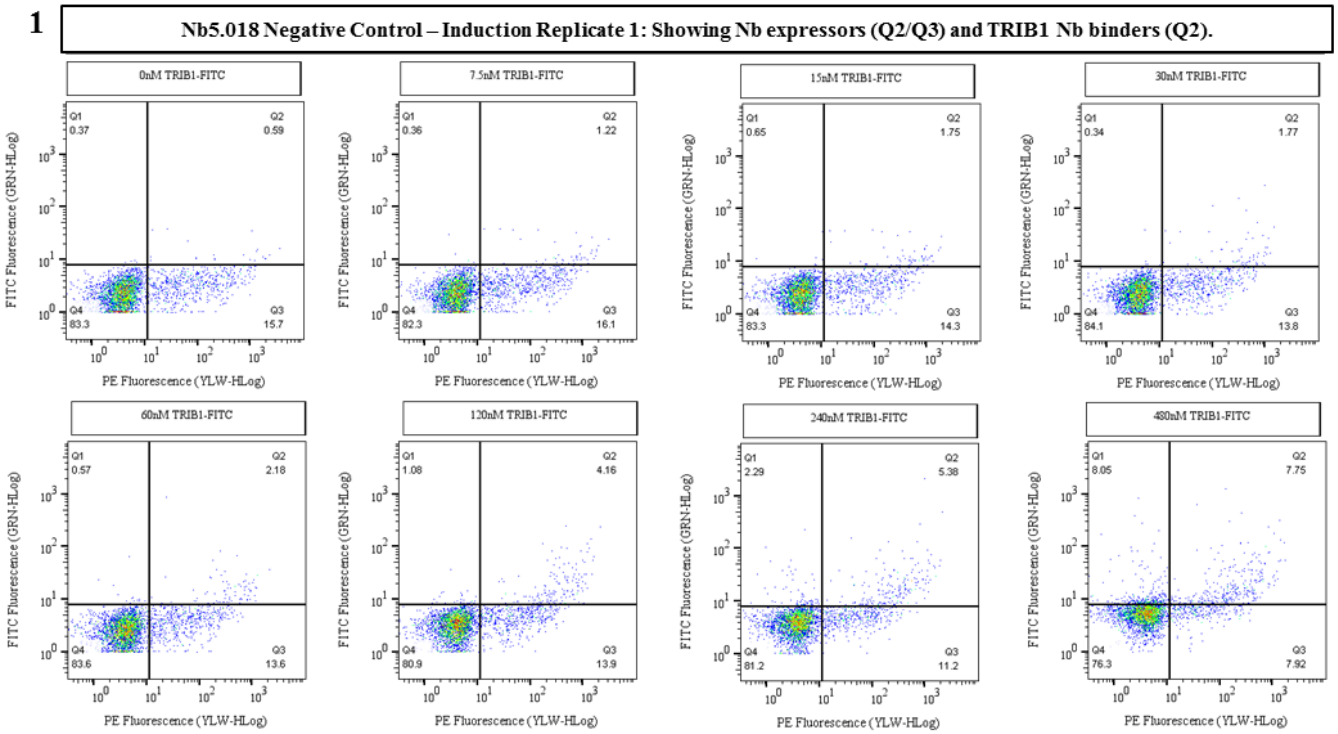

2

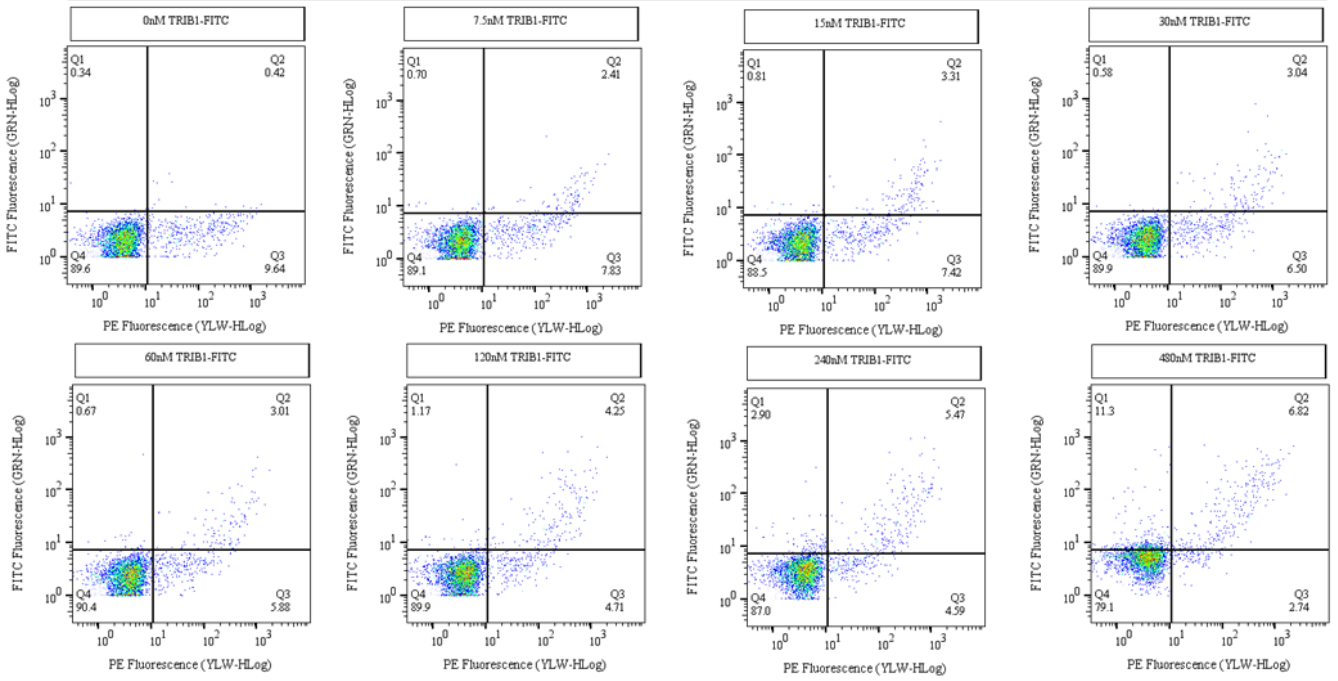

Appendix E: **Affinity characterisation of TRIB1-Nb yeast clones Nb2.012 and Nb2.029 via yeast surface display system and flow cytometry.** Dot plots representing an induction replicate of Nb binding results to TRIB1-FITC (titrations of 0-480 nM) were generated in FlowJo – **1.** Nb2.012 and **2.** Nb2.029. A quadrant gate was set using an unlabelled control, to show the different yeast populations.

1

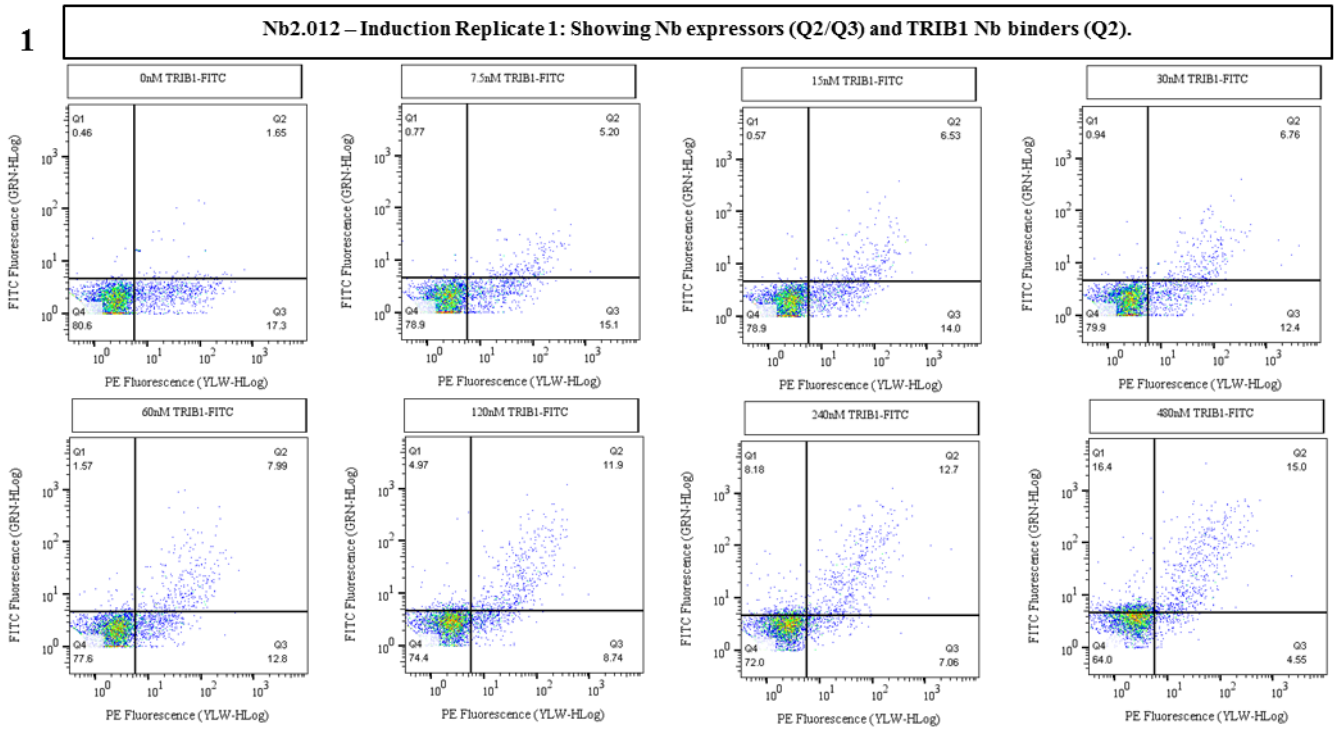

2

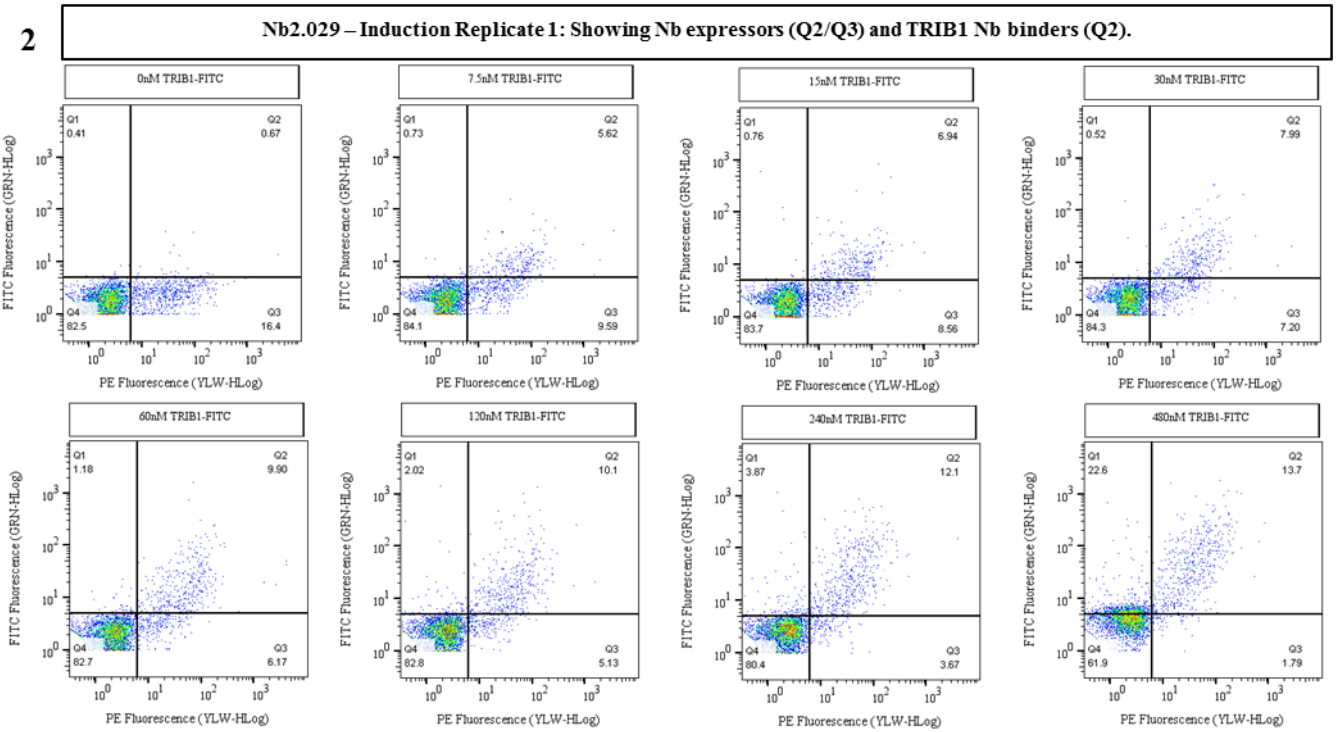

Appendix F: **Affinity characterisation of TRIB1-Nb yeast clones Nb2.031 and Nb2.038 via yeast surface display system and flow cytometry.** Dot plots representing an induction replicate of Nb binding results to TRIB1-FITC (titrations of 0-480 nM) were generated in FlowJo – **1.** Nb2.031 and **2.** Nb2.038. A quadrant gate was set using an unlabelled control, to show the different yeast populations.

1

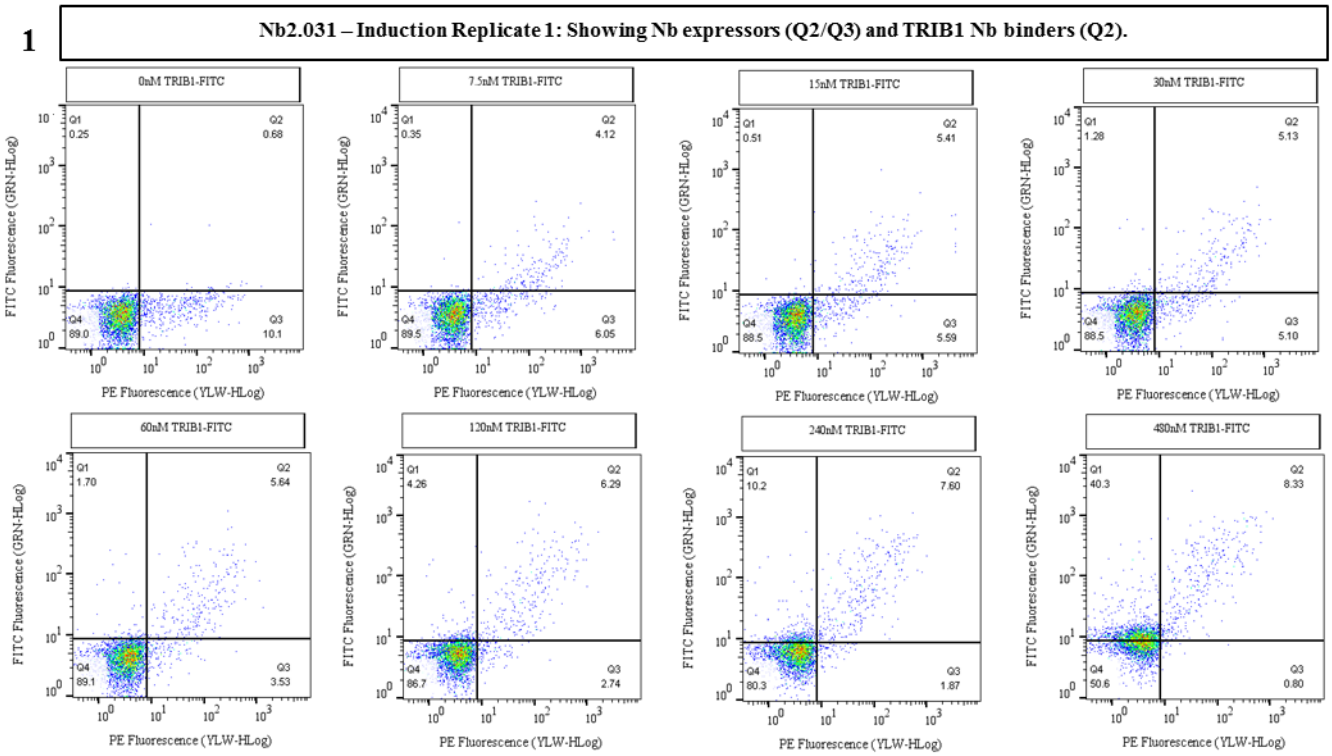

2

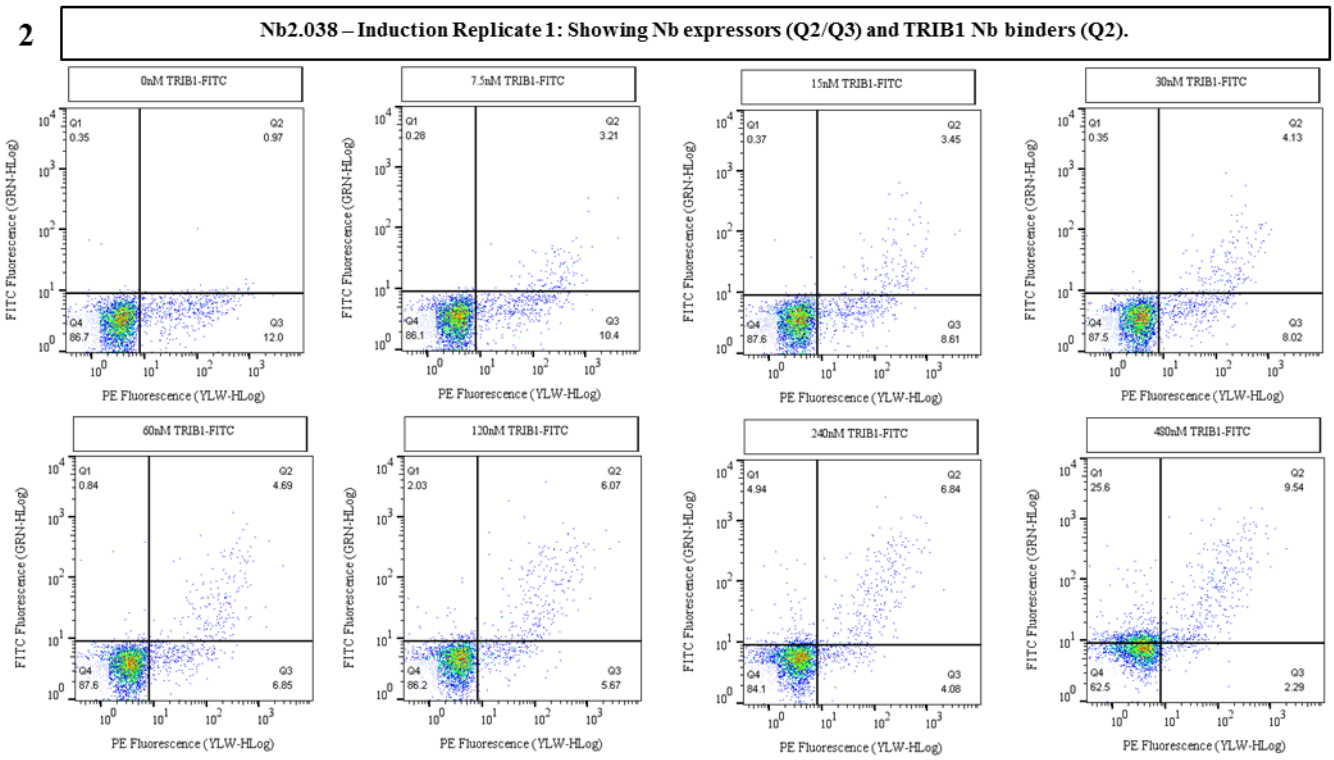

Appendix G: **Affinity characterisation of TRIB1-Nb yeast clones Nb2.049 and Nb2.060 via yeast surface display system and flow cytometry.** Dot plots representing an induction replicate of Nb binding results to TRIB1-FITC (titrations of 0-480 nM) were generated in FlowJo – **1.** Nb2.049 and **2.** Nb2.060. A quadrant gate was set using an unlabelled control, to show the different yeast populations.

1 **Nb2.049 – Induction Replicate 1: Showing Nb expressors (Q2/Q3) and TRIB1 Nb binders (Q2).**

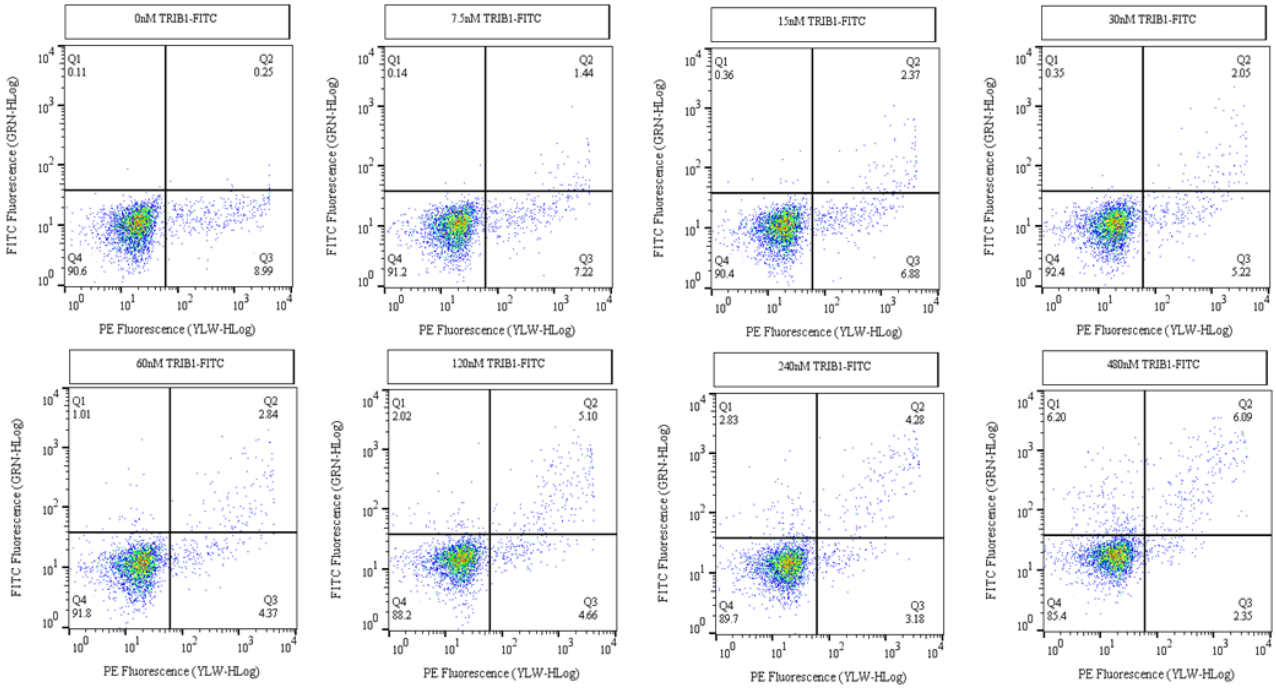

2 **Nb2.060 – Induction Replicate 1: Showing Nb expressors (Q2/Q3) and TRIB1 Nb binders (Q2).**

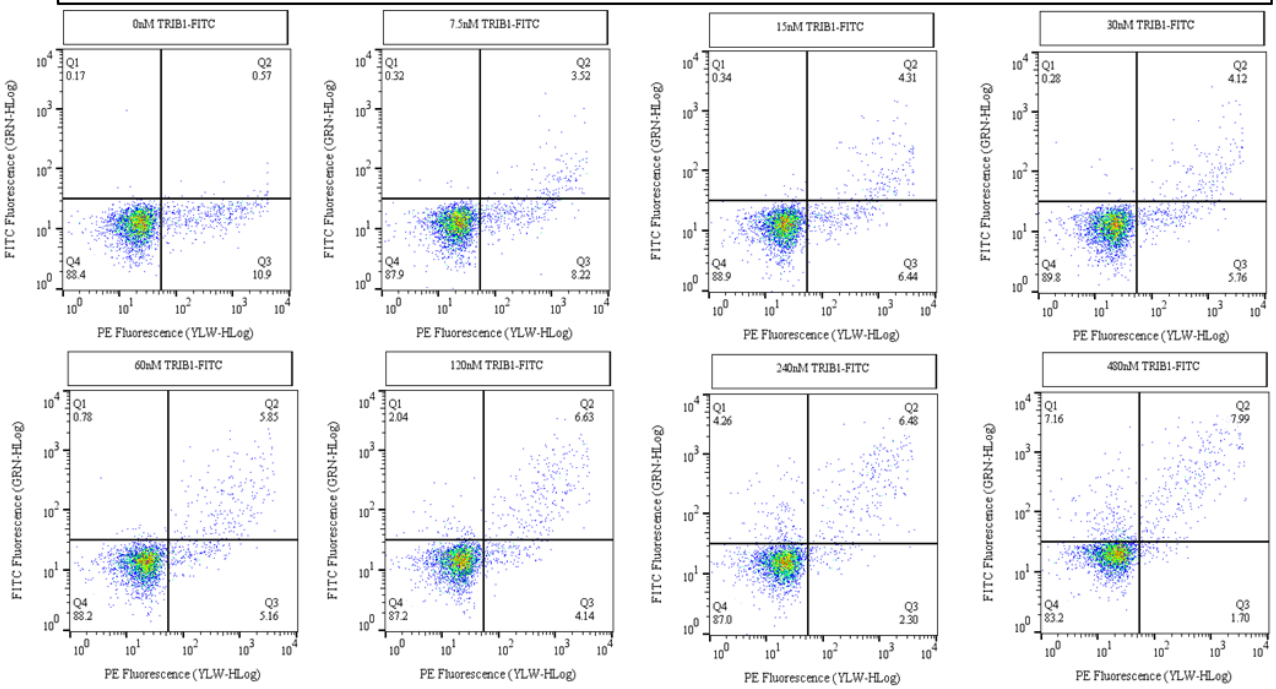

Appendix H: **Affinity characterisation of TRIB1-Nb yeast clones Nb2.066 and Nb2.074 via yeast surface display system and flow cytometry.** Dot plots representing an induction replicate of Nb binding results to TRIB1-FITC (titrations of 0-480 nM) were generated in FlowJo – **1.** Nb2.066 and **2.** Nb2.074. A quadrant gate was set using an unlabelled control, to show the different yeast populations.

1 **Nb2.066 – Induction Replicate 1: Showing Nb expressors (Q2/Q3) and TRIB1 Nb binders (Q2).**

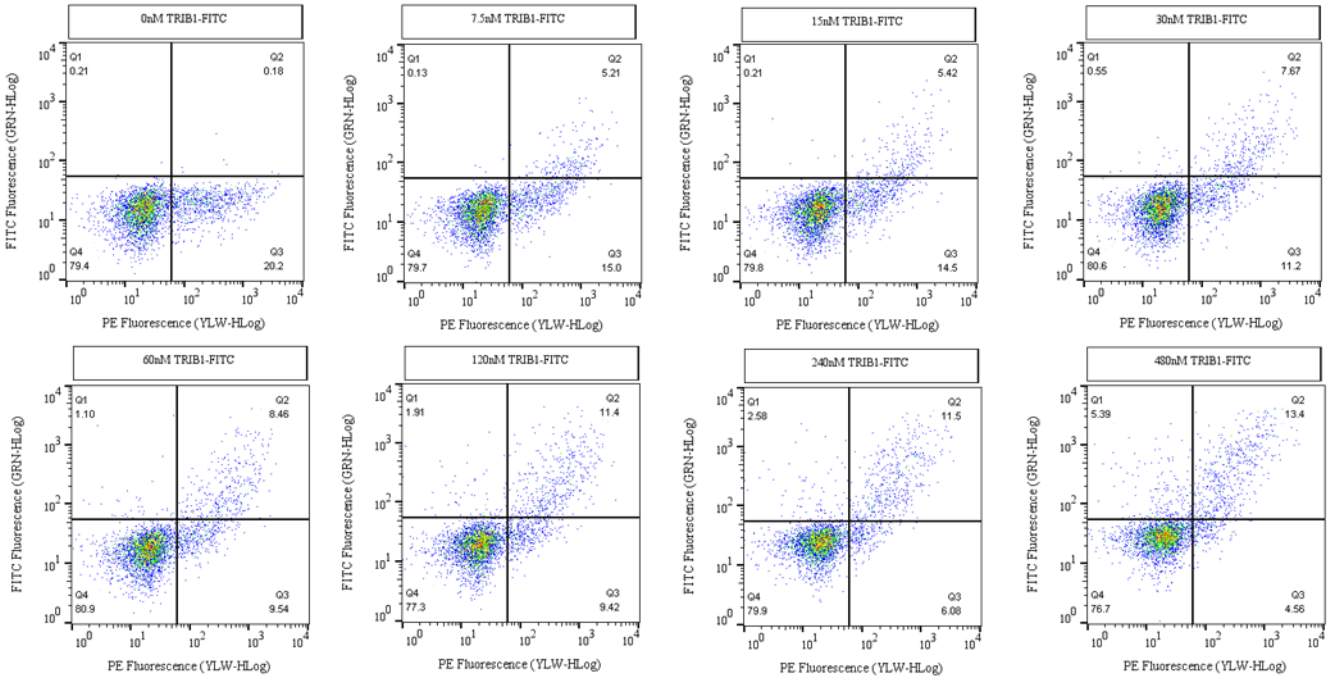

2 **Nb2.074 – Induction Replicate 1: Showing Nb expressors (Q2/Q3) and TRIB1 Nb binders (Q2).**

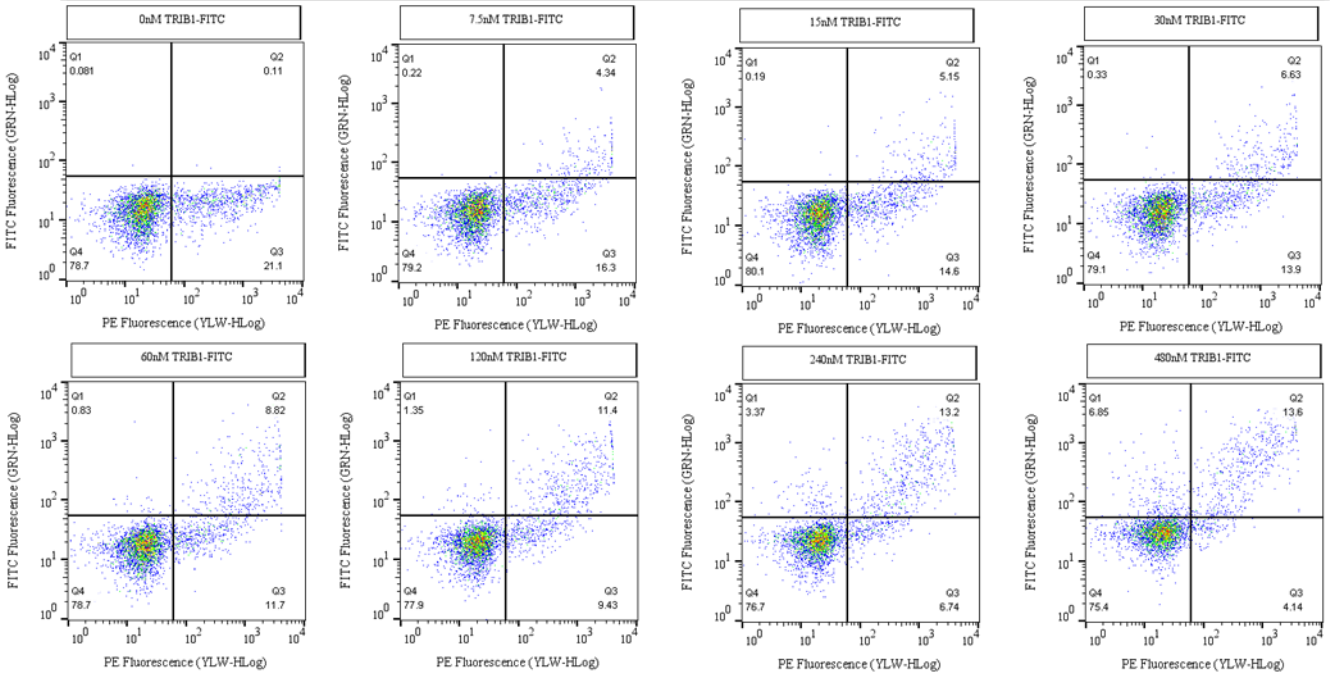

Appendix I: **Raw data of affinity characterisation of TRIB1-Nbs using FITC mean fluorescence intensity (MFI) from flow cytometric analysis of yeast surface display system.** In FlowJo, the FITC MFI was calculated from the Nb-expressing (Nb Pos) population. **1-14.** Shows table of flow cytometry analysis of affinity characterisation experiments exemplified by *Appendices D-H*, with each separate experiment (represented by row) run through with the negative control, Nb5.018. **15.** Shows table of flow cytometry analysis of second affinity characterisation (ran with Nb5.18) of Nb2.038, Nb2.049, and Nb2.066 – 12 TRIB1-FITC titrations were done (0-480 nM).

1

	Nb5.018	Induction Replicates		
	[TRIB1-FITC] (nM)	1	2	3
FITC Mean Fluorescence Intensity (MFI)	0	15.5	17.2	17.7
	7.5	15.1	12.7	15.2
	15	14	31.6	15.2
	30	24.9	24.3	20.8
	60	28.1	22.1	13.4
	120	26.8	26.5	29.8
	240	38	32.5	31.5
	480	33.3	29.6	40.5

2

	Nb2.011	Induction Replicates		
	[TRIB1-FITC] (nM)	1	2	3
FITC Mean Fluorescence Intensity (MFI)	0	14	20.5	11.6
	7.5	20.5	24.6	18.9
	15	29.8	24	23.4
	30	40.6	28.1	26.9
	60	36.7	47.5	24.4
	120	68.3	70.8	51.8
	240	74.5	70.9	63.1
	480	90.6	95.2	78.7

3

	Nb5.018	Induction Replicates		
	[TRIB1-FITC] (nM)	1	2	3
FITC Mean Fluorescence Intensity (MFI)	0	9.28	9.95	12
	7.5	23.9	15.2	19.4
	15	18.5	27	28
	30	16.4	15.5	38.2
	60	38	19.7	23.3
	120	40.6	29.5	30.9
	240	50.3	38.1	25.8
	480	39	42.4	49.1

4

	Nb2.012	Induction Replicates		
	[TRIB1-FITC] (nM)	1	2	3
FITC Mean Fluorescence Intensity (MFI)	0	17.4	8.78	10.8
	7.5	11.2	17	18.2
	15	19.5	20.8	19
	30	20.6	23.4	24.5
	60	36.8	27.6	31
	120	45	52.1	57
	240	66.1	62.7	71.1
	480	82.6	91.7	95.1

5

	Nb2.029	Induction Replicates		
	[TRIB1-FITC] (nM)	1	2	3
FITC Mean Fluorescence Intensity (MFI)	0	9.76	28.6	19.1
	7.5	12.2	13.7	15.1
	15	18.8	19.5	17.5
	30	20.3	24	28.6
	60	31.5	31.1	28.8
	120	39.1	44.2	44.9
	240	53.4	56.3	74
	480	85.3	88.5	69.3

6

	Nb5.018	Induction Replicates		
	[TRIB1-FITC] (nM)	1	2	3
FITC Mean Fluorescence Intensity (MFI)	0	14.9	11.5	67.7
	7.5	21.6	39	19.8
	15	31.4	45.9	32.3
	30	38.7	40	36.8
	60	60.6	48.6	49.8
	120	66.4	67.8	58.2
	240	54.7	88.2	62
	480	71.8	69.3	118

7

	Nb2.031	Induction Replicates		
	[TRIB1-FITC] (nM)	1	2	3
FITC Mean Fluorescence Intensity (MFI)	0	17.1	21	15.7
	7.5	29.3	31.1	31.2
	15	45.3	46.4	41.6
	30	45.7	57.8	52.5
	60	70	96.5	79.9
	120	112	136	128
	240	121	176	170
	480	182	233	231

8

	Nb2.038	Induction Replicates		
	[TRIB1-FITC] (nM)	1	2	3
FITC Mean Fluorescence Intensity (MFI)	0	12.8	10.8	19
	7.5	25.8	27.8	22.4
	15	49.4	39.9	28.5
	30	47.8	59.8	48.1
	60	84.9	64.6	53.4
	120	124	70.6	93.8
	240	145	129	121
	480	135	132	57.2

9

	Nb5.018	Induction Replicates		
	[TRIB1-FITC] (nM)	1	2	3
FITC Mean Fluorescence Intensity (MFI)	0	133	114	60.7
	7.5	96.4	83.8	109
	15	205	142	156
	30	101	108	171
	60	212	231	259
	120	270	265	475
	240	407	403	611
	480	441	501	636

10

	Nb2.049	Induction Replicates		
	[TRIB1-FITC] (nM)	1	2	3
FITC Mean Fluorescence Intensity (MFI)	0	55.5	44.5	116
	7.5	107	153	144
	15	162	217	176
	30	241	200	244
	60	306	303	350
	120	350	446	421
	240	668	545	560
	480	812	880	888

11

	Nb2.060	Induction Replicates		
	[TRIB1-FITC] (nM)	1	2	3
FITC Mean Fluorescence Intensity (MFI)	0	48	114	142
	7.5	120	97	105
	15	164	152	146
	30	190	194	152
	60	268	253	143
	120	355	359	283
	240	541	555	396
	480	779	709	703

12

	Nb5.018	Induction Replicates		
	[TRIB1-FITC] (nM)	1	2	3
FITC Mean Fluorescence Intensity (MFI)	0	102	81	1815
	7.5	323	194	307
	15	144	163	151
	30	151	179	236
	60	188	329	322
	120	184	261	246
	240	255	294	312
	480	388	407	326

13

	Nb2.066	Induction Replicates		
	[TRIB1-FITC] (nM)	1	2	3
FITC Mean Fluorescence Intensity (MFI)	0	105	64.1	803
	7.5	158	152	162
	15	212	197	205
	30	242	182	230
	60	334	281	350
	120	415	405	406
	240	494	458	542
	480	667	504	788

14

	Nb2.074	Induction Replicates		
	[TRIB1-FITC] (nM)	1	2	3
FITC Mean Fluorescence Intensity (MFI)	0	75.8	150	87.6
	7.5	160	171	165
	15	201	219	197
	30	218	241	225
	60	341	411	363
	120	344	536	490
	240	554	651	621
	480	778	964	868

		Nb5.018			Nb2.038			Nb2.049			Nb2.066		
	[TRIB1-FITC] (nM)	1	2	3	1	2	3	1	2	3	1	2	3
FITC Mean Fluorescence Intensity (MFI)	0	24.8	26.3	26.0	28.9	27.8	24.2	27.3	29.5	27.8	36.6	37.8	33.6
	1	26.7	25.5	27.3	25.6	29.4	27.5	30.1	29.1	29.1	40.4	41.0	37.3
	2	26.8	27.8	27.8	29.4	42.7	33.2	32.7	36.8	33.7	49.5	44.3	41.4
	4	26.9	25.8	28.0	33.1	33.2	31.4	37.8	32.2	34.3	50.6	48.6	46.4
	8	30.2	30.1	30.2	39.4	42.9	39.6	53.1	53.3	39.8	69.7	69.0	62.9
	10	33.8	35.9	29.4	35.8	42.4	35.2	52.1	47.1	43.0	73.3	79.9	70.3
	15	40.2	37.5	39.9	60.5	67.4	60.1	77.6	64.3	70.6	94.1	111.0	76.8
	30	46.3	50.1	41.6	64.6	59.7	71.5	98.3	106.0	68.9	106.0	123.0	107.0
	60	62.2	63.4	86.7	120.0	112.0	142.0	142.0	111.0	119.0	143.0	178.0	183.0
	120	98.3	89.1	106.0	181.0	212.0	202.0	208.0	216.0	174.0	275.0	268.0	250.0
	240	153.0	200.0	187.0	253.0	342.0	301.0	358.0	363.0	266.0	446.0	604.0	436.0
	480	273.0	285.0	416.0	508.0	518.0	581.0	635.0	687.0	668.0	772.0	791.0	734.0

Appendix J: **Determining presence of TRIB1-Nb binding to TRIB2 proteins using FITC mean fluorescence intensity (MFI) from flow cytometric analysis of yeast surface display system.** Nbs expressed on the surface of *S. cerevesiae* were labelled with αHA-PE then incubated with 200 nM TRIB2 labelled with FITC. As a measure of Nb binding TRIB2, FITC MFI was measured using Guava ExpressPlus and analysed using FlowJo software *(n=3)*. **1.** Shows dot plots of flow cytometry data: The first row is an example of the labelling controls performed for each Nb tested, using Nb2.011; the second row shows 1/3 induction replicates performed to determine whether TRIB1-Nbs (Nb2.011 – positive control, Nb2.038, Nb2.066) had any affinity to bind TRIB2; Nb5.018 was used as a negative non TRIB2 binding control. The 3 TRIB1-Nbs tested were shown to have some affinity to bind TRIB2 at 200 nM. **2.** A table showing the raw data of FITC MFI generated from the Nb-expressing (Nb Pos) population, representing TRIB1-Nb binding TRIB2 proteins**. 3.** Shows a column graph of TRIB2 binding TRIB1-Nbs, generated using GraphPad Prism8.4.3, with mean and SD (standard deviation).

1

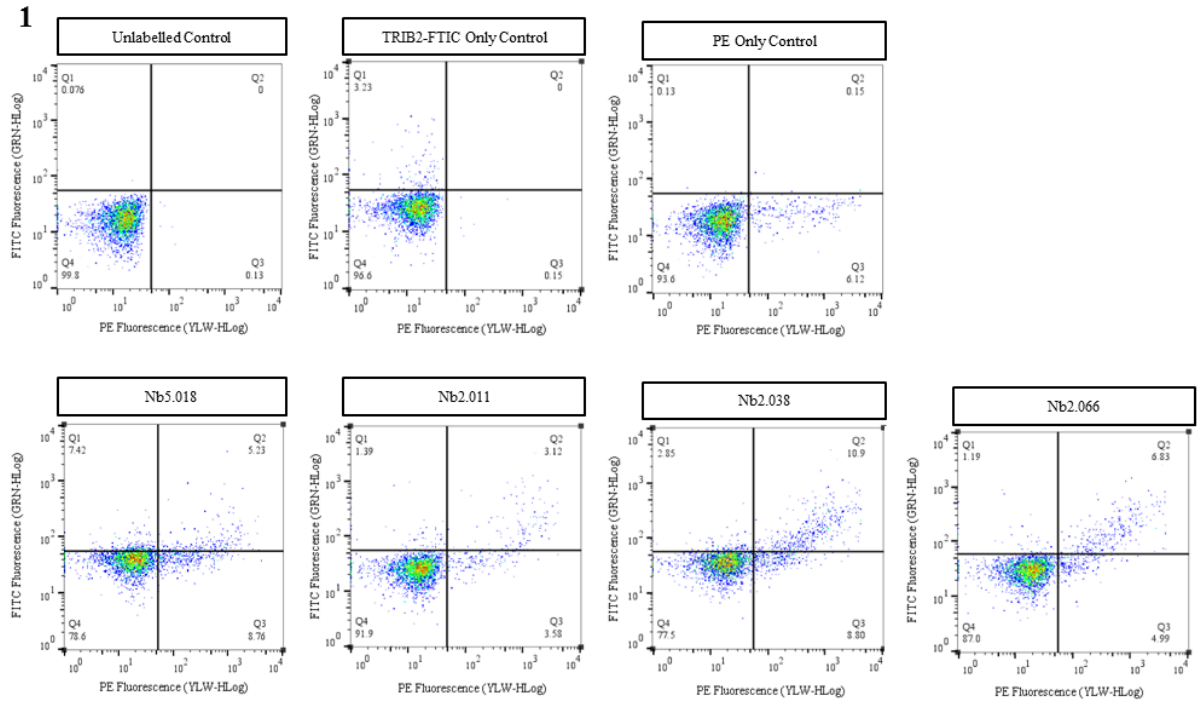

2

		FITC Mean Fluorescence Intensity (MFI)		
	Technical Relplicates	**1**	**2**	**3**
Nanobody	**Nb5.018**	66.5	54.2	68.5
	Nb2.011	126	120	115
	Nb2.038	114	107	116
	Nb2.066	132	125	129

3

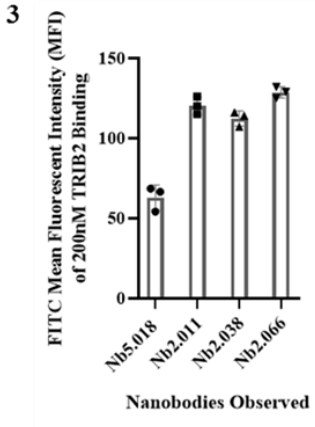

Appendix K: **Competition assay to determine the specificity of TRIB1-Nb over TRIB2 using FITC mean fluorescence intensity (MFI) from flow cytometric analysis of yeast surface display system.** Nbs expressed on the surface of *S. cerevesiae* were labelled with αHA-PE then incubated with a fixed concentration of TRIB1-FITC at 200 nM against increasing molar ratio of unlabelled TRIB2 proteins (0X, 1X, 5X, 10X). As a measure of affinity, FITC MFI was measured using Guava ExpressPlus and analysed using FlowJo *(n=3)*. **1.** Shows dot plots of 1/3 induction replicates performed to determine the specificity of TRIB1-Nbs (Nb2.011, Nb2.038, Nb2.066). **2**.Shows dot plots, an example of the labelling controls performed for each Nb tested, using Nb2.011. **3.** A table showing the raw data of FITC MFI generated from the Nb-expressing (Nb Pos) population, representing TRIB1-Nb binding to TRIB2 under increasing molar ratio concentrations of TRIB2. **4.** A table showing the results of a one-way ANOVA with Dunnett's post-hoc test performed on competition assay data from *Appendix K.2* (normalised to mean Nb5.018 data to account for non-specific binding), using GraphPad Prism 8.4.3.

1

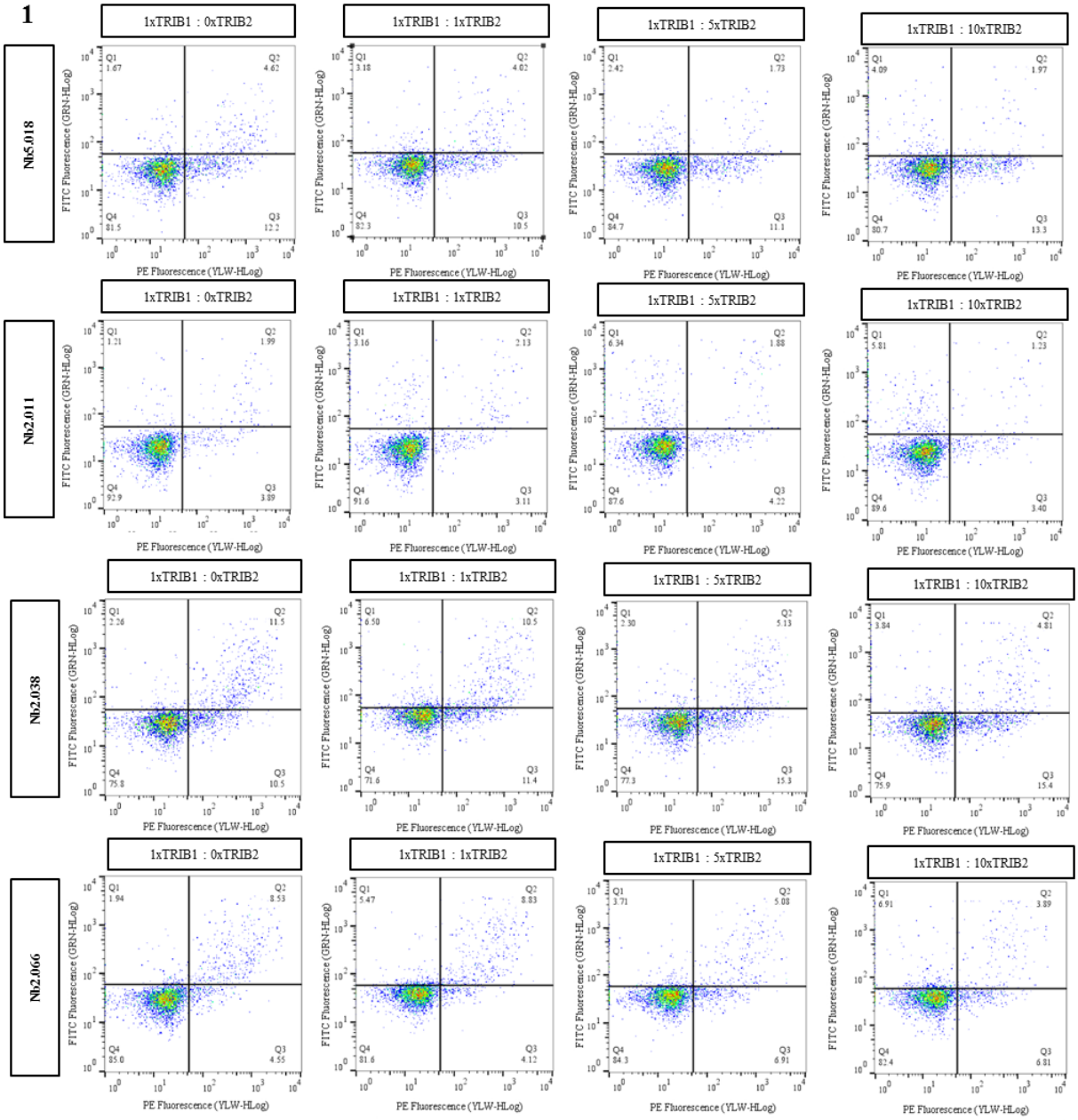

2

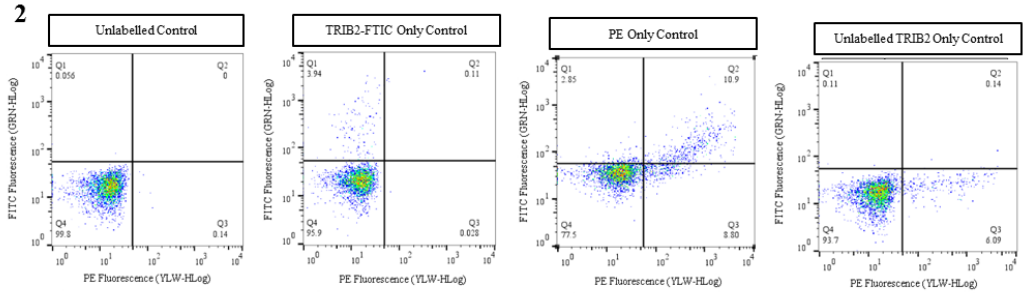

3

Nanobody	Molar Ratio of TRIB1-FITC:TRIB2 (200 nM)	Technical Replicates 1	2	3	
Nb5.018	1:0	88.4	113	146	FITC Mean Fluorescence Intensity (MFI)
	1:1	106	133	142	
	1:5	60	72.2	68.3	
	1:10	92.1	105	131	
Nb2.011	1:0	51.2	46.2	110	
	1:1	111	89.0	224	
	1:5	268	252	174	
	1:10	226	201	207	
Nb2.038	1:0	111.2	65.2	106	
	1:1	82.0	75.0	77.0	
	1:5	50.2	72.2	55.2	
	1:10	49.6	59.6	145	
Nb2.066	1:0	137	104	101	
	1:1	211	185	179	
	1:5	131	160	136	
	1:10	175	130	102	

4

Analysis of Competition Assay to Determine TRIB1-Nb Specificity over TRIB2:

Nanobody	Dunnett's multiple comparisons test	Mean 1	Mean 2	Mean Difference	95% CI of difference	Significant?	Adjusted P Value
Nb2.011	1:0 vs 1:1	69.1	141	-72.2	-185 to 40.6	No	0.228
	1:0 vs 1:5	69.1	231	-162	-275 to -49.4	Yes	0.0083
	1:0 vs 1:10	69.1	211	-142	-255 to -29.4	Yes	0.0168
Nb2.038	1:0 vs 1:1	94.1	78.0	16.1	-53.7 to 86.0	No	0.845
	1:0 vs 1:5	94.1	59.2	34.9	-34.9 to 105	No	0.392
	1:0 vs 1:10	94.1	84.7	9.40	-60.5 to 79.3	No	0.961
Nb2.066	1:0 vs 1:1	114	192	-77.7	-134 to -21.5	Yes	0.0103
	1:0 vs 1:5	114	142	-28.3	-84.5 to 27.9	No	0.386
	1:0 vs 1:10	114	136	-21.7	-77.9 to 34.5	No	0.575